



# Plantwide Control for Biodiesel Production from PFAD

Apichat Saejio

A Thesis Submitted in Partial Fulfillment of the Requirements for the  
Degree of Doctor of Philosophy in Chemical Engineering

Prince of Songkla University

2015

Copyright of Prince of Songkla University



# Plantwide Control for Biodiesel Production from PFAD

Apichat Saejio

A Thesis Submitted in Partial Fulfillment of the Requirements for the  
Degree of Doctor of Philosophy in Chemical Engineering

Prince of Songkla University

2015

Copyright of Prince of Songkla University

Thesis Title            Plantwide Control for Biodiesel Production from PFAD  
 Author                    Mr. Apichat Saejjo  
 Major Program        Chemical Engineering

---

Major Advisor

.....  
 (Asst. Prof. Dr. Kulchanat Prasertsit)

Examining Committee:

.....Chairperson  
 (Asst. Prof. Dr. Juraivan Ratanapisit)

.....Committee  
 (Asst. Prof. Dr. Kulchanat Prasertsit)

.....Committee  
 (Assoc. Prof. Dr. Pakamas Chetpattananondh)

.....Committee  
 (Asst. Prof. Dr. Pornsiri Kaewpradit)

.....Committee  
 (Dr. Sutham Sukmanee)

The Graduate School, Prince of Songkla University, has approved this thesis as partial fulfillment of the requirements for the Doctor of Philosophy Degree in Chemical Engineering.

.....  
 (Assoc. Prof. Dr. Teerapol Srichana)

Dean of Graduate School

This is to certify that the work here submitted is the result of the candidate's own investigations. Due acknowledgment has been made of any assistance received.

.....Signature

(Asst. Prof. Dr. Kulchanat Prasertsit)

Major Advisor

.....Signature

(Mr. Apichat Saejio)

Candidate

I hereby certify that this work has not been accepted in substance for any degree, and is not being currently submitted in candidature for any degree.

.....Signature

(Mr. Apichat Saejio)

Candidate

ชื่อวิทยานิพนธ์	ระบบควบคุมแบบแพลนท์ไวด์สำหรับการผลิตไบโอดีเซล
ผู้เขียน	นายอภิชาติ แซ่จิ๋ว
สาขาวิชา	วิศวกรรมเคมี
ปีการศึกษา	2558

### บทคัดย่อ

งานวิจัยนี้ได้จำลองการผลิตไบโอดีเซลจากส่วนกลั่นกรดไขมันปาล์ม และ ออกแบบระบบควบคุมแบบแพลนท์ไวด์ด้วยโปรแกรม ASPEN PLUS และ ASPEN PLUS DYNAMICS V 8.4 โดยแบ่งการศึกษาออกเป็น 4 ส่วน คือ 1) การหาค่าจลนพลศาสตร์ของ ปฏิกริยาเอสเตอริฟิเคชันจากส่วนกลั่นกรดไขมันปาล์มแบบต่อเนื่อง 2) การจำลองในสภาวะคงตัว 3) การจำลองระบบควบคุม และ 4) การจัดการพลังงาน

ส่วนกลั่นกรดไขมันปาล์มเหลว และสารละลายเมทานอลกับกรดซัลฟิวริกถูก ป้อนเข้าในการถั่งปฏิกรณ์แบบกวนต่อเนื่อง โดยมีสัดส่วนเชิงโมลระหว่างส่วนกลั่นกรดไขมัน ปาล์มและเมทานอลเป็น 1 : 8 ปริมาณกรดซัลฟิวริกเป็น 1.83% โดยน้ำหนักของส่วนกลั่นกรดไขมัน ปาล์มซึ่งทำหน้าที่เป็นตัวเร่งปฏิกริยา ดำเนินการที่อุณหภูมิ 60 70 และ 80 องศาเซลเซียส และที่ เวลา 10 20 และ 30 นาที จากการทดลองพบว่าอันดับของปฏิกริยาไปข้างหน้าเป็นปฏิกริยาอันดับ หนึ่ง และสำหรับปฏิกริยาย้อนกลับเป็นปฏิกริยาอันดับสอง ค่าจลนพลศาสตร์ที่ได้ถูกนำไปใช้ในการ จำลองกระบวนการผลิตต่อไป

ในการจำลองการผลิตไบโอดีเซลจากส่วนกลั่นกรดไขมันปาล์มนั้นประกอบไปด้วย การทำปฏิกริยาเอสเตอริฟิเคชัน การทำปฏิกริยาทรานส์เอสเตอริฟิเคชัน การทำปฏิกริยาสะเทิน การทำบริสุทธิ์ และการแยกเมทานอลกลับคืน ผลจากการจำลองระบบพบว่ากระบวนการผลิตไบ โอดีเซลนี้สามารถผลิตไบโอดีเซลที่ผ่านมาตรฐานตามมอก. 2548 ได้

ในระบบควบคุมการผลิตได้มีการออกแบบโครงสร้างควบคุมแพลนท์ไวด์ไว้ 2 แบบคือ แบบดั้งเดิม และแบบตามความต้องการ โดยทั้งสองโครงสร้างนั้นตัวควบคุมจะถูกตั้งค่า ด้วยระเบียบวิธีไทรส-ไลเบน และซิกเลอร์-นิโคลน์ จากการทดลองพบว่าระเบียบวิธีซิกเลอร์-นิโคลน์ มีประสิทธิภาพที่ดีกว่า และทั้งสองโครงสร้างควบคุมนั้นสามารถที่จะกำจัดตัวแปรบวกรวนออกไป

ได้ นอกจากนั้นการควบคุมอุณหภูมิในหอกลั่นนั้นสามารถใช้แทนการควบคุมองค์ประกอบของสารได้

ในการจัดการพลังงาน อุปกรณ์แลกเปลี่ยนความร้อนได้ถูกติดตั้งแทนเครื่องให้ความร้อนและเครื่องทำความเย็น ที่ตำแหน่งกระแสน้ำของหอกลั่นเมทานอล อุปกรณ์แลกเปลี่ยนความร้อนทำการถ่ายโอนความร้อนจากกระแสน้ำไปสู่อุปกรณ์ทำความเย็นซึ่งใช้น้ำในกระบวนการล้างไปโอดีเซล จากนั้นจึงทำการทดสอบระบบควบคุมพบว่าสามารถที่จะควบคุมระบบให้เป็นเข้าสู่ค่าตามที่ต้องการได้

Thesis Title	Plantwide Control for Biodiesel Production from PFAD
Author	Mr. Apichat Saejio
Major Program	Chemical Engineering
Academic Year	2015

## ABSTRACT

In the research, the plantwide control for biodiesel production process using the esterification reaction of palm fatty acid distillate (PFAD) was simulated by ASPEN PLUS and ASPEN PLUS DYNAMICS V8.4. This study was divided into four parts: 1) Kinetics of continuous PFAD esterification estimation, 2) Steady state simulation, 3) Dynamic and control simulation and 4) Energy management.

Melted PFAD and methanol-sulfuric acid solution were fed into a continuous stirred tank reactor (CSTR). The molar ratio of PFAD to methanol was 1 : 8, and the catalyst amount (sulfuric acid/PFAD) of 1.83 weight%. The reaction temperature was varied at 60, 70, and 80°C. The reaction mixture was sampled at retention time 10, 20, and 30 min. The esterification experimental results indicated that the forward reaction was first order, and the backward reaction was second order. Furthermore, the kinetic data from the experiment were used for simulation in this work.

In the steady state simulation, the biodiesel process from PFAD was simulated including: esterification, transesterification, neutralization, purification and methanol recovery processes. Simulation results shown the specification of biodiesel was standardized Thai Industrial Standard (TIS) 2005.

For the plantwide control system, conventional and on demand control structures were proposed. Both structures were tuned by Tyreus – Luyben and Ziegler – Nichols tuning methods with considering of dynamic performance to eliminate disturbances or setpoint change; Ziegler – Nichols tuning method provides better



performance than using Tyreus – Luyben tuning method. Moreover, the designed temperature control tray could control the methanol composition in distillate stream instead of composition control.

In addition, heat exchanger was added instead of a cooler and a heater at the bottom stream of methanol recovery column. It transferred heat from bottom stream to water that was fed into water washing column. After that, the dynamic responses were tested. It also reached to the desired setpoint.

## ACKNOWLEDGMENT

First and foremost, I would like to thank my advisor Asst. Prof. Dr. Kulchanat Prasertsit not only for her supervision and guidance but also for her patience and composure and for giving me the opportunity to complete a Ph.D. program.

I would also thank the rest of my thesis committee members for their valuable times and suggestions helped me to improve the thesis in any ways.

My gratitude goes to the Department of Chemical Engineering, Faculty of Engineering, Graduate school of Prince of Songkla University and the Specialized R&D Center for Alternative Energy from Palm Oil and Oil Crops for supporting my study.

I would like to express my deepest appreciation to all lectures in the Department of Chemical Engineering, Prince of Songkla University for their helpful.

Big thanks also goes to all my friends. They have provided me the great friendship.

Many thanks to those who contributed, directly and indirectly, to accomplishing all the works presented in this study.

Finally, I am indebted and thankful to my family for their love, encouragement, and supporting throughout my study.

APICHAT SAEJIO

## CONTENT

บทคัดย่อ	V
ABSTRACT	VII
ACKNOWLEDGMENT	IX
CONTENT	X
LIST OF TABLES	XIII
LIST OF FIGURES	XIV
CHAPTER 1 INTRODUCTION	1
1.1 BACKGROUND AND RATIONALE	1
1.2 OBJECTIVE	2
1.3 SCOPE	2
1.4 THEORIES	2
1.4.1 Biodiesel production	2
1.4.2 Control system	7
1.5 LITERATURE REVIEW	12
CHAPTER 2 RESEARCH METHODOLOGY	17
2.1 MATERIALS	17
2.1.2 Raw material	17
2.1.3 Chemicals	17
2.2 EQUIPMENTS AND INSTRUMENTS	17
2.3 METHODOLOGY	18
2.3.1 Kinetics of esterification	18
2.3.2 Steady state process simulation	19
2.3.3 Dynamic simulation and control	19
2.3.4 Energy management	20

**CONTENT (continuous)**

<b>CHAPTER 3 RESULT AND DISCUSSION</b>	<b>21</b>
3.1 KINETICS OF ESTERIFICATION	21
3.2 STEADY STATE PROCESS SIMULATION	25
3.2.1 Esterification	26
3.2.2 Methanol recovery I	26
3.2.3 Neutralization	27
3.2.4 Transesterification	27
3.2.5 Methanol recovery II	28
3.2.6 Water washing (liquid – liquid extraction)	28
3.3 DYNAMICS SIMULATION AND CONTROL	33
3.3.1 Conventional control structure (CS I)	33
3.3.2 On demand control structure (CS II)	38
3.3.3 Selection of temperature control tray	44
3.3.4 Controller tuning	46
3.3.5 Control robustness	50
3.3.6 Dynamic performance	71
3.4 ENERGY MANAGEMENT	73
<b>CHAPTER 4 CONCLUSION</b>	<b>100</b>
4.1 CONCLUSION	100
4.2 RECOMMENDATION	101
<b>REFERENCES</b>	<b>102</b>
<b>APPENDIX</b>	<b>105</b>
<b>APPENDIX A CALIBRATION CURVE OF THE PUMP</b>	<b>106</b>
<b>APPENDIX B ULTIMATE GAIN AND ULTIMATE PERIOD OF THE PROCESS</b>	<b>107</b>

CONTENT (continuous)

APPENDIX C CONFERENCE PROCEEDING	109
VITAE	116

## LIST OF TABLES

Table 1-1 Fatty acid profile of PFAD.	4
Table 1-2 Fuel properties of Thai standard biodiesel.	7
Table 1-3 Controller parameters setting.	11
Table 2-1 Conditions for robustness test for both control structures.	20
Table 3-1 Arrhenius parameters and summation of absolute error of each model.	23
Table 3-2 Data of biodiesel production from PFAD simulation.	29
Table 3-3 Control degrees of freedom for biodiesel production process from PFAD.	34
Table 3-4 Controlled and manipulated variables of control structure I.	36
Table 3-5 Controlled and manipulated variables of control structure II.	40
Table 3-6 Controller settings for control structure I.	48
Table 3-7 Controller settings for control structure II.	49
Table 3-8 Robustness, IAE and maximum settling time of control structure I.	72
Table 3-9 Robustness, IAE and maximum settling time of control structure II.	72
Table 3-10 Heat exchanger specification.	75
Table 3-11 Controller setting by ZN tuning method for control structure I and II with heat exchanger.	76

## LIST OF FIGURES

Fig. 1-1 Transesterification of triglyceride.	5
Fig. 1-2 Esterification of free fatty acid.	5
Fig. 1-3 Auto tuning using a relay feedback method.	11
Fig. 3-1 Effect of temperature on FFA content.	22
Fig. 3-2 Predicted data versus experimental data parity plot.	24
Fig. 3-3 Biodiesel production from PFAD process (esterification and methanol recovery I).	25
Fig. 3-4 Biodiesel production from PFAD process (neutralization, transesterification and methanol recovery II).	26
Fig. 3-5 Biodiesel production from PFAD process (water washing and flash drum).	27
Fig. 3-6 Biodiesel production from PFAD process (entire the process).	32
Fig. 3-7 Control structure I (PFAD feed flow rate control).	42
Fig. 3-8 Control structure II (Production flow rate control).	43
Fig. 3-9 Temperature profile of methanol recovery column I.	44
Fig. 3-10 Temperature profile of methanol recovery column II.	45
Fig. 3-11 Effect of changes in column boilup $\pm 10\%$ on temperature profile of column I.	45
Fig. 3-12 Effect of changes in column boilup $\pm 10\%$ on the temperature profile of column II.	46
Fig. 3-13 Flow dynamic responses of TL and ZN-tuned control structure I for PFAD feed rate change.	51
Fig. 3-14 Level dynamic responses of TL and ZN-tuned control structure I for PFAD feed rate change.	52
Fig. 3-15 Pressure and temperature dynamic responses of TL and ZN-tuned control structure I for PFAD feed rate change.	53
Fig. 3-16 Temperature dynamic responses of TL and ZN-tuned control structure I for R1 temperature change.	55

## LIST OF FIGURES (continuous)

Fig. 3-17 Flow and pressure dynamic responses of TL and ZN-tuned control structure I for R1 temperature change.	56
Fig. 3-18 Level dynamic responses of TL and ZN-tuned control structure I for R1 temperature change.	57
Fig. 3-19 Temperature dynamic responses of TL and ZN-tuned control structure II for R1 temperature change.	58
Fig. 3-20 Flow and pressure dynamic responses of TL and ZN-tuned control structure II for R1 temperature change.	59
Fig. 3-21 Level dynamic responses of TL and ZN-tuned control structure II for R1 temperature change.	60
Fig. 3-22 Temperature dynamic responses of TL and ZN-tuned control structure I for FFA in PFAD change.	62
Fig. 3-23 Flow and pressure dynamic responses of TL and ZN-tuned control structure I for FFA in PFAD change.	63
Fig. 3-24 Level dynamic responses of TL and ZN-tuned control structure I for FFA in PFAD change.	64
Fig. 3-25 Temperature dynamic responses of TL and ZN-tuned control structure II for FFA in PFAD change.	65
Fig. 3-26 Flow and pressure dynamic responses of TL and ZN-tuned control structure II for FFA in PFAD change.	66
Fig. 3-27 Level dynamic responses of TL and ZN-tuned control structure II for FFA in PFAD change.	67
Fig. 3-28 Flow dynamic responses of TL and ZN-tuned control structure II for production rate change.	68
Fig. 3-29 Temperature dynamic responses of TL and ZN-tuned control structure II for production rate change.	69



## LIST OF FIGURES (continuous)

Fig. 3-30 Level and pressure dynamic responses of TL and ZN-tuned control structure II for production rate change.	70
Fig. 3-31 Biodiesel production from PFAD process with heat exchanger.	74
Fig. 3-32 Flow dynamic responses of ZN-tuned control structure I with heat exchanger for PFAD feed rate change.	77
Fig. 3-33 Level dynamic responses of ZN-tuned control structure I with heat exchanger for PFAD feed rate change.	78
Fig. 3-34 Temperature dynamic responses of ZN-tuned control structure I with heat exchanger for PFAD feed rate change.	79
Fig. 3-35 Pressure dynamic responses of ZN-tuned control structure I with heat exchanger for PFAD feed rate change.	80
Fig. 3-36 Temperature dynamic responses of ZN-tuned control structure I with heat exchanger for R1 temperature change.	81
Fig. 3-37 Flow and pressure dynamic responses of ZN-tuned control structure I with heat exchanger for R1 temperature change.	82
Fig. 3-38 Level dynamic responses of ZN-tuned control structure I with heat exchanger for R1 temperature change.	83
Fig. 3-39 Temperature dynamic responses of ZN-tuned control structure I with heat exchanger for FFA in PFAD change.	84
Fig. 3-40 Flow and pressure dynamic responses of ZN-tuned control structure I with heat exchanger for FFA in PFAD change.	85
Fig. 3-41 Level dynamic responses of ZN-tuned control structure I with heat exchanger for FFA in PFAD change.	86
Fig. 3-42 Flow dynamic responses of ZN-tuned control structure II with heat exchanger for biodiesel production rate change.	87
Fig. 3-43 Temperature dynamic responses of ZN-tuned control structure II with heat exchanger for biodiesel production rate change.	88

## LIST OF FIGURES (continuous)

Fig. 3-44	Level and pressure dynamic responses of ZN-tuned control structure II with heat exchanger for biodiesel production rate change.	89
Fig. 3-45	Temperature dynamic responses of ZN-tuned control structure II with heat exchanger for R1 temperature change.	91
Fig. 3-46	Flow and pressure dynamic responses of ZN-tuned control structure II with heat exchanger for R1 temperature change.	92
Fig. 3-47	Level dynamic responses of ZN-tuned control structure II with heat exchanger for R1 temperature change.	93
Fig. 3-48	Temperature dynamic responses of ZN-tuned control structure II with heat exchanger for FFA in PFAD change.	94
Fig. 3-49	Flow and pressure dynamic responses of ZN-tuned control structure II with heat exchanger for FFA in PFAD change.	95
Fig. 3-50	Level dynamic responses of ZN-tuned control structure II with heat exchanger for FFA in PFAD change.	96
Fig. 3-51	IAE responses of $\pm 10\%$ PFAD feed rate change of control structure I for the process with and without heat exchanger.	97
Fig. 3-52	IAE responses of $\pm 10\%$ production rate change of control structure II for the process with and without heat exchanger.	98
Fig. 3-53	IAE responses of $\pm 10^{\circ}\text{C}$ of esterification reactor temperature change for the process with and without heat exchanger.	98
Fig. 3-54	IAE responses of FFA content in PFAD change in range of 92 - 98% for the process with and without heat exchanger.	99

## CHAPTER 1

### INTRODUCTION

#### 1.1 Background and rationale

Since energy consumption is increasing worldwide but the energy resources such as diesel and gasoline are decreased. So it is necessary to find the new energy sources to meet the demand. One of the favorite alternative energy replacing diesel is biodiesel.

Biodiesel is made from oil or fat: palm oil, waste cooking oil, and sunflower oil and alcohol. The physical properties of biodiesel are similar to petroleum based diesel, but it has lower emission and toxicity. Biodiesel production is a simple process mainly using oil and alcohol with alkali-catalyst in transesterification. However, the transesterification must use low free fatty acid (FFA) oil which is more expensive than high FFA feedstock such as Palm fatty acid distillate (PFAD) because if FFA content in oil is higher than 1%, the FFA can react with a alkali catalyst to produce soap and stop the reaction [1].

PFAD is a byproduct of the palm oil refining process. It has high FFA content but low price so it is selected to react with alcohol in sulfuric acid catalyst-esterification in order to convert FFA to fatty acid methyl ester (FAME) or biodiesel and byproduct water.

In the production process, general plants are consists of several unit operations. Thus, the control system is required to achieve the process purpose, such as product quality, safe and smooth process operation [2].

The goal of this research is to design the control structures of biodiesel production process from PFAD which can achieve the control objectives as well as safety. In particular, this research can be separated into four sections: kinetics determination for PFAD esterification, steady state and dynamics simulation, and heat management.

## 1.2 Objective

- 1) To study and design biodiesel production process from PFAD with ASPEN PLUS.
- 2) To design appropriate control structures for the biodiesel plant.

## 1.3 Scope

- 1) Oleic acid, palmitic acid, and triolein are used representative of PFAD composition.
- 2) Two-step reaction is acid catalyzed reaction followed by alkali catalyzed reaction.
- 3) PID-controllers are used for control the system.
- 4) Simulation the biodiesel process and control system by using ASPEN PLUS V8.4 and ASPEN DYNAMICS V8.4.

## 1.4 Theories

### 1.4.1 Biodiesel production

Biodiesel is a short chain alcohol with a long chain fatty acid ester supplied from vegetable oil or animal fats. If methanol (MeOH) is used in the reaction, product of the reaction is fatty acid methyl ester (FAME). There are properties

resembled diesel, low emission and non-toxic. Four primary processes [3] for biodiesel production are 1) Direct used or blending, 2) Micro emulsion, 3) Thermal cracking and 4) Transesterification.

PFAD is by product from palm oil refinery process. It has FFA content about 90-98 weight% and traces of impurities [4]; the composition of PFAD as shown in Table 1-1.

Generally catalysts in biodiesel process are acid or alkali base such as sodium hydroxide (NaOH), potassium hydroxide (KOH), sulfuric acid ( $H_2SO_4$ ), and hydrochloric acid (HCl). For high FFA content in feedstocks, alkali base catalyzed biodiesel production will form soap. It causes difficult ester - glycerol phase separation, so pretreatment process is required for high FFA feedstock [1].

There are 4 techniques [1] to convert FFA to biodiesel and reduce the FFA content, and that techniques are:

- 1) Enzymatic methods: This method is expensive but water is less effect on this.
- 2) Glycerolysis: Glycerol is added to feedstock to react with FFA and zinc chloride as catalyst to produce mono- and diglyceride at high temperature.
- 3) Acid catalysis: Sulfuric acid is used as catalyst in esterification of FFA and transesterification of triglyceride to produce FAME. This procedure does not form soap.
- 4) Acid catalysis followed by alkali catalysis: First step, using an acid catalyst to convert FFA to methyl ester. When the FFA content lower than 0.5%; an alkali catalyst is used for converting triglyceride to methyl ester.

**Table 1-1** Fatty acid profile of PFAD [4].

Fatty acid	Weight%
Myristic acid	1.0
Palmitic acid	45.6
Palmitoleic acid	0.2
Tetracosenoic acid	0.6
Oleic acid	33.3
Linoleic acid	7.7
Ecosanoic acid	0.3
Linolenic acid	0.3
Ecosenoic acid	0.2
Stearic acid	3.8

Mainly reactions used to produce the biodiesel were:

- 1) Transesterification [3]: Triglyceride reacts with alcohol such as methanol under suitable condition. Three fatty acid chains are released from glycerol skeleton and combine with alcohol. It produces FAME, and glycerol is by product. The reaction was shown in Fig. 1-1.

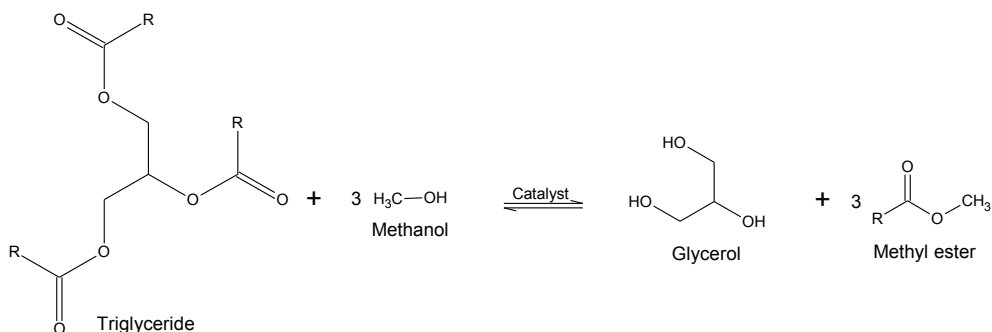


Fig. 1-1 Transesterification of triglyceride [1].

2) Esterification: FFA reacts with methanol in the presence of an acid catalyst. The yields of the reaction are FAME and water which is by product. The reaction was shown in Fig. 1-2.

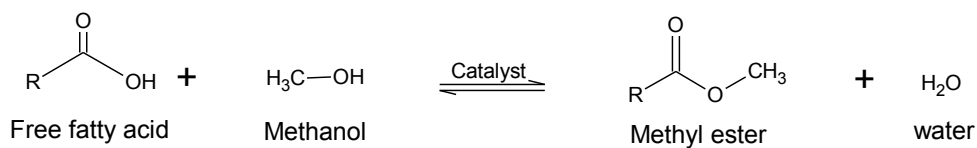


Fig. 1-2 Esterification of free fatty acid [1].

The reaction rate constant [5],  $k$  is almost strongly dependent on temperature. Thus, Eqs (1-1) showed the specific reaction rate is dependent on temperature that was called Arrhenius equation.

$$k(T) = A \exp(-E_a/RT) \quad (1-1)$$

$A$  pre-exponential factor or frequency factor;  $E_a$  activation energy (J/mol);

$R$  gas constant = 8.314 J/mol·K;  $T$  absolute temperature (K)

There are four steps of biodiesel production from PFAD [6]:

- 1) Reaction: PFAD, alcohol and acid catalyst are fed into a continuous stirred tank reactor (CSTR). The reaction temperature is kept about 65-75 °C. Excess alcohol is used to ensure oil converting to ester completely.
- 2) Separation: Once the reaction is complete; unreacted alcohol, biodiesel, residual FFA and glycerides, mono- di- tri- glyceride, are separated by gravity separation in settling vessel since the biodiesel phase is denser than alcohol.
- 3) Purification: FFA in FAME phase is neutralized with NaOH solution since transesterification of glycerides with alcohol in alkali catalyst in FAME phase has soap (from FFA and NaOH) as a byproduct. This soap is removed at the bottom of the separator.
- 4) Washing: The esterified product is washed by the water spray tank or liquid - liquid extractor, and then it flows to the separator to separate water. Finally, the biodiesel is flashed residual water with a flash evaporation process or distillation.

Thai standard of biodiesel properties as shown in Table 1-2 is considered.



**Table 1-2** Fuel properties of Thai standard biodiesel [7].

Properties	Unit	Specification
Methyl ester	wt%	96.5 (minimum)
Density at 15 °C	kg/m <sup>3</sup>	860-900
Viscosity at 40 °C	cSt	3.5-5.0
Flash point	°C	120 (minimum)
Water	wt%	0.050 (maximum)
Corrosion strip copper	number	1 (maximum)
Acid value	mgKOH/g	0.50 (maximum)
Monoglyceride	wt%	0.8 (maximum)
Diglyceride	wt%	0.2 (maximum)
Triglyceride	wt%	0.2 (maximum)

#### 1.4.2 Control system [2]

##### 1) Plantwide process control

In the control system, Luyben defined the method and strategies of control system for individual unit and plantwide [2]. The designing of process control system has to consider the control objective, control degree of freedom, energy management system, production rate, product quality, recycle loop, and inventories and component balance. Integration of control of individual unit has slightly different from

plantwide control because of the interconnection of unit operations. Steps of plantwide process control design are:

1. Establish control objective: by evaluating the steady state design and dynamic control objectives of the process. This step is the most important of the control system since different control objectives lead to different control structures. There are many control objectives, for example, reactor yield, product specification and environmental restriction.

Instead of composition control, there are mainly two criteria for selecting which tray temperature control can be used because of its fast response and cheaper than using composition control [2].

- 1) The steepest slope: this procedure is to look at the steady state temperature profile. Where there is a large temperature change or steepest indicate that the important component is changing.
- 2) Manipulated variable change sensitivity: finding the control tray which is the most sensitive to changes in manipulated variable. In steady state, heat input is made small change. The changed results of the tray temperature profile show the largest change temperature tray that is a very sensitive tray. It is a temperature control tray.

2. Determine control degrees of freedom by counting the number of control valves which are available. The number of degrees of freedom for control represents manipulated variables respect to controlled variables.

3. Establish energy management system to prevent energy propagation from the process. The heat from exothermic process must be eliminated by direct reactor utilities or other unit operations. If heat integration is employed, the control system must be ensured that it can prevent the propagation of energy disturbance and the heat is spread and not recycled.

Heat transfer between streams can lead to units interaction and process instability. Partial vaporization or condensation and a small change in stream composition may occur during heat transfer. As a result, heat transfer between streams is not enough, and dynamic performance is poor and complex. Heaters, coolers or heat exchanger bypass lines

4. Set production rate. One of choices for setting production rate is one of main reactor variables that is the prevailing variable of the reactor. For liquid phase reactor, there are many dominant variables, such as reactor temperature, concentration of limiting reactant, reaction time and flow rate.

In addition, the chose variable must provide the smooth process and reject disturbance. That variable not only has a direct and rapid effect on the reaction rate, but also has the least effect on separation units.

5. Control product quality and safety operation with low environmental constraints. The important quantities for control are economic and operational reasons, so the selected manipulated variables must have dynamic relationships between the controlled and manipulated variables that give small time constants and deadtimes and large steady state gains. The first gives small closed loop time constants and then prevents problems with the range ability.

6. Fix flow rate in all recycle loops and control pressures and levels. In chemical process a flow controller should be installed in every liquid recycle loop. This way can prevent problems in recycle streams that can happen if all flows in the recycle loops are controlled using level controllers.

Inventory loop should be controlled with manipulated variable that give the largest effect on its unit. Moreover, P controller can be used in nonreactive level loops.

7. Check component balances. Component balances are important in the process with recycle streams. They frequently affect variable that can be used to set

the production rate. Purge streams can also be used to control the amount of high or low boiling impurities in a recycle stream.

8. Set control individual unit operations. For example, high temperature endothermic reactions are controlled using fuel flow rate to a furnace, Crystallization manipulate refrigeration load to control temperature.

9. Optimize economics or improve dynamic controllability. After managing all of the basic requirements, the remaining degrees of freedom including control valves are tuned. These control valves can be used to improve dynamic response and to optimize steady state economic process.

## 2) Control parameters tuning

For Proportional-Integral-Derivative controller (PID) parameters [8]. The characteristics of the process are shown in the terms of ultimate gain ( $K_u$ ), ultimate period ( $P_u$ ), and ultimate frequency ( $\omega_u$ ), it can be determined by auto tune variation method (ATV) proposed by Åström and Hägglund in 1984. For this test, feedback controller is temporarily replaced by a relay controller. The controlled variable ( $x$ ) has shown the continuous oscillation because of the manipulated variable ( $m$ ) variation as shown in Fig. 1-3. The ultimate gain and ultimate frequency are calculated by using Eqs. (1-2) and Eqs. (1-3) respectively.

$$K_u = \frac{4h}{\pi a} \quad (1-2)$$

$$\omega_u = \frac{2\pi}{P_u} \quad (1-3)$$

$K_u$  and  $P_u$  are used to calculate controller parameters which are controller gain ( $K_c$ ), integral time constant ( $\tau_i$ ) and derivative time constant ( $\tau_D$ ) by using Ziegler-Nichols (ZN) or Tyreus-Luyben (TL) setting as shown in Table 1-3.

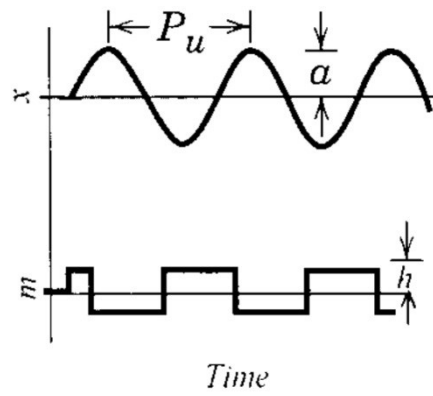


Fig. 1-3 Auto tuning using a relay feedback method [2].

Table 1-3 Controller parameters setting [8].

ZN	$K_c$	$\tau_I$	$\tau_D$
P	$0.5K_u$	-	-
PI	$0.45K_u$	$P_u/1.2$	-
PID	$0.6K_u$	$P_u/2$	$P_u/8$
TL	$K_c$	$\tau_I$	$\tau_D$
PI	$0.31K_u$	$2.2P_u$	-
PID	$0.45K_u$	$2.2P_u$	$P_u/6.3$

### 3) Control evaluation

The optimal objective of controller setting is to minimize an integral error criterion [2]. There are three integral error criteria that are:

#### 1) Integral of the absolute value of the error (IAE):

$$IAE = \int_0^{\infty} |e(t)| dt \quad (1-4)$$

#### 2) Integral of the squared error (ISE):

$$ISE = \int_0^{\infty} e(t)^2 dt \quad (1-5)$$

#### 3) Integral of the time-weighted absolute error (ITAE):

$$ITAE = \int_0^{\infty} t|e(t)| dt \quad (1-6)$$

$e(t)$  is the difference value between the setpoint and controlled variable value for each time.

## 1.5 Literature review

Zhang et al. (2003) [9] studied four different continuous biodiesel processes, and an assessment of four processes was evaluated. These processes included alkali catalyzed process with virgin vegetable oil, alkali catalyzed process with waste cooking oil, acid catalyzed with waste cooking oil and acid catalyzed using hexane extraction. All processes were simulated using HYSYS. The thermodynamic

property packages NRTL and UNIQUAC were recommended to simulate since the reaction mixture had the polar components that were methanol and glycerol. From the assessment analysis, vegetable oil with the alkali catalyst process needed the fewest unit operations. However the feedstock cost of this process was higher than others. The acid catalyzed process using waste cooking oil was simpler and suitable for raw material cost competition.

Chongkhong et al. (2007) [4] studied biodiesel production from esterification of PFAD. The optimal condition of continuous production process was PFAD to methanol molar ratio at 1 : 8, 1.834 wt% of sulfuric acid, reaction temperature 70°C, and retention time 1 hr. It could decrease FFA from 93 wt% to 1.402 wt%. After that, biodiesel was purified to obtain the highest yield that was neutralization with 3 M sodium hydroxide solution followed by transesterification with 0.396 M sodium hydroxide in methanol solution.

Aranda et al. (2008) [10] studied PFAD esterification with homogeneous catalyst in batch process. The main compositions of fatty acid were palmitic acid and oleic acid. The results informed that sulfuric acid and methanesulfonic acid were the best catalysts, and methanol gave higher yield than ethanol. Additionally, kinetics of reaction was studied the rate of reaction with respect to fatty acid in first order and zero order on alcohol, excess of alcohol used.

ASPEN PLUS biodiesel model manual (2008) [11] simulated the transesterification biodiesel from palm oil. It suggested that the suitable property method for biodiesel simulation was Dortmund modified UNIFAC. Major units in the process, transesterification reactor, catalyst removal unit, and water washing column were represented by RCSTR, RStoic, and liquid – liquid extractor, respectively, and this model could be used as a guide for economical process or change of feedstock.

West et al. (2008) [12] investigated four continuous biodiesel production that were homogeneous alkali catalyzed process, homogeneous acid catalyzed process,

heterogeneous acid catalyzed process and supercritical alcohol process. Those processes were designed and simulated using HYSYS. The NRTL thermodynamic property method was employed for calculating thermodynamic and activity parameters, and the UNIFAC property package was also selected for estimating unavailable parameters. Feedstock flow rate was set around 1000 kg/hr. The stoichiometric reactor was used in the reaction simulation part; the reaction conversion was in the range of 94 – 100%.

S. Glisic and D. Skala (2009) [13] investigated energy consumption of supercritical biodiesel process, and compared with the homogeneous alkali catalyst process. Triolein, oleic acid; and methyl oleate were used to represent raw material and product, respectively. The UNIQUAC and the UNIFAC-LL were employed in the low pressure section of supercritical process. The UNIQUAC and the NRTL were used for the alkali catalyst process, also. The results showed that the consumption of energy was very close; still, purification of supercritical process was easier because of the non-catalyzed process.

Tesser et al. (2009) [14] studied esterification kinetics which FFA reacted with methanol and catalyzed with ionic-exchange sulphonic acid resins in a batch reactor. Kinetics results informed the kinetic model of non-catalytic reaction was second order in FFA and first order in methanol; moreover, the model of catalyzed esterification was assumed pseudo-homogeneous that neglected the solid phase, so the kinetic outcome was first order in FFA and methanol.

Yadav et al. (2010) [15] investigated PFAD biodiesel process optimization. The results informed that 1 : 10 molar ratio of PFAD to methanol at 65°C was the optimum process condition; it gave a maximum conversion 94.4%. Moreover, the kinetic esterification was studied, and found that overall reaction order was second order.



Shen et al. (2011) [16] researched the design and control biodiesel production with internal recycle and phase separation in the reactor system. A decanter was added after the reactor to separate liquid into two phases. Glycerol phase was the methanol rich phase that was recycled back to the reactor. That could reduce annual cost and energy consumption. The UNIFAC property method was selected for this simulation and control. Plantwide controllability results indicated that the proposed process could handle the process with dynamic stability and a settle time less than 10 hr.

Lee et al (2011) [17] studied process simulation and economic analysis of biodiesel production processes that were alkali catalyzed fresh vegetable oil process; acid catalyzed pretreatment with alkali catalyzed waste vegetable oil process; and supercritical methanol of waste vegetable oil process. For simulation, the selected property package was NRTL which was fulfilled by UNIFAC model. The alkali catalyzed fresh vegetable oil process had lowest total capital investment. The supercritical process, however, was the most feasible process in economic.

A. A. Kiss and C. S. Bildea (2011) [18] investigated the design and plantwide control of an energy integrated biodiesel production using reactive distillation and reactive absorption. ASPEN PLUS DYNAMICS and UNIFAC-Dortmund modified thermodynamic properties method were used to simulate in this work. The proposed process could improve efficiency and reduce the energy consumption. Furthermore, the proposed control structure could control the process and product purity to meet the standard.

C. S. Bildea and A. A. Kiss (2011) [19] studied dynamics and control of a biodiesel process by reactive absorption. Four proposed control structures were basic structure (fixing the alcohol inlet flow by ratio controller), improving the basic control structure by manipulating the alcohol/acid ratio, improving the basic control structure by controlling influent acid temperature and fixing the acid inlet flow. The main results of this study showed these control structures could be controlled and operate efficiently.

Cho et al. (2012) [20] studied biodiesel production from PFAD without a catalyst and simulation for economic analysis. The reaction performed in a semi batch reactor; the reaction mixture was sampled and analyzed the FFA content. In the simulation, the Wilson-RK and UNIFAC were used as the thermodynamic properties. The analyzed results informed total manufacturing cost of this process was cheaper than alkali and supercritical processes, but it required capital cost higher than the alkali process.

Cheng et al (2014) [21] studied plantwide control for a biodiesel production process using heterogeneous sugar catalyst. The mainly thermodynamic property in this work was UNIFAC. The results indicated that the energy consumption of biodiesel production of the proposed process saved for an acid oil feed. Dynamic simulation showed that the proposed process could handle production rate and feed composition changes employing the plantwide control structure.

D. S. Patle, Z. Ahmad, and G. P. Rangaiah (2014) [22] investigated plantwide control of biodiesel production from waste cooking oil using integrated framework of simulation and heuristics methodology. Production flow rate, fresh methanol, recycled methanol and overall conversion were disturbances of the process. The proposed control structure could handle and eliminate all of tested disturbance, and the biodiesel specification was maintained despite the large disturbances.

## CHAPTER 2

### RESEARCH METHODOLOGY

#### 2.1 Materials

##### 2.1.2 Raw material

PFAD was obtained from Chumporn Palm Oil Industry PLC., Thailand.

##### 2.1.3 Chemicals

- 1) Methanol ( $\text{CH}_3\text{OH}$ ) 99.5% commercial grade
- 2) Sulfuric acid ( $\text{H}_2\text{SO}_4$ ) 98% commercial grade
- 3) Sodium hydroxide ( $\text{NaOH}$ ) 99% commercial grade

#### 2.2 Equipments and instruments

- 1) A continuous stirred tank reactor 0.57 L
- 2) Peristaltic pumps (model BT300-2J)
- 3) Heater and temperature controller sets

## 2.3 Methodology

PFAD esterification was studied in continuous process experiment to analyze the kinetics of the reaction.

The biodiesel production process from PFAD was simulated using ASPEN PLUS V8.4 in steady state and dynamics. The conventional control structure and on demand control structures were proposed and tested the performance. After that, a heat exchanger was installed in the process for saving the energy and cost.

There are proceeding as follows:

### 2.3.1 Kinetics of esterification

The PFAD was melted to a desired temperature (50, 60, and 70°C) before feeding into a CSTR. Methanol (molar ratio of methanol to PFAD was 8 : 1) was mixed with sulfuric acid which was of catalyst (1.834 weight% of PFAD) [4] and fed into the reactor along.

The temperature of the mixture in the reactor was set using the heater and temperature controller set. The reaction mixture would overflow when it reached for retention time (10, 20, and 30 min). Retention time was adjusted by PFAD and mixed methanol flow rates. The mixture was sampled after the process reached to steady state that was four times of retention time. Then, the sample was washed by 50°C hot water and separated by pouring into a separation funnel to remove un-reacted methanol and impurities. The top phase was a water rich phase and the bottom phase was a biodiesel rich phase. The washed sample that was a biodiesel rich phase was dried for 1 hr at 105°C to eliminate residual water. Finally, it was analyzed FFA content by AOCS Official Method Ca 5a-40 [23].

Kinetic models related to the reaction were proposed to find a suitable model for prediction and simulation. The concentration of each component in the reaction mixture was estimated based on FFA concentration using material balance calculation. The least absolute error method was used to fit the models.

### 2.3.2 Steady state process simulation

Biodiesel esterification production process from PFAD was simulated using a commercial simulation software ASPEN PLUS V8.4. The simulation was performed from beginning reactants to end product that was biodiesel. The conditions of this simulation employed the optimal conditions of Chongkhong et al. research [4]; however, the kinetics of esterification reaction used the result from a kinetic model study of this work. The Winn-Underwood- Gilliland method was used for calculation of minimum number of stages and reflux ratio that was DSTWU unit (shortcut model) in ASPEN PLUS.

### 2.3.3 Dynamic simulation and control

Two control structures which were conventional (feed flow rate controlled) and on demand (production rate controlled) control structures were designed for the biodiesel production process. Controllers of these structures were tuned using Tyreus – Luyben (TL) and Ziegler – Nichols (ZN) tuning method [8] for each structure. Finally, the performance and robustness test of both structures were verified, and IAE criteria results was showed the characteristic of the apiece control structure. The conditions for robustness test for both structures were shown in Table 2-1.

**Table 2-1** Conditions for robustness test for both control structures.

Control structures	Test conditions
Conventional structure	<ul style="list-style-type: none"> <li>- PFAD feed flow rate</li> <li>- Esterification reactor temperature</li> <li>- PFAD composition</li> </ul>
On demand structure	<ul style="list-style-type: none"> <li>- Biodiesel production rate</li> <li>- Esterification reactor temperature</li> <li>- PFAD composition</li> </ul>

#### 2.3.4 Energy management

Heat integration of distillation column with other units was used to reduce the energy consumption. The bottom stream of methanol recovery column II was hot fluid, and water stream of water washing column was cold stream. Cooler at bottom stream was removed, and heat exchanger was added instead of it. So, the energy consumption of the process is decreased. The specification of the heat exchanger was designed to remove heat from bottom stream and transfer to the water stream. After that, the dynamic simulation and dynamic performance were performed to test the stability of the process.

## CHAPTER 3

### RESULT AND DISCUSSION

#### 3.1 Kinetics of esterification

PFAD compositions contained 93% FFA, 2.7% triglyceride, and impurities. The major types of FFA in PFAD were palmitic acid and oleic acid [4, 15].

In preliminary study, the kinetics models of PFAD esterification were fit using least square error method with S. Chongkhong et al.'s data [4]. The results as shown in APPENDIX C found that the forward reaction rate respected on FFA and methanol. Meanwhile, the backward reaction rate respected on methyl ester and water. The model gave the best fit result at molar ratio of PFAD : methanol 1 : 8 that was the optimum condition for biodiesel production from PFAD also.

The PFAD was preheated and pumped into a CSTR. Methanol was blended with sulfuric acid (1.834 weight% of PFAD) and fed into the reactor. The molar ratio of methanol to PFAD was set 8 : 1. In esterification, FFA in PFAD reacted with methanol to produce FAME and water. Then, the reacted mixture was sampled and analyzed the FFA content as shown in Fig. 3-1. It was indicated that FFA content rapidly decreased in the first 10 min. After that, the FFA conversion was slower. The higher reaction temperature gave a higher conversion rate of FFA.

Six kinetic models were proposed to fit the data as shown in Eqs. (3-1) – (3-6). The least relative absolute error (RAE) method was applied for finding the suitable model. RAE values were estimated using Eqs. (3-7). The summation of RAE and Arrhenius parameters of each model were shown in Table 3-1.

Experimental data—concentration of methanol, FAME and water—estimated based on FFA concentration material balance and predicted data of each equation (Eqs. (3-1) – (3-6)) were calculated by ASPEN PLUS simulation.

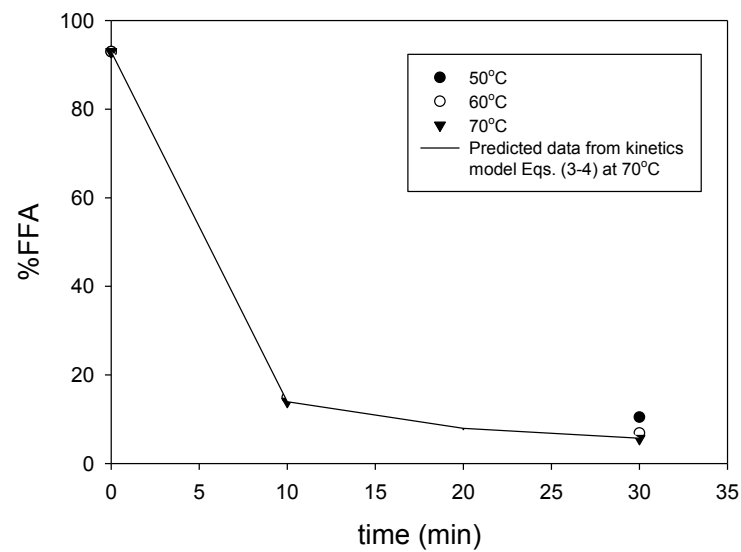


Fig. 3-1 Effect of temperature on FFA content (molar ratio of methanol to PFAD 8 : 1).

$$r = k_f [\text{FFA}] \quad (3-1)$$

$$r = k_f [\text{FFA}][\text{methanol}] \quad (3-2)$$

$$r = k_f [\text{FFA}] - k_b [\text{FAME}] \quad (3-3)$$

$$r = k_f [\text{FFA}] - k_b [\text{FAME}][\text{water}] \quad (3-4)$$

$$r = k_f [\text{FFA}][\text{methanol}] - k_b [\text{FAME}] \quad (3-5)$$



$$r = k_f [\text{FFA}][\text{methanol}] - k_b [\text{FAME}][\text{water}] \quad (3-6)$$

$k_f$  forward reaction kinetic constant;

$k_b$  backward reaction kinetic constant.

$$\text{RAE} = \sum \left| \frac{\text{exp} - \text{cal}}{\text{exp}} \right| \quad (3-7)$$

exp experimental value;

cal calculated value.

**Table 3-1** Arrhenius parameters and summation of absolute error of each model.

Model	A	$E_a$ (kJ/mol)	$A_b$	$E_{a_b}$ (kJ/mol)	RAE	$R^2$
Eqs. (3-1)	6.47	18.772	-	-	1.1938	0.7272
Eqs. (3-2)	0.61	18.781	-	-	1.0091	0.7323
Eqs. (3-3)	6.47	18.772	1952.82	49.869	1.0176	0.7480
Eqs. (3-4)	6.82	18.772	50.01	38.126	0.9742	0.7718
Eqs. (3-5)	6.46	18.547	14.63	20.199	2.6799	0.1332
Eqs. (3-6)	5.99	19.239	13.30	21.324	2.6675	0.2142

These results showed Eqs (3-4) had the least RAE or least deviation. Fig. 3-2 indicated that predicted data and experimental data of FFA mass fraction were hardly different; this model could be used to predict the reaction rate. Thus, Eqs (3-4)

was selected for next simulation work. It could be expressed in the forms of palmitic acid and oleic acid as written in Eqs. (3-8) and (3-9), and they were assumed which rate of disappearing of palmitic acid and oleic acid were equal. The forward reaction order was a pseudo first order that respect on FFA, while methanol concentration was assumed which it was excess and constant corresponding to Yadav et al. work (2010) [15]. The backward reaction order was the second order that respect on FAME and water. Besides, these results had similar results with preliminary study.

$$r = k_f [\text{palmitic acid}] - k_b [\text{methyl palmitate}][\text{water}] \quad (3-8)$$

$$r = k_f [\text{oleic acid}] - k_b [\text{methyl oleate}][\text{water}] \quad (3-9)$$

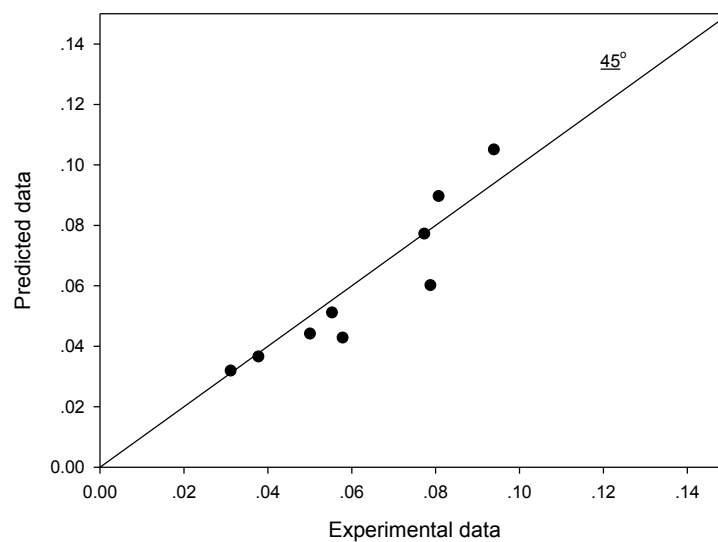


Fig. 3-2 Predicted data versus experimental data parity plot (from Eqs. (3-8) and (3-9)).

### 3.2 Steady state process simulation

The biodiesel production process was simulated by ASPEN PLUS V8.4. Thermodynamic package Dortmund modified UNIFAC was employed to obtain the activity coefficients and other properties because the polar components in the process were methanol and glycerol [9, 11-13, 16-18, 21]. The PFAD chemical content consisting of 53.75 wt% palmitic acid, 39.25 wt% oleic acid and 7 wt% triolein was assumed.

All of unit operations of this process and process flow diagram were presented in Fig. 3-6, and process stream data was shown in Table 3-2. The process consists of esterification, transesterification, purification, and recovery sections. Entire volumes of liquid in this process are specified at 50% liquid holdup, partially filled.

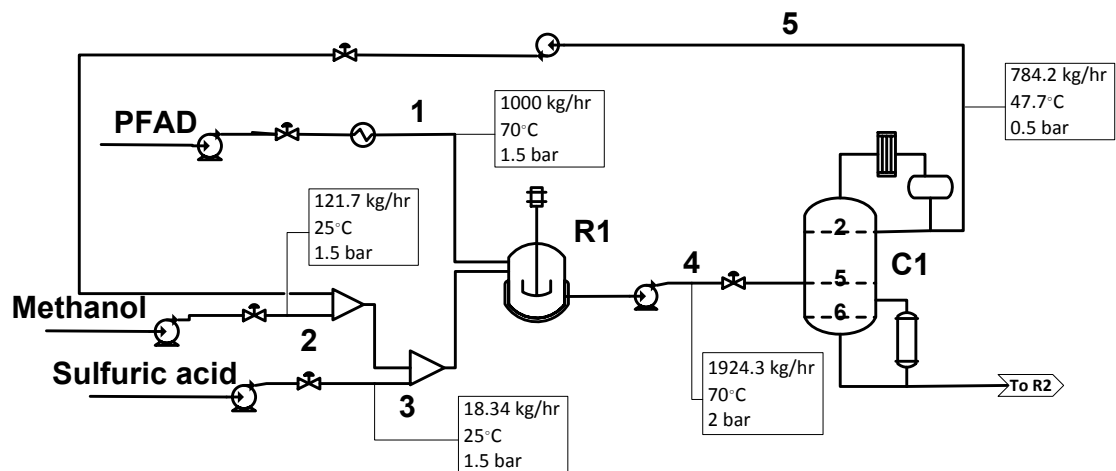


Fig. 3-3 Biodiesel production from PFAD process  
(esterification and methanol recovery I).

### 3.2.1 Esterification

1000 kg/hr PFAD and sulfuric acid in methanol were fed into the esterification reactor (R1) at the optimum operating conditions: a reaction temperature of 70°C, retention time 60 min, and a molar ratio of PFAD to methanol 1:8. FFA from PFAD was converted to FAME using the kinetic parameters from previous work data. This unit was shown in Fig. 3-3.

### 3.2.2 Methanol recovery I

The excess methanol was recovered using the first vacuum distillation column (C1) which the bottom temperature under was kept under 100°C. The seven-stage column (minimum 6) which the first stage was condenser, and the 7<sup>th</sup> stage was reboiler was operated at 9.16 of a mass reflux ratio (minimum 0.42), 0.5 bar of condenser pressure, and all reactants were fed above the 5<sup>th</sup> stage to achieve 99.5% of methanol purity in a recycle stream back to the R1. This unit was shown in Fig. 3-3.

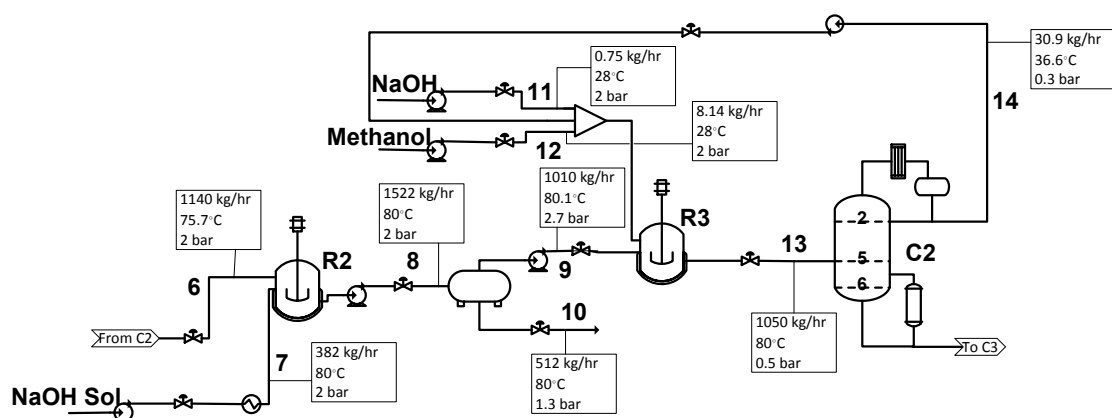


Fig. 3-4 Biodiesel production from PFAD process

(neutralization, transesterification and methanol recovery II).

### 3.2.3 Neutralization

The esterified mixture was fed into the second reactor (R2) for neutralization. Therefore, 20 weight% of 3 M of Sodium hydroxide solution reacted with both sulfuric acid (esterification catalyst) and remain FFA. Neutralization was operated at a temperature of 80°C for 15 min. The mixture of neutralization was separated by a decanter. The upper phase that was FAME rich phase and lower phase was a water rich phase. This unit was shown in Fig. 3-4.

### 3.2.4 Transesterification

FAME rich phase was fed into the transesterification reactor (R3). For transesterification, triglyceride reacts with methanol in a present of sodium hydroxide as catalyst. The 99% triolein conversion was assumed. Operating conditions were reaction temperature of 80°C, retention time 15 min, and 3.85 weight% of 0.396 M sodium hydroxide in methanol solution of the neutralized stream. This unit was shown in Fig. 3-4.

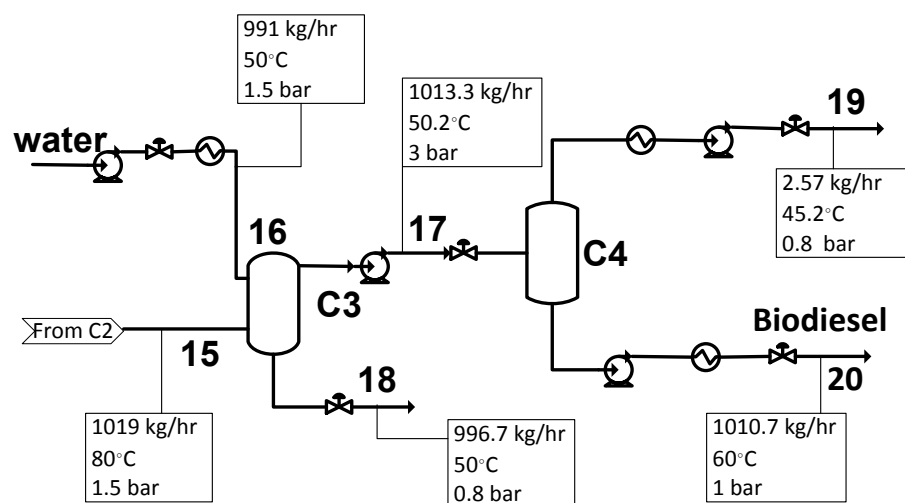


Fig. 3-5 Biodiesel production from PFAD process (water washing and flash drum).

### 3.2.5 Methanol recovery II

The second vacuum distillation column (C2) was necessary for the methanol recovery process after neutralization. The seven-stage column (minimum 2) that the first stage was condenser, and the 7<sup>th</sup> stage was reboiler was operated at 3.11 of a mass reflux ratio (minimum 0.1), 0.3 bar pressure of condenser, and the mixture was fed above the 5<sup>th</sup> stage to achieve 99.5% of methanol purity in a recycle stream back into the R3. This unit was shown in Fig. 3-4.

### 3.2.6 Water washing (liquid – liquid extraction)

The transesterified product was washed using 50°C of water in order to remove the impurities and undesired products. Finally, the washed FAME was flashed to remove residual water at 100°C and 0.1 bar for meeting the biodiesel standard. These units were shown in Fig. 3-5.



Table 3-2 Data of biodiesel production from PFAD simulation (cont).

Stream No.	8	9	10	11	12	13	14
Molar flow (kmol/hr)	27.38	3.38	24.00	0.02	0.25	4.62	0.96
Mass flow (kg/hr)	1522.04	1010.08	511.96	0.75	8.14	1049.87	30.90
Vol. flow (m <sup>3</sup> /hr)	1.92	1.32	0.47	0.00	0.01	1.33	0.04
Temperature (°C)	80.09	80.12	80.01	28.12	28.23	80.05	36.59
Pressure (bar)	2	2.7	1.3	2	2	0.5	0.3
Mass fraction							
Oleic acid	0.000	0.000	0.000	0.000	0.000	0.000	0.000
Palmitic acid	0.000	0.000	0.000	0.000	0.000	0.000	0.000
Triolein	0.046	0.069	0.000	0.000	0.000	0.001	0.000
Methanol	0.010	0.000	0.031	0.000	1.000	0.030	0.995
Methyl Oleate	0.356	0.537	0.000	0.000	0.000	0.583	0.000
Methyl Palmitate	0.261	0.394	0.000	0.000	0.000	0.379	0.000
Water	0.268	0.000	0.795	0.000	0.000	0.000	0.000
NaOH	0.015	0.000	0.045	1.000	0.000	0.001	0.005
H <sub>2</sub> SO <sub>4</sub>	0.000	0.000	0.000	0.000	0.000	0.000	0.000
Na <sub>2</sub> SO <sub>4</sub>	0.000	0.000	0.000	0.000	0.000	0.007	0.000
Na-oleate	0.017	0.000	0.052	0.000	0.000	0.000	0.000
Na-palmitate	0.015	0.000	0.044	0.000	0.000	0.000	0.000





R1: Esterification reactor

R2: Neutralization reactor

C2: Methanol recovery column II

C4: Flash drum

C1: Methanol recovery column I

R3: Transesterification reactor

C3: Water washing column

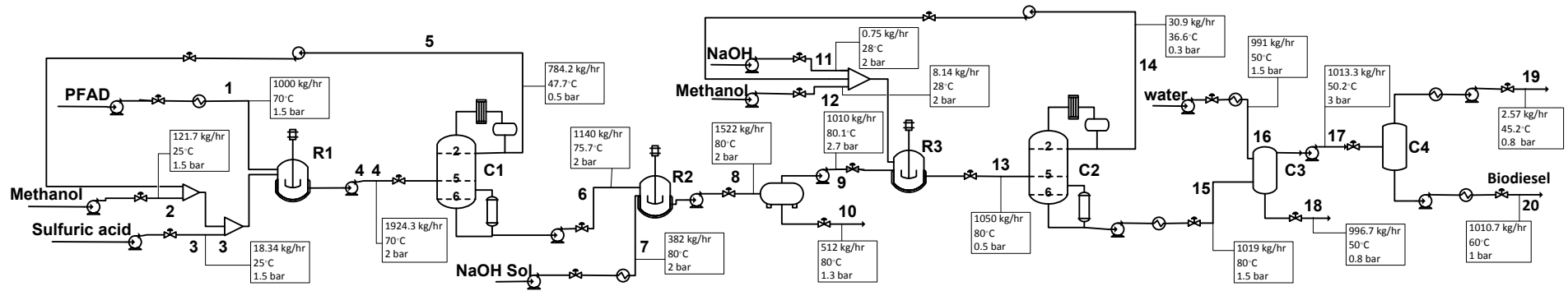


Fig. 3-6 Biodiesel production from PFAD process (entire the process).

### 3.3 Dynamics simulation and control

The control system was requisite to eliminate disturbance and other changes in the production process. Moreover, unit operations had to be controlled to the desire conditions. So two control structures including conventional and on demand control structures were proposed in this work.

#### 3.3.1 Conventional control structure (CS I)

The plantwide control strategy was applied to this structure [2, 24]; therefore, the design procedures were

- 1) The control objectives of this process were
  1. The biodiesel product quality was higher than 96.5% as reported by TIS 2005 [7].
  2. The esterification reactor feed molar ratio of PFAD to methanol had to be 1 : 8
  3. The temperatures of all streams, especially at reboilers, were not over the decomposition temperature of biodiesel (275<sup>o</sup>C) [25].
- 2) The number of control degrees of freedom for biodiesel production process control was shown in Table 3-3.

**Table 3-3** Control degrees of freedom for biodiesel production process from PFAD.

Unit operation	Control valves available	Degrees of freedom
Esterification reactor (R1)	Fresh feed of PFAD, methanol, and sulfuric acid; reactor heater; outlet stream; PFAD feed heater	6
Methanol recovery column I (C1)	Distillate and bottom stream; reflux stream; heater of condenser and reboiler	5
Neutralization reactor (R2)	Sodium hydroxide solution stream and heater; reactor heater; outlet stream;	4
Decanter	Upper and lower phase stream	2
Transesterification reactor (R3)	Fresh feed of sodium hydroxide and methanol; reactor heater; outlet stream	4
Methanol recovery column II (C2)	Distillate and bottom stream; heater of condenser and Reboiler; outlet stream heater	5
Water washing column (C3)	Water feed stream; heater of water stream; top and bottom stream	4
Flash drum (C4)	Top and bottom stream; Heater of drum, top, and bottom stream;	5
Total		35

3) Since biodiesel production from PFAD process was low temperature operation. Esterification and transesterification were endothermic reactions, so the heat duty of reactors required enough to keep the reaction temperatures to the desired temperatures using directly heated heaters, and the complex heat exchanger network may not be required.

4) The PFAD flow rate was dominating variable which increased reactor holdup. Because the esterification was not aggressive reaction and sensitive to heat, the reaction temperature was hardly impacted the reaction conversion. Other variables in the reactor shall be selected instead of reactor temperature. The flow rate of PFAD dominating variable increases reactor holdup and could indirectly control production rate. Hence, it was selected for setting production rate.

5) Biodiesel quality must be maintained at least 96.5%. The water washing unit was used for removing methanol, catalyst, and other impurities. Water fed to wash the reaction mixture should have enough volume being equal a quantity of biodiesel. After that, the residual water in biodiesel was flashed out from the product.

6) Flow rate should be fixed in all recycle loops. In first recycle loop, it had a high reflux ratio (more than 4); the distillate flow rate was controlled to handle reflux ratio. Another recycle loop, this distillation column had a moderate reflux ratio; the reflux flow rate was fixed, and level of the reflux drum was controlled by manipulating a distillate flow rate.

Three pressures were controlled: in the two distillation columns and in a flash drum. Two pressure controls of distillation columns were achieved by manipulating heat removal of condenser unit. Pressure of flash drum was controlled by changing vapor product flow rate.

For liquid level control, all of the liquid levels were controlled by manipulating the effluent flow.

7) Unconverted FFA and sulfuric acid feed stream were eliminated in neutralization reactor and removed at the bottom stream of settling drum. Methanol in the first step of reaction, it was removed in the bottom stream of settling drum; in the second step methanol was removed in the bottom stream of water washing column. The inventory of biodiesel was accounted for via level control in methanol column II sump receiver, and the purity of biodiesel was controlled by temperature and quantity of water washing and temperature of flash drum.

8) Several control valves remain unassigned. Heaters were used for controlling temperatures of the reactor, preheated stream, and other units and streams. PFAD, fresh feed methanol, sulfuric acid, sodium hydroxide solution, and washing water were controlled by flow controller.

9) The regulatory strategy had been established as shown in Fig. 3-7, and set of controlled and manipulated variables was shown in Table 3-4. According to S. Chongkhong et al. [4], the setpoints of the process in this work were optimized.

**Table 3-4** Controlled and manipulated variables of control structure I.

Unit operation	Controlled variable	Manipulated variable
Esterification reactor (R1)	Temperature	Reactor duty
	Level	Effluence flow rate
	Flow into reactor	PFAD flow rate
	Methanol and sulfuric acid feed ratios	Methanol and sulfuric acid flow rates
Methanol recovery column I (C1)	5 <sup>th</sup> stage temperature	Reboiler duty
	Sump level	Bottom flow rate
	Condenser pressure	Condenser duty
	Reflux ratio	Distillate flow rate
	Reflux drum level	Reflux flow rate

Table 3-4 Controlled and manipulated variables of control structure I (cont).

Neutralization reactor (R2)	Temperature	Reactor duty
	Level	Effluence flow rate
	Sodium hydroxide solution feed ratio	Sodium hydroxide solution flow rate
Decanter	Upper phase level	Upper phase effluence flow rate
	Lower phase level	Lower phase effluence flow rate
Transesterification reactor (R3)	Temperature	Reactor duty
	Level	Effluence flow rate
	Sodium hydroxide and methanol feed ratios	Sodium hydroxide and methanol flow rates
Methanol recovery column II (C2)	5 <sup>th</sup> stage temperature	Reboiler duty
	Sump level	Bottom flow rate
	Condenser pressure	Condenser duty
	Reflux drum level	Distillate flow rate
	Bottom flow temperature	Cooler duty

Table 3-4 Controlled and manipulated variables of control structure I (cont).

Water washing column (C3)	Washing water temperature	Heater duty
	Water feed ratio	Water flow rate
	Upper phase level	Upper phase effluence flow rate
	Lower phase level	Lower phase effluence flow rate
Flash drum (C4)	Temperature	Column duty
	Level	Effluence liquid flow rate
	Pressure	Effluence vapor flow rate

### 3.3.2 On demand control structure (CS II)

In this structure, the biodiesel flow rate was controlled with the setpoint of flow controller coming from demand of biodiesel. Levels were controlled in the opposite direction from flows that was called reverse direction to flow [2]. When the biodiesel production rate was changed, the responses of flow rates were changed back through the process sequentially. There were nine steps of plantwide process control design procedure similar to CS I as shown below.

- 1) The control objectives of this process were
  1. The biodiesel product quality was higher than 96.5% as reported by TIS 2005 [7].
  2. The biodiesel production rate was controlled by flow controller and set on the demand.



3. The temperature of any streams and especial at reboilers was not over the decomposition temperature of biodiesel.
- 2) The same number of degrees of freedoms exist that were 35.
- 3) The energy management system was same CS I.
- 4) Production rate was set by the bottom stream of flash drum that was biodiesel production flow rate.
- 5) The water washing unit and flash drum controlled product purity which was equal or above 96.5%.
- 6) For liquid level control, all of the liquid levels were controlled by manipulating the influent flow that had to use the level controller in the reverse direction to flow strategy [2].
- 7) The purity of biodiesel was controlled by temperature and quantity of water washing and temperature of flash drum like the previous structure.
- 8) Individual unit operations control was set up, and all of control valves had been assigned as shown in Fig 3-8.
- 9) Setpoints and conditions of the unit operations were used the optimized data that were similar CS I setpoints, and set of controlled and manipulated variables was shown in Table 3-5.

Table 3-5 Controlled and manipulated variables of control structure II.

Unit operation	Controlled variable	Manipulated variable
Esterification reactor (R1)	Temperature	Reactor duty
	Level	PFAD flow rate
	Methanol and sulfuric acid feed ratios	Methanol and sulfuric acid flow rates
Methanol recovery column I (C1)	5 <sup>th</sup> stage temperature	Reboiler duty
	Sump level	Influent flow rate
	Condenser pressure	Condenser duty
	Reflux ratio	Distillate flow rate
	Reflux drum level	Reflux flow rate
Neutralization reactor (R2)	Temperature	Reactor duty
	Level	Influent flow rate
	Sodium hydroxide solution feed ratio	Sodium hydroxide solution flow rate
Decanter	Upper phase level	Upper phase influent flow rate
	Lower phase level	Lower phase effluence flow rate

Table 3-5 Controlled and manipulated variables of control structure II (cont).

Transesterification reactor (R3)	Temperature	Reactor duty
	Level	Influent flow rate
	Sodium hydroxide and methanol feed ratios	Sodium hydroxide and methanol flow rates
Methanol recovery column II (C2)	5 <sup>th</sup> stage temperature	Reboiler duty
	Sump level	Influent flow rate
	Condenser pressure	Condenser duty
	Reflux drum level	Distillate flow rate
	Bottom flow temperature	Cooler duty
Water washing column (C3)	Washing water temperature	Heater duty
	Water feed ratio	Water flow rate
	Upper phase level	Upper phase influent flow rate
	Lower phase level	Lower phase effluence flow rate
Flash drum (C4)	Temperature	Column duty
	Level	Influent flow rate
	Pressure	Effluence vapor flow rate
	Biodiesel production rate	Effluence liquid flow rate

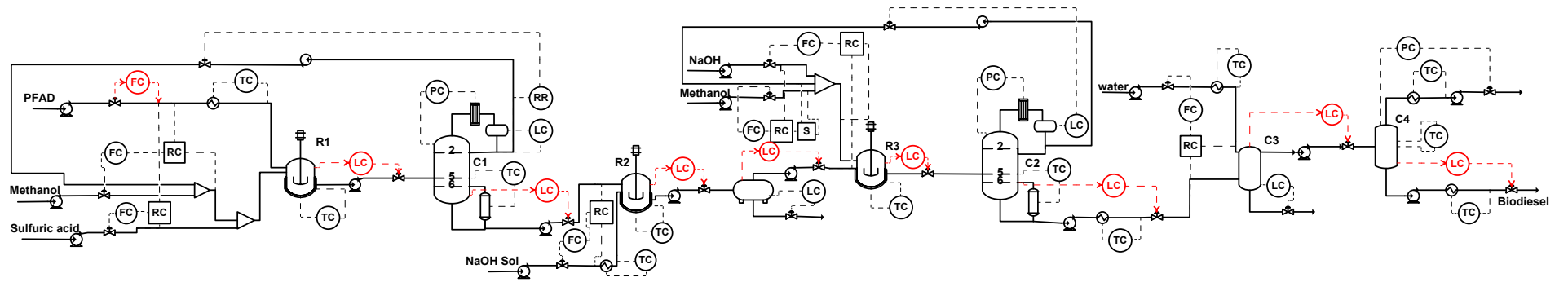


Fig. 3-7 Control structure I (PFAD feed flow rate control).

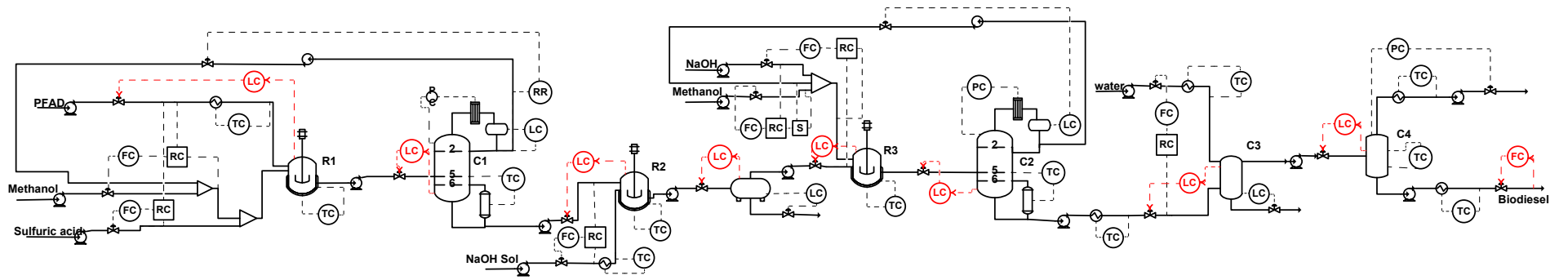


Fig. 3-8 Control structure II (Production flow rate control).

### 3.3.3 Selection of temperature control tray

Two methanol recovery columns used tray temperature control instead of composition control because it was faster response and cheaper than composition control. Large change in temperature from tray to tray in the column indicated that tray could be selected for controlling the temperature. The temperature profiles at steady state of methanol recovery I and II are shown in Fig. 3-9 and Fig. 3-10, respectively.

In Fig. 3-9 and Fig. 3-10, the slopes of temperature profile were the steepest around trays 5 or 6, so the effect of changes in column reboiler duty ( $\pm 10\%$ ) was used to confirm a selecting tray. Fig. 3-11 and Fig. 3-12 show the temperature profiles changing the most from tray to tray at the 5<sup>th</sup> tray for both columns, even though the C1 shows less sensitive than C2 since the C2 had less methanol than C1. Therefore, these trays were selected as a tray temperature control.

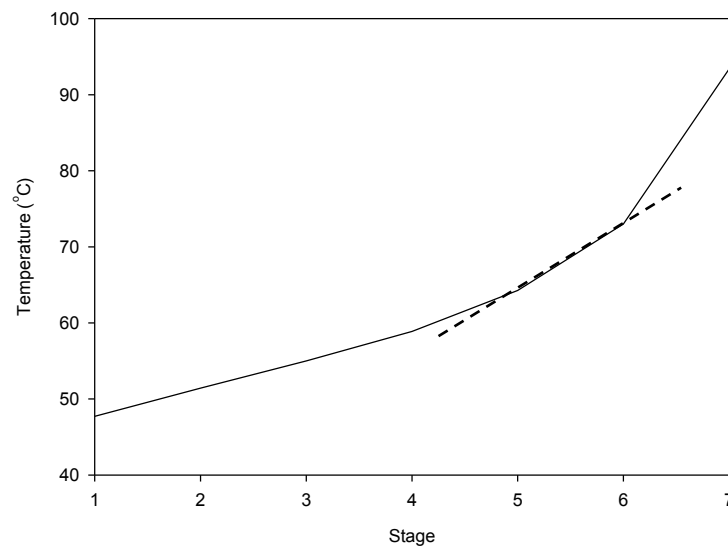


Fig. 3-9 Temperature profile of methanol recovery column I.

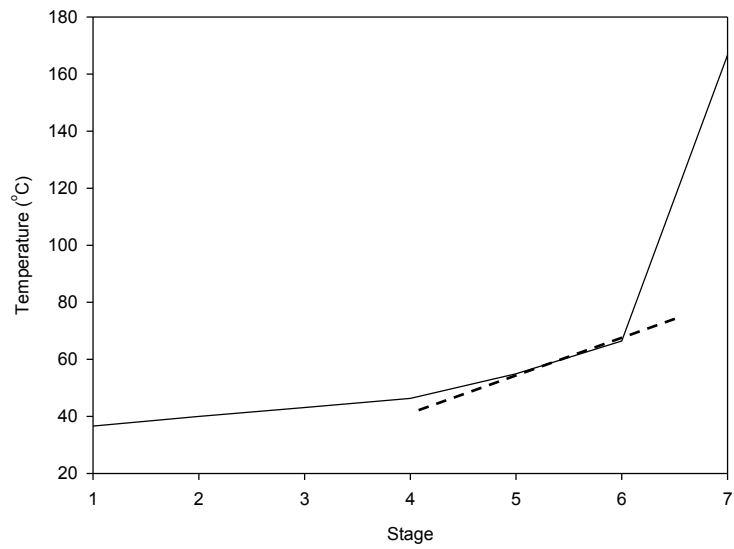


Fig. 3-10 Temperature profile of methanol recovery column II.

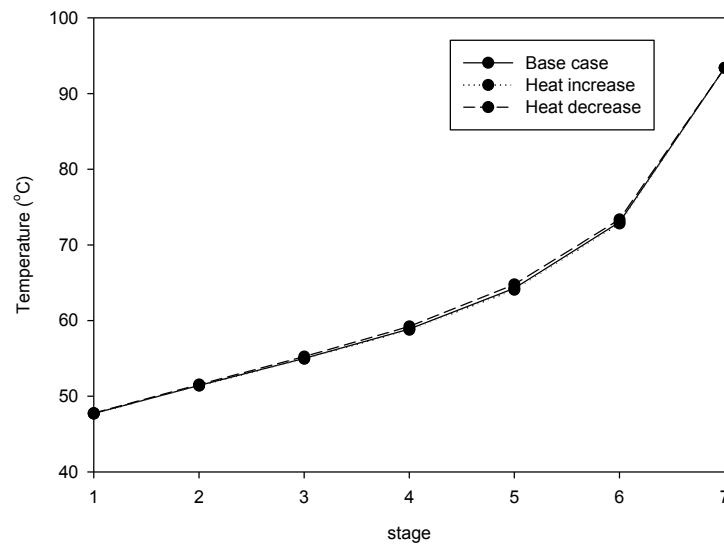


Fig. 3-11 Effect of changes in column boilup  $\pm 10\%$  on temperature profile of column I.

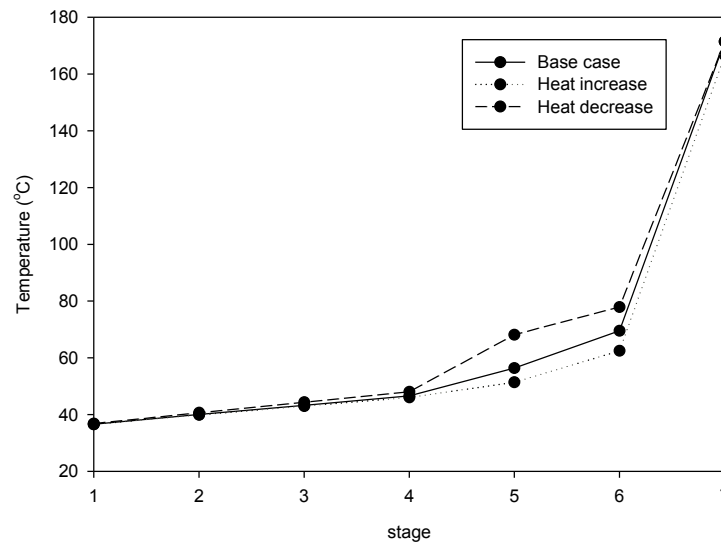


Fig. 3-12 Effect of changes in column boilup  $\pm 10\%$  on the temperature profile of column II.

### 3.3.4 Controller tuning

After the control structures had been established; the controllers were tuned using ATV to obtain the ultimate gain and frequency of the temperature closed loops. Two different tuning methods which were TL and ZN were applied to calculate PI controller parameters. Moreover, temperature measurement was assumed as a 2-first order with 0.5 min lag model or  $\left(\frac{e^{-0.5s}}{\tau s + 1}\right)^2$  [24]. PI temperature controller parameters for control structure I and II were shown in Table 3-6 and Table 3-6, respectively. On the other hand, flow, pressure and level control parameters were used heuristic values [24]. Flow and pressure controllers were PI controllers. Flow controller had  $K_c = 0.5$ ,  $\tau_i = 0.3$  min. Pressure controller had  $K_c = 2$ ,  $\tau_i = 10$  min. And level controllers were P controllers which were  $K_c = 2$  for normal liquid level and  $K_c = 10$  for liquid level-sensitive level such as reactors, reflux drums.



Table 3-6 and Table 3-7 show gains and integral time constants for all controllers of control structure I and II, respectively. They were found that the controller gains of both structures were rarely different. However, they had some control loops that gave the different gains. Since the objectives of two control structures were opposite, the responses of control loops — temperatures of the 5<sup>th</sup> tray distillation column I, transesterification reactor temperature and 5<sup>th</sup> tray temperature of distillation column II — were different.

Table 3-6 Controller settings for control structure I.

Controlled variable	Manipulated variable	TL		ZN	
		$K_c$	$\tau_I$ (min)	$K_c$	$\tau_I$ (min)
PFAD feed	Heat duty	42.52	13.2	61.87	5
R1	Reactor duty	2.27	13.2	2.83	5
Tray 5 <sup>th</sup> of C1	Reboiler duty	1.56	2.64	2.15	1.5
Sodium hydroxide feed to R2	Heat duty	3.29	13.2	18.1	1.5
R2	Reactor duty	7.51	13.2	10.97	5
R3	Reactor duty	90.08	13.2	135.11	5
Tray 5 <sup>th</sup> of C2	Reboiler duty	3.21	18.48	4.39	7
Bottom stream of C2	Heat duty	7.51	2.64	13.0	1
Water feed to C3	Heat duty	8.59	7.92	15.14	3.5
C4	Heat duty	2.83	15.84	4.06	6.5
Bottom stream of C4	Heat duty	3.57	6.6	5.19	2.5
Top stream of C4	Heat duty	1.06	2.64	2.93	1

Table 3-7 Controller settings for control structure II.

Controlled variable	Manipulated variable	TL		ZN	
		$K_c$	$\tau_I$ (min)	$K_c$	$\tau_I$ (min)
PFAD feed	Heat duty	42.52	13.2	61.85	5
R1	Reactor duty	2.44	11.88	3.53	4.5
Tray 5 <sup>th</sup> of C1	Reboiler duty	3.89	2.64	5.53	1
Sodium hydroxide feed to R2	Heat duty	4.08	3.96	5.37	2.5
R2	Reactor duty	6.73	13.2	9.87	5
R3	Reactor duty	34.15	13.2	87.77	3.5
Tray 5 <sup>th</sup> of C2	Reboiler duty	10.98	26.4	15.92	10
Bottom stream of C2	Heat duty	5.19	7.92	13.29	3
Water feed to C3	Heat duty	9.37	9.24	13.90	3
C4	Heat duty	2.68	15.84	3.96	6
Bottom stream of C4	Heat duty	3.53	6.6	5.10	2.5
Top stream of C4	Heat duty	0.70	3.96	3.83	2

### 3.3.5 Control robustness

#### 1) PFAD feed flow rate change

The increased and decreased feed flow rate dynamic responses which the controllers were tuned by TL and ZN methods. The fresh feed PFAD into the esterification reactor was increased from 1000 kg/hr to 1100 kg/hr and decreased from 1000 kg/hr to 900 kg/hr at 0.5 hr ( $\pm 10\%$  of setpoint) as shown in Fig. 3-13 (a). This change was applied to control structure I only, the control structure II did not have flow control in feed stream.

The PFAD feed rate changing affected on fresh feed methanol and other feed streams (Fig. 3-13 (b-f)) due to the controllers had to keep the ratios reaching to the setpoint.

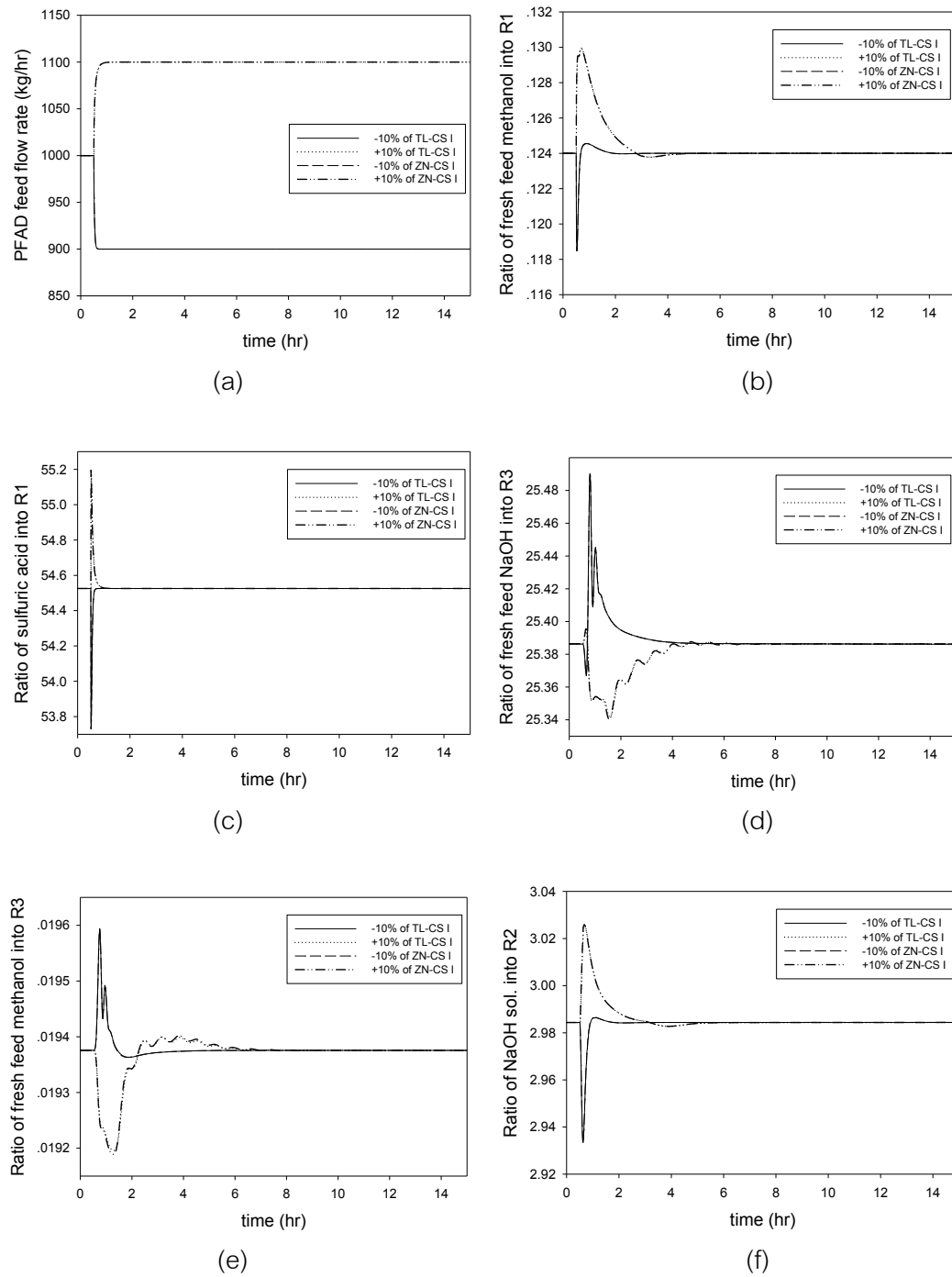


Fig. 3-13 Flow dynamic responses of TL and ZN-tuned control structure I for PFAD feed rate change.

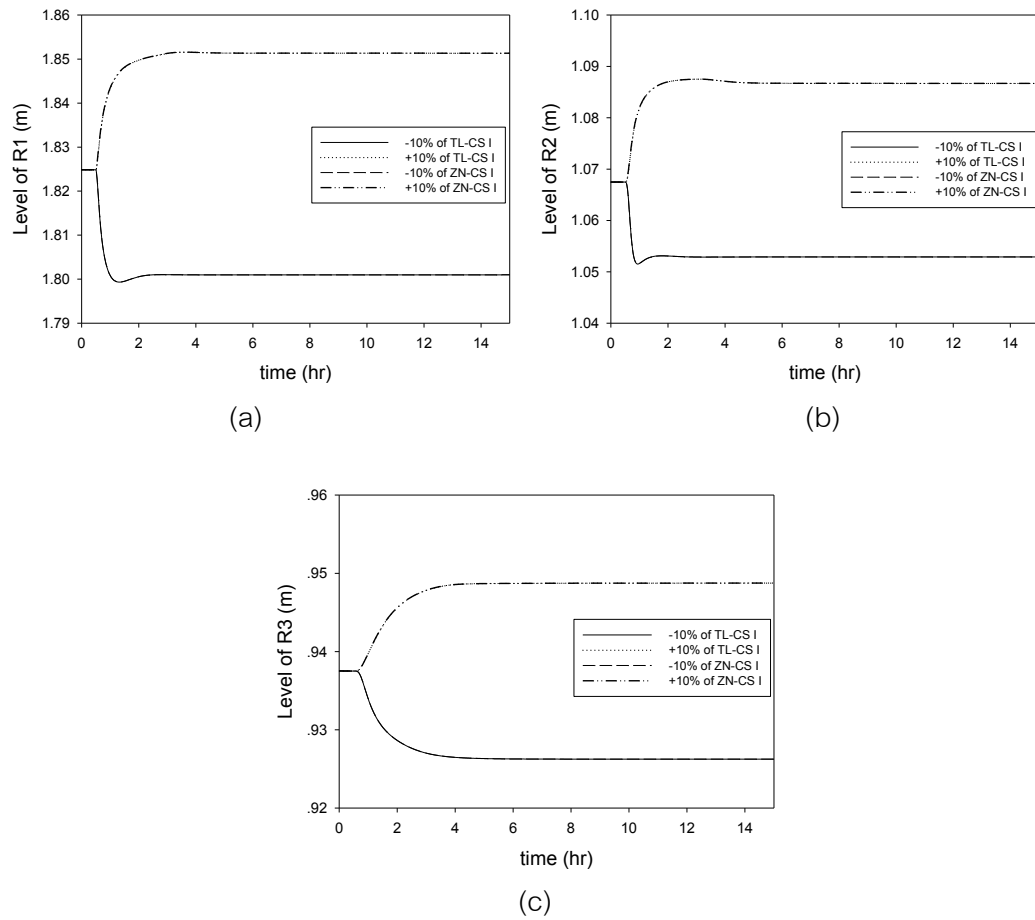


Fig. 3-14 Level dynamic responses of TL and ZN-tuned control structure I for PFAD feed rate change.

Level controls were gotten that effect also as shown in Fig. 3-14 (a-c). The level responses had offset because of effect of P controller.

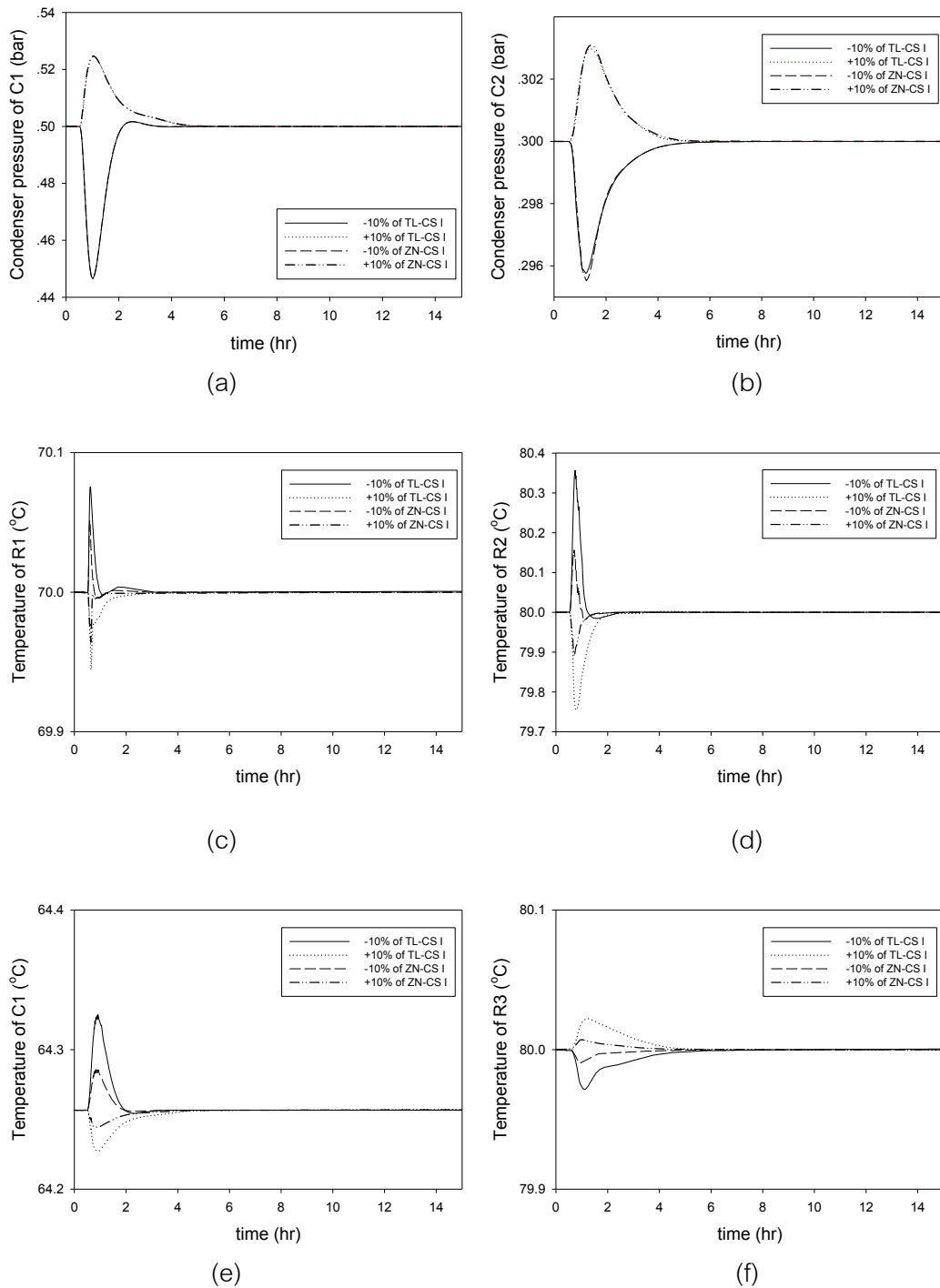


Fig. 3-15 Pressure and temperature dynamic responses of TL and ZN-tuned control structure I for PFAD feed rate change.

The pressure (Fig. 3-15 (a, b)) and temperature (Fig. 3-15 (c-f)) responses had small change indicated that PFAD feed rate had less effect on them since the temperature and pressure controllers had fast response to adjust the manipulated variables.

The Dynamic responses of the control system tuned by ZN method gave similar results as the TL method, while ZN setting gave the lower overshoot. Overall responses of control structure I for PFAD feed rate change, the process variables reached to steady state within 4 hr. The product specifications still met the standard.

## 2) Temperature of esterification reactor change

The reactor temperature of esterification reaction was changed from primary setpoint  $70^{\circ}\text{C}$  to  $80^{\circ}\text{C}$  and from primary setpoint  $70^{\circ}\text{C}$  to  $60^{\circ}\text{C}$  as shown in Fig. 3-16 (a) and Fig. 3-19 (a) for control structure I and II, respectively.

This temperature changing affected on nearly units that were distillation column I and neutralization reactor. They had small variation and could settle to set value immediately as shown in Fig. 3-16 (b-e). Furthermore, the TL setting provided quite oscillatory responses.

For responses of flow in control structure I, Fig. 3-17 (a-d) were the results of process streams ratios that were controlled to reach the setpoint.

Fig. 3-17 (e-f) were the pressure responses in control structure I. They showed the pressure controllers could handle the temperature change.



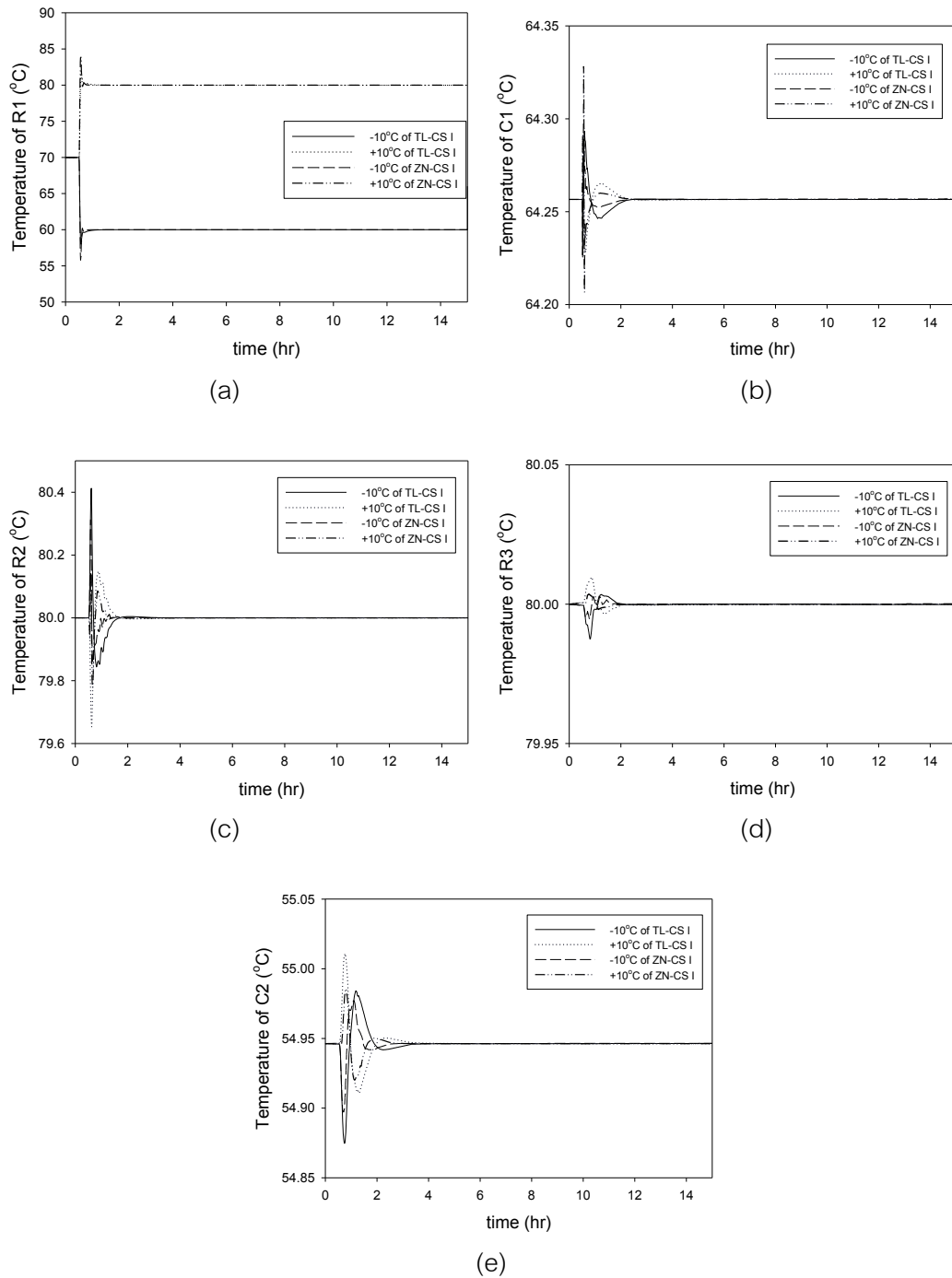


Fig. 3-16 Temperature dynamic responses of TL and ZN-tuned control structure I for R1 temperature change.

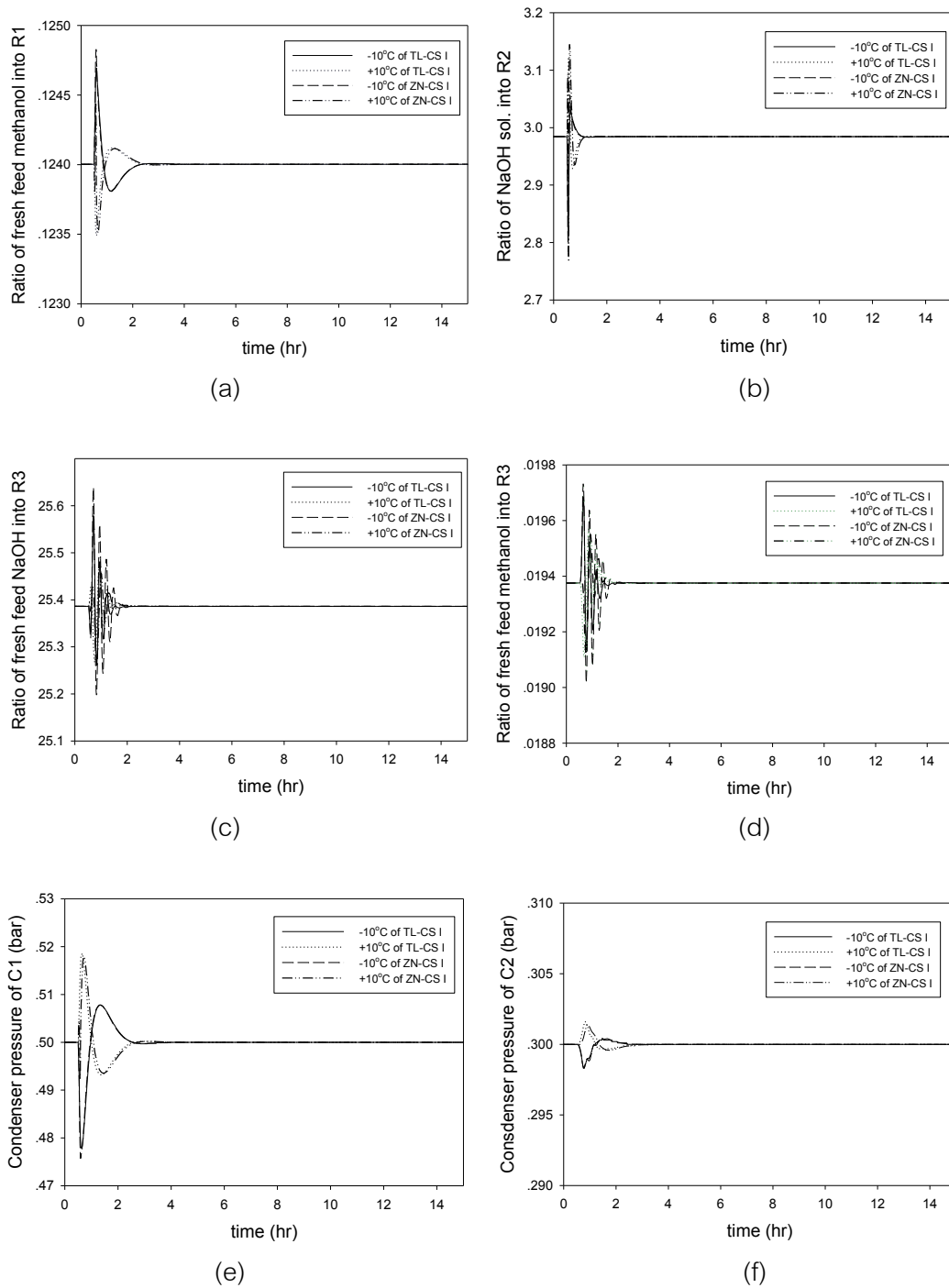


Fig. 3-17 Flow and pressure dynamic responses of TL and ZN-tuned control structure I for R1 temperature change.

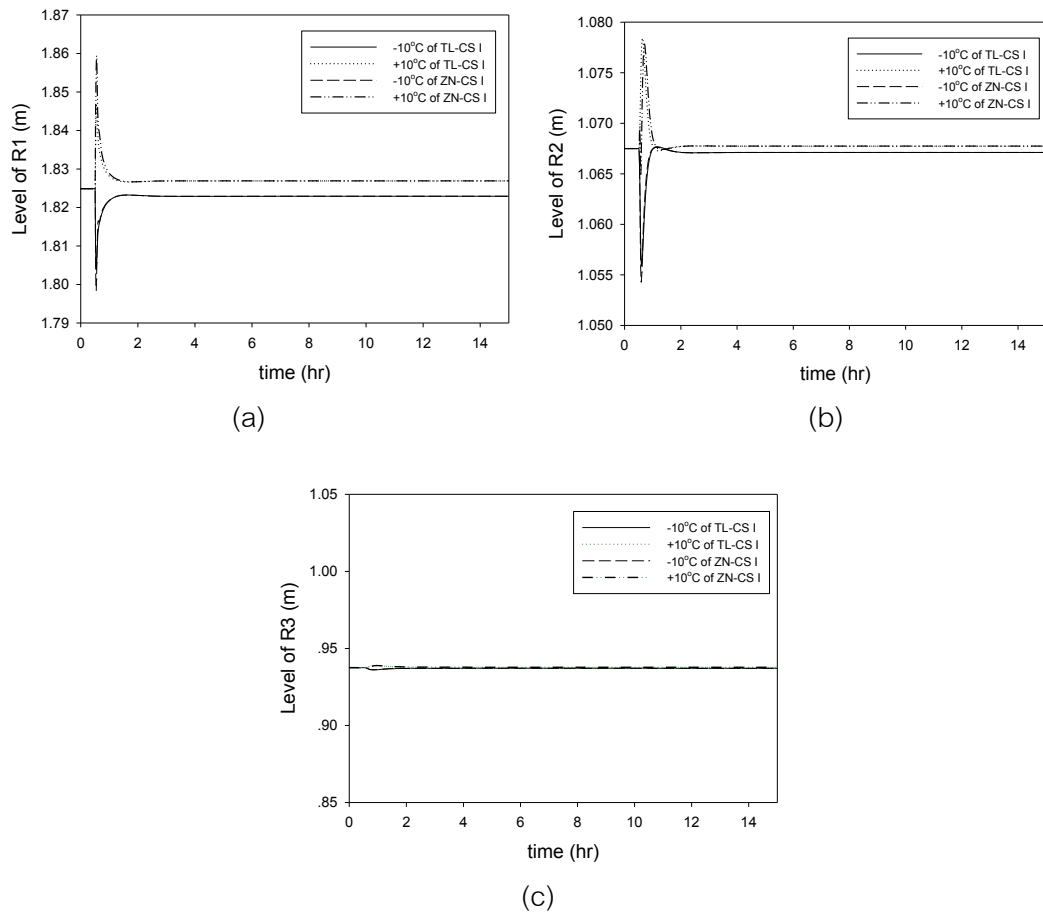


Fig. 3-18 Level dynamic responses of TL and ZN-tuned control structure I for R1 temperature change.

The level dynamic responses were shown in Fig. 3-18 (a-c). The level controller could keep the process variables to reach the setpoint with their offset. However, the small level offset could be neglected, and the process still achieved setpoints.

For control structure II, esterification reactor temperature change gave the effect on process variables less than control structure I as shown in Fig. 3-19 (c, e) compared with Fig. 3-16 (c, e).

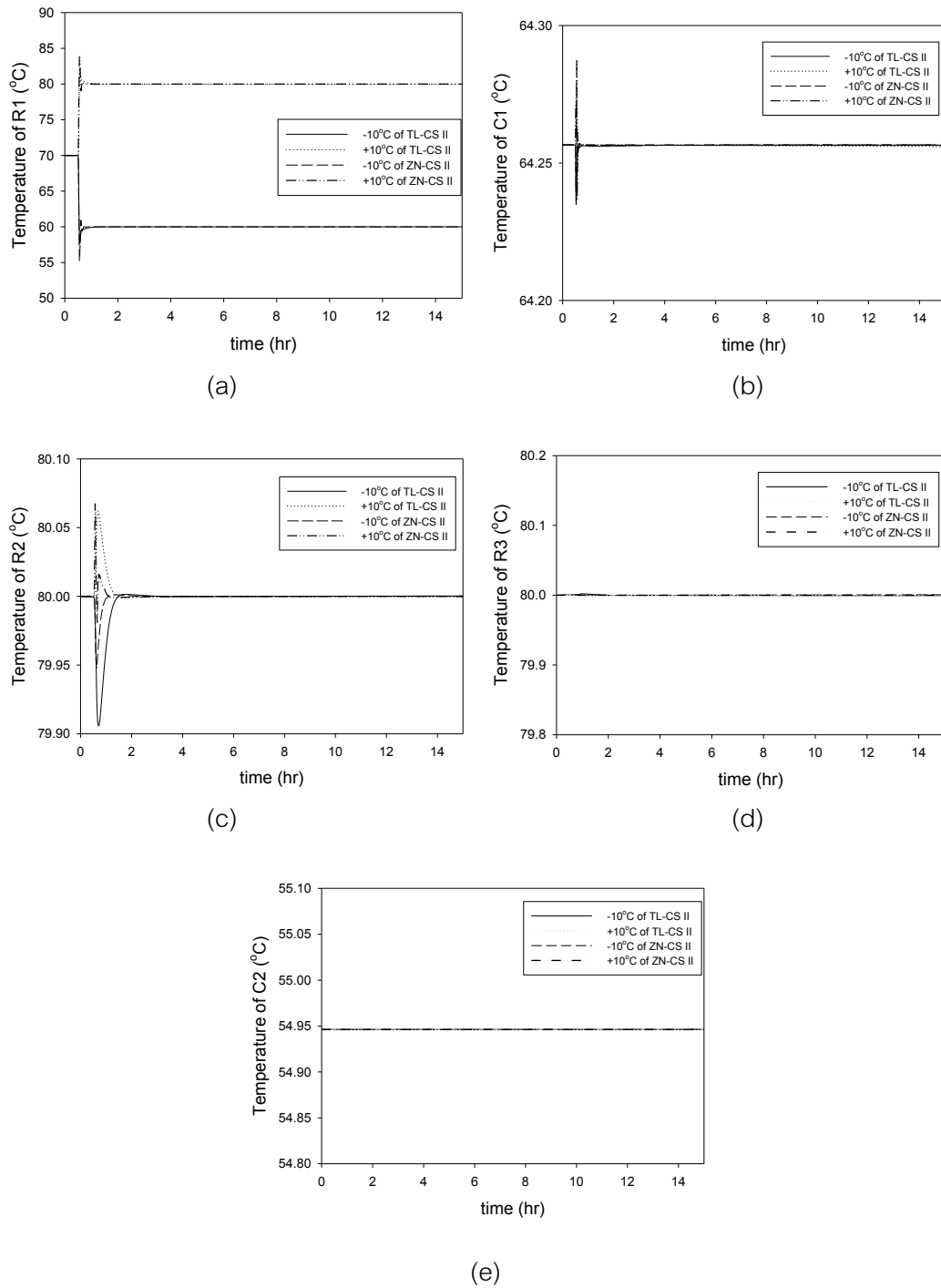


Fig. 3-19 Temperature dynamic responses of TL and ZN-tuned control structure II for R1 temperature change.

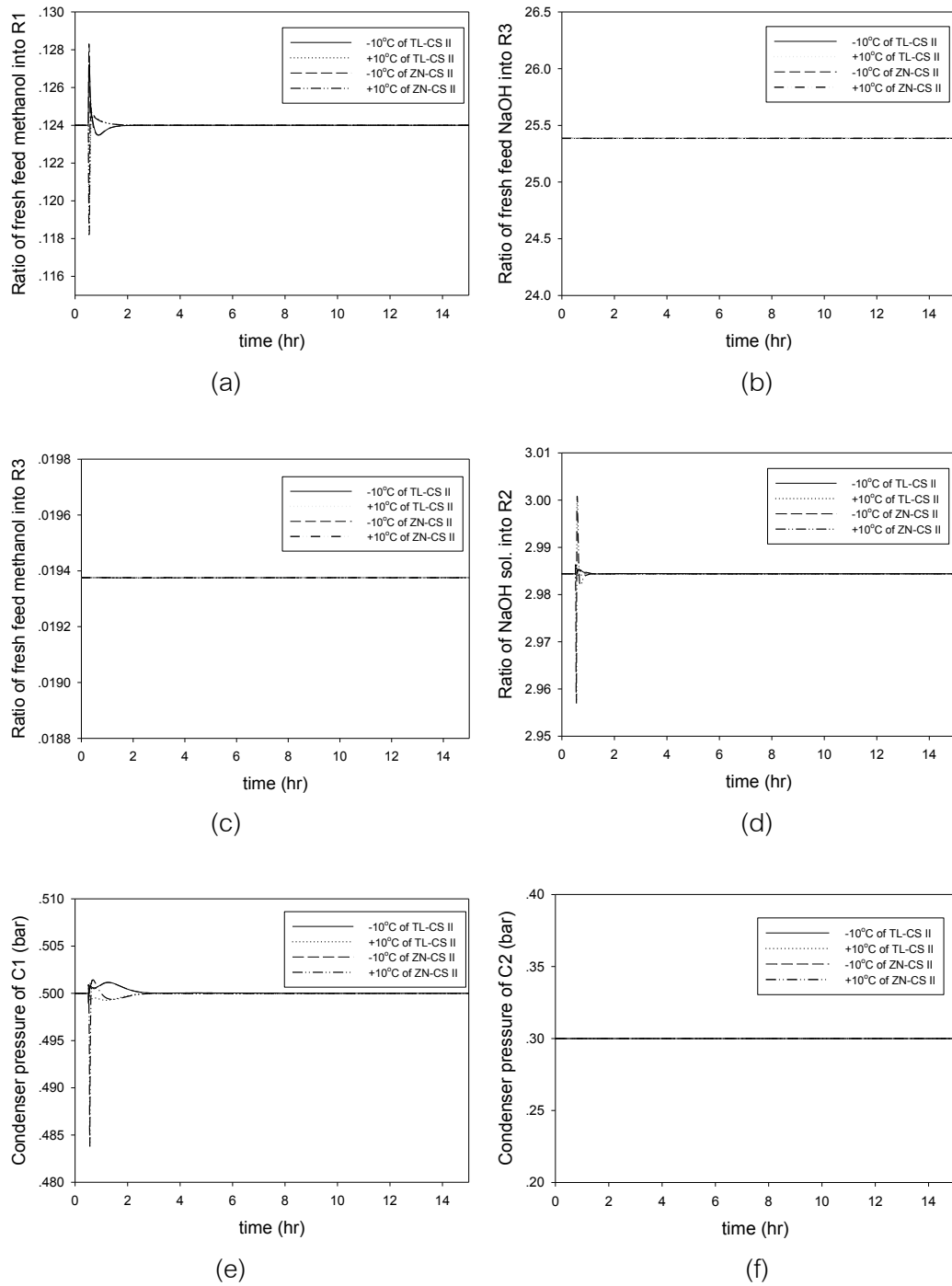


Fig. 3-20 Flow and pressure dynamic responses of TL and ZN-tuned control structure II for R1 temperature change.

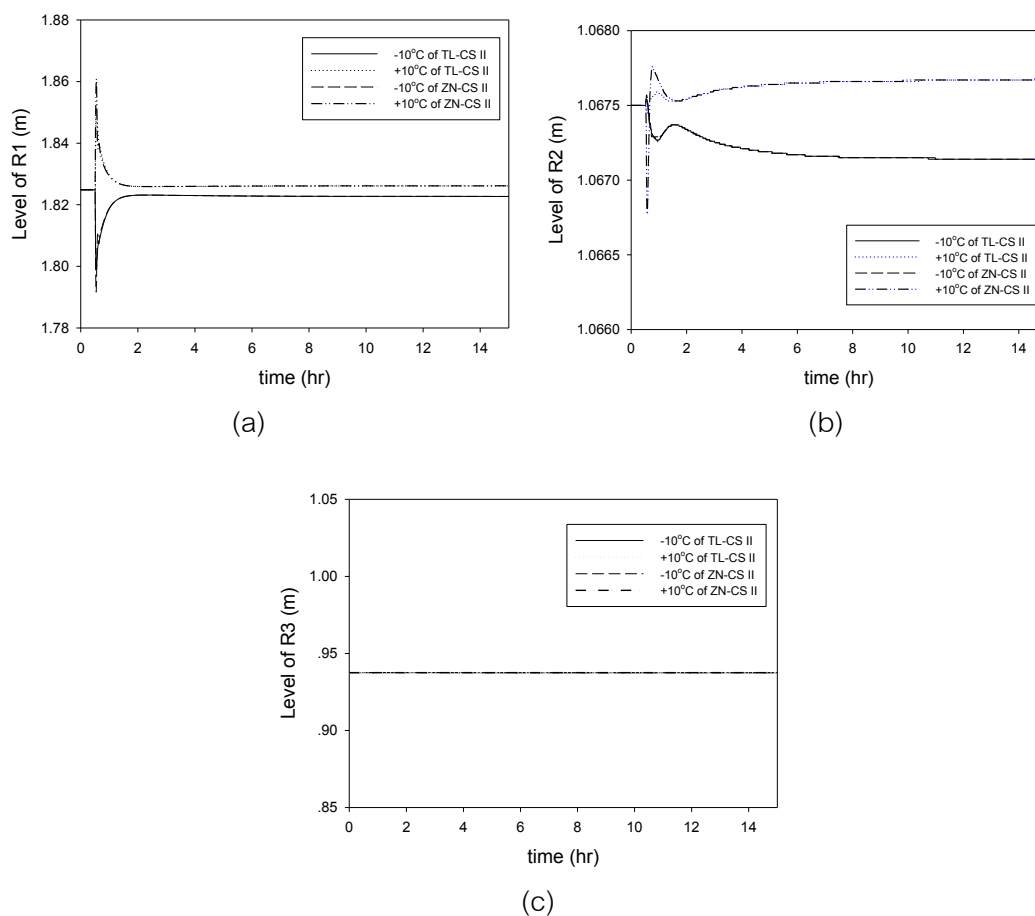


Fig. 3-21 Level dynamic responses of TL and ZN-tuned control structure II for R1 temperature change.

The temperature dynamic responses when the esterification reactor temperature changed were shown in Fig. 3-19 (a-e).

The dynamic responses when the esterification reactor temperature changed of flow and pressure controllers were shown in Fig. 3-20 (a-d) and Fig. 3-20 (e, f), respectively. In addition, the TL tuned level responses were shown in Fig. 3-21 (a-c).

The temperature of reactor change mainly impacted on control structure I more than control structure II. However, the temperature changing of esterification reactor that had less effect on other process variables because temperature controllers in both control structures were tight installed. Increasing temperature resulted in

reaction conversion had a slightly increasing value as well as decreasing temperature that the conversion tiny decreased.

### 3) FFA content in PFAD change

The FFA content in PFAD was increased from 93% to 98 % and decreased from 93% to 92%.

For control structure I, Fig. 3-22 (a-e), Fig. 3-23 (a-d), Fig. 3-23 (e, f) and Fig. 3-24 (a-c) showed the process dynamic responses of PFAD composition change for temperature, flow, pressure, and level controllers that were tuned employing TL and ZN tuning method. The results informed that the uncertain composition of PFAD rarely affected to process variables, and the controllers had fast response to move the process variables back to the setpoint. The responses of TL tuned temperature controllers had overshoot more than ZN tuned controllers.

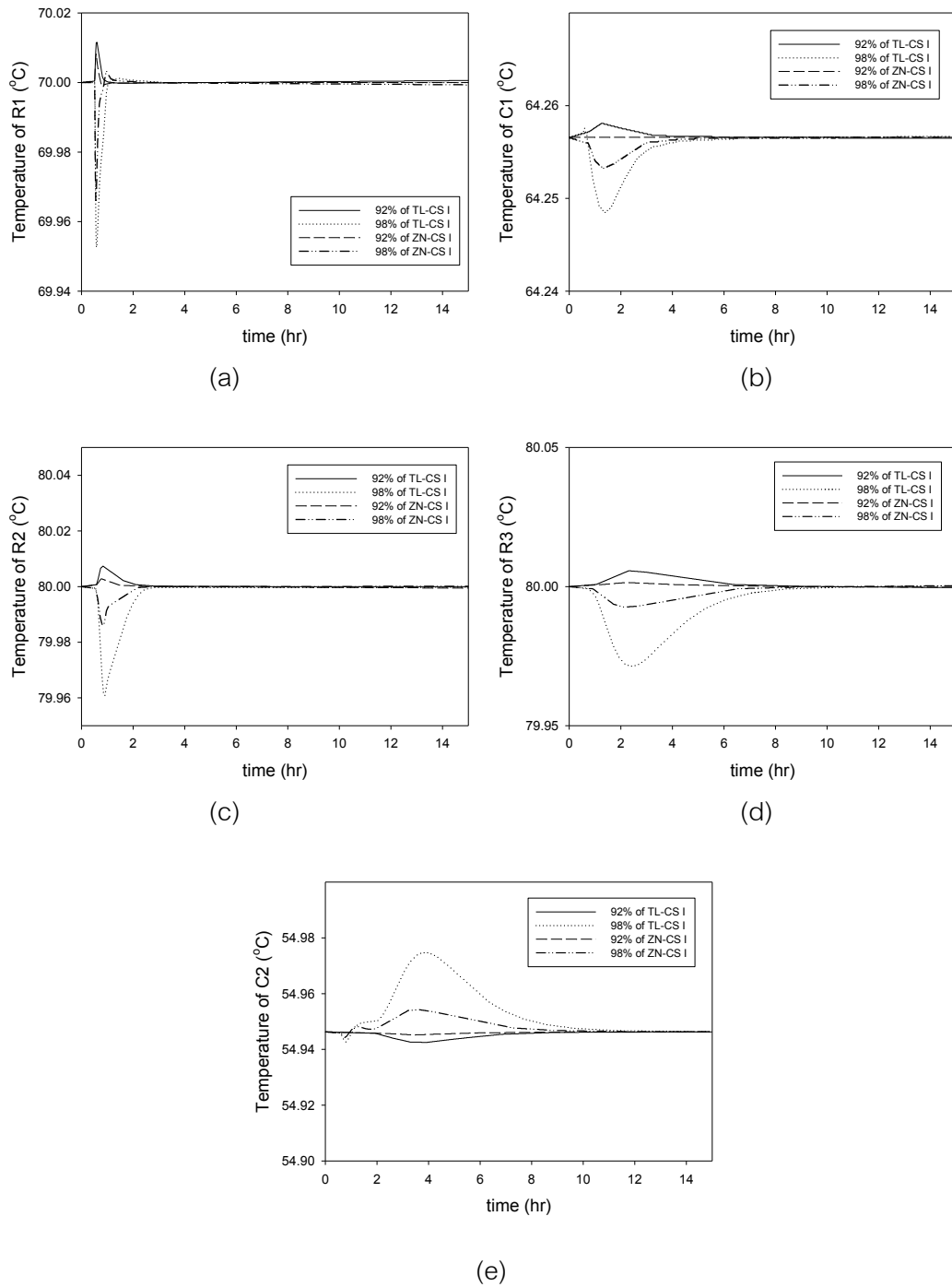


Fig. 3-22 Temperature dynamic responses of TL and ZN-tuned control structure I for FFA in PFAD change.



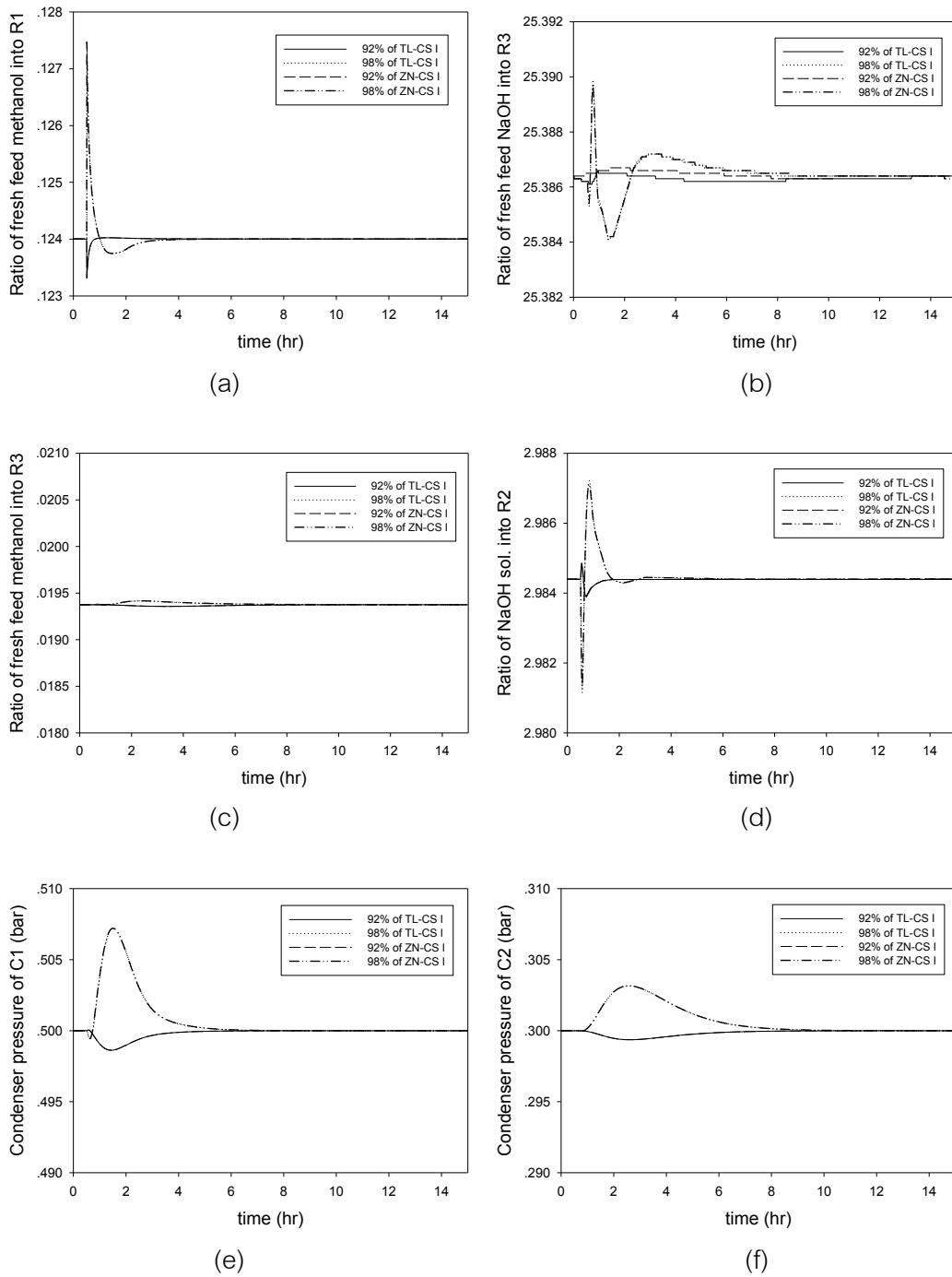


Fig. 3-23 Flow and pressure dynamic responses of TL and ZN-tuned control structure I for FFA in PFAD change.

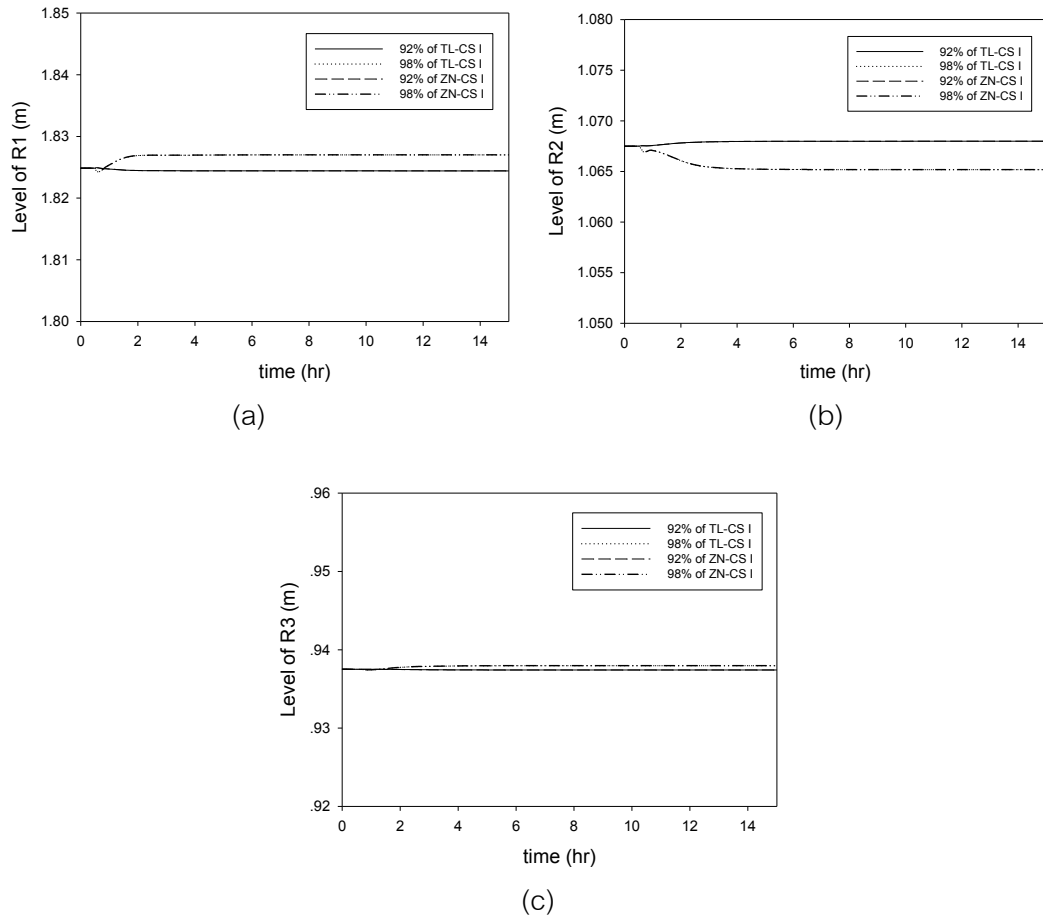


Fig. 3-24 Level dynamic responses of TL and ZN-tuned control structure I for FFA in PFAD change.

For control structure II, Fig. 3-25 (a-e), Fig. 3-26 (a-d), Fig. 3-26 (e, f) and Fig. 3-27 (a-c) displayed the process dynamic responses of temperature, flow, pressure, and level controllers for PFAD composition change.

The all results indicated the changing of the PFAD compositions had slightly effect to all process variables. Thus, the control structures could reject this disturbance that was uncertain FFA content in feed stock in a range of 92% - 98%, and the biodiesel specification had still accepted.

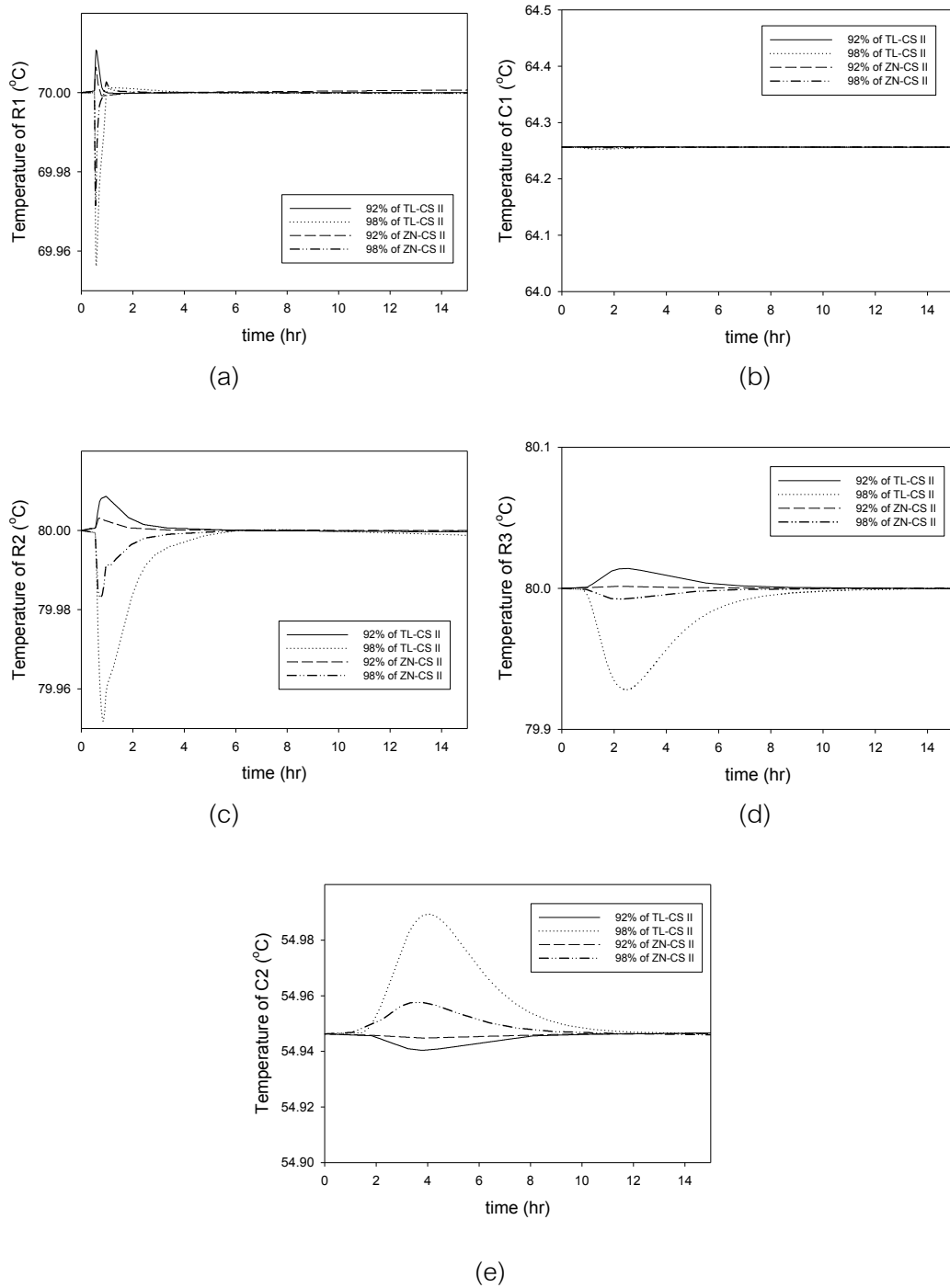


Fig. 3-25 Temperature dynamic responses of TL and ZN-tuned control structure II for FFA in PFAD change.

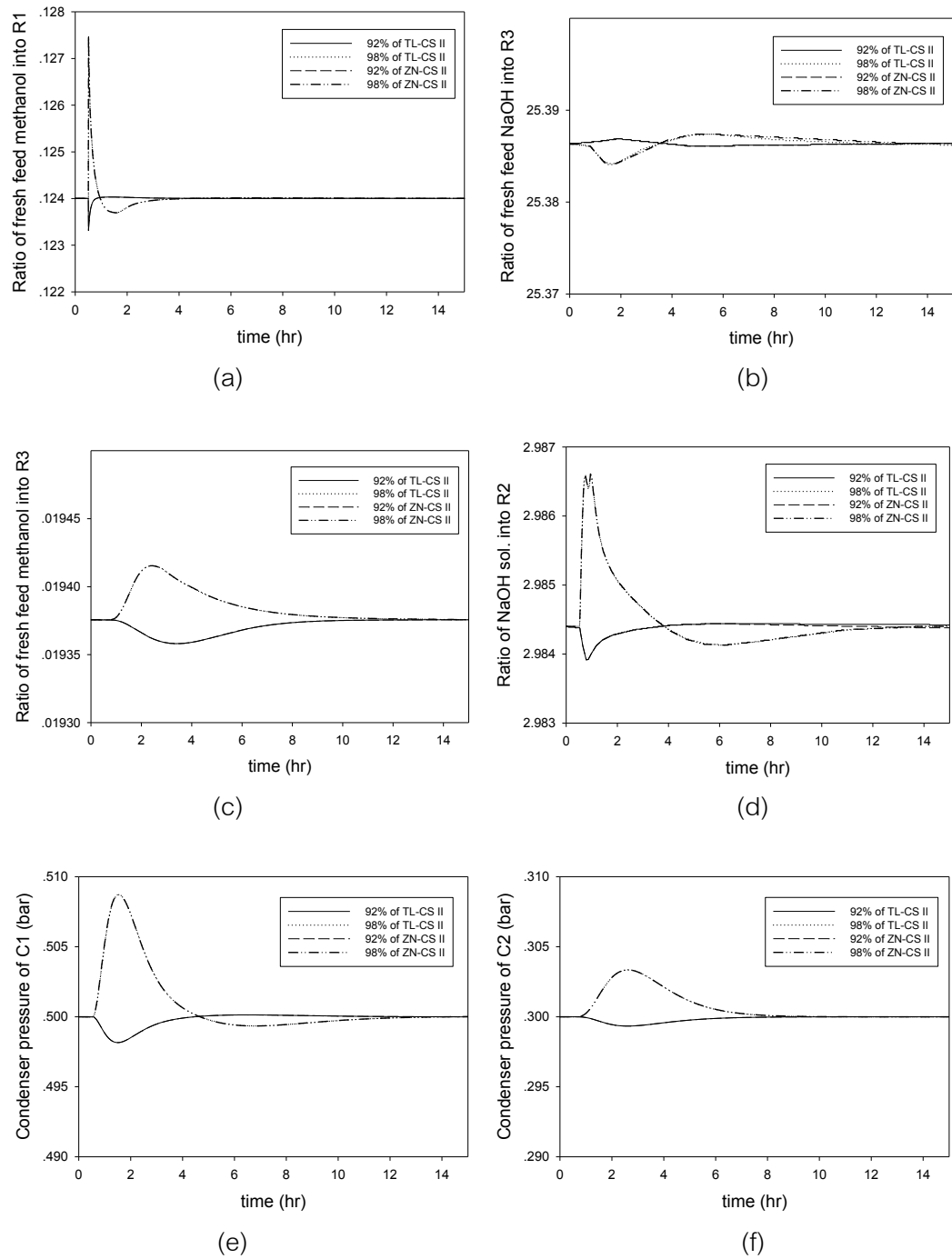


Fig. 3-26 Flow and pressure dynamic responses of TL and ZN-tuned control structure II for FFA in PFAD change.

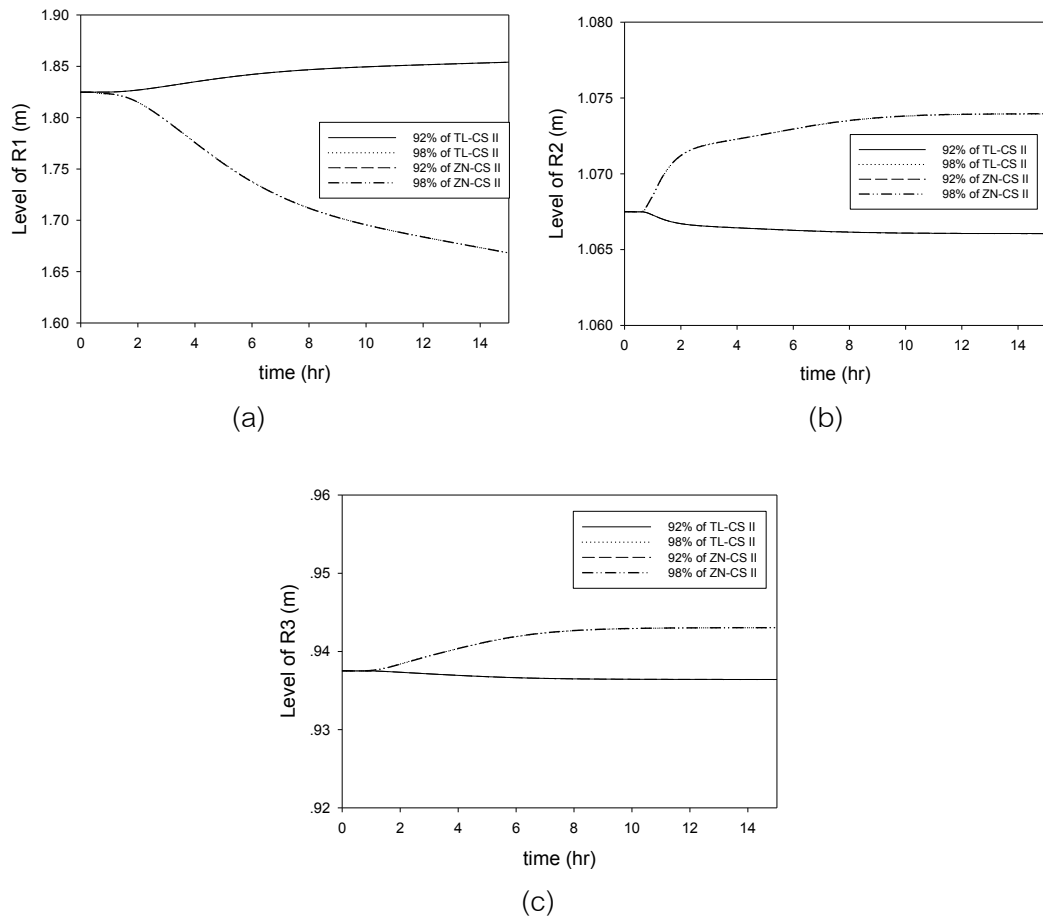


Fig. 3-27 Level dynamic responses of TL and ZN-tuned control structure II for FFA in PFAD change.

#### 4) Biodiesel production rate change

The biodiesel production rate was changed from 1010.7 kg/hr to 1111.8 kg/hr (+10%) and from 1010.7 kg/hr to 909.6 kg/hr (-10%) as shown in Fig. 3-28 (a). This testing was applied on control structure II only.

For flow controllers, the dynamic response results were displayed in Fig. 3-28 (b-f).

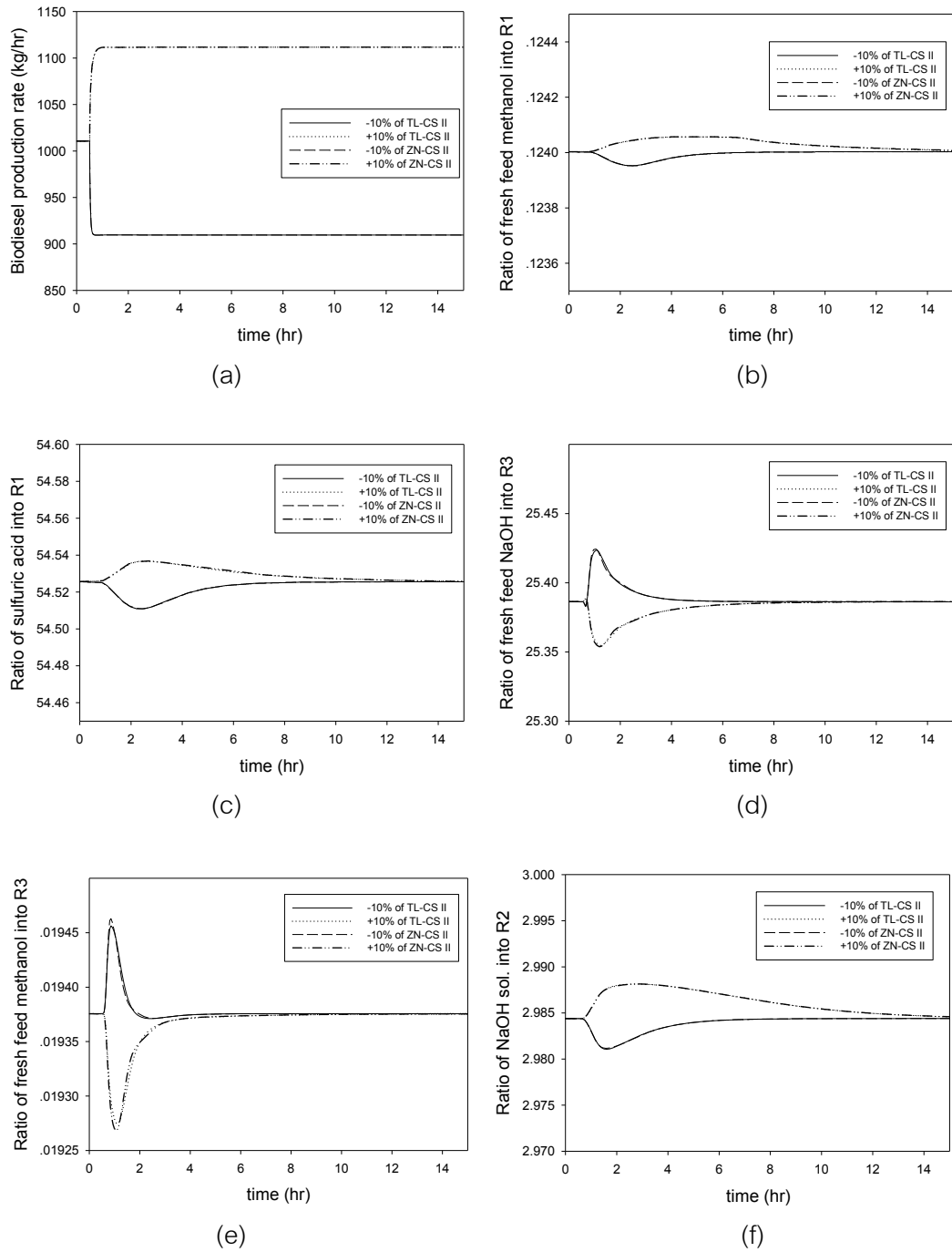


Fig. 3-28 Flow dynamic responses of TL and ZN-tuned control structure II for production rate change.

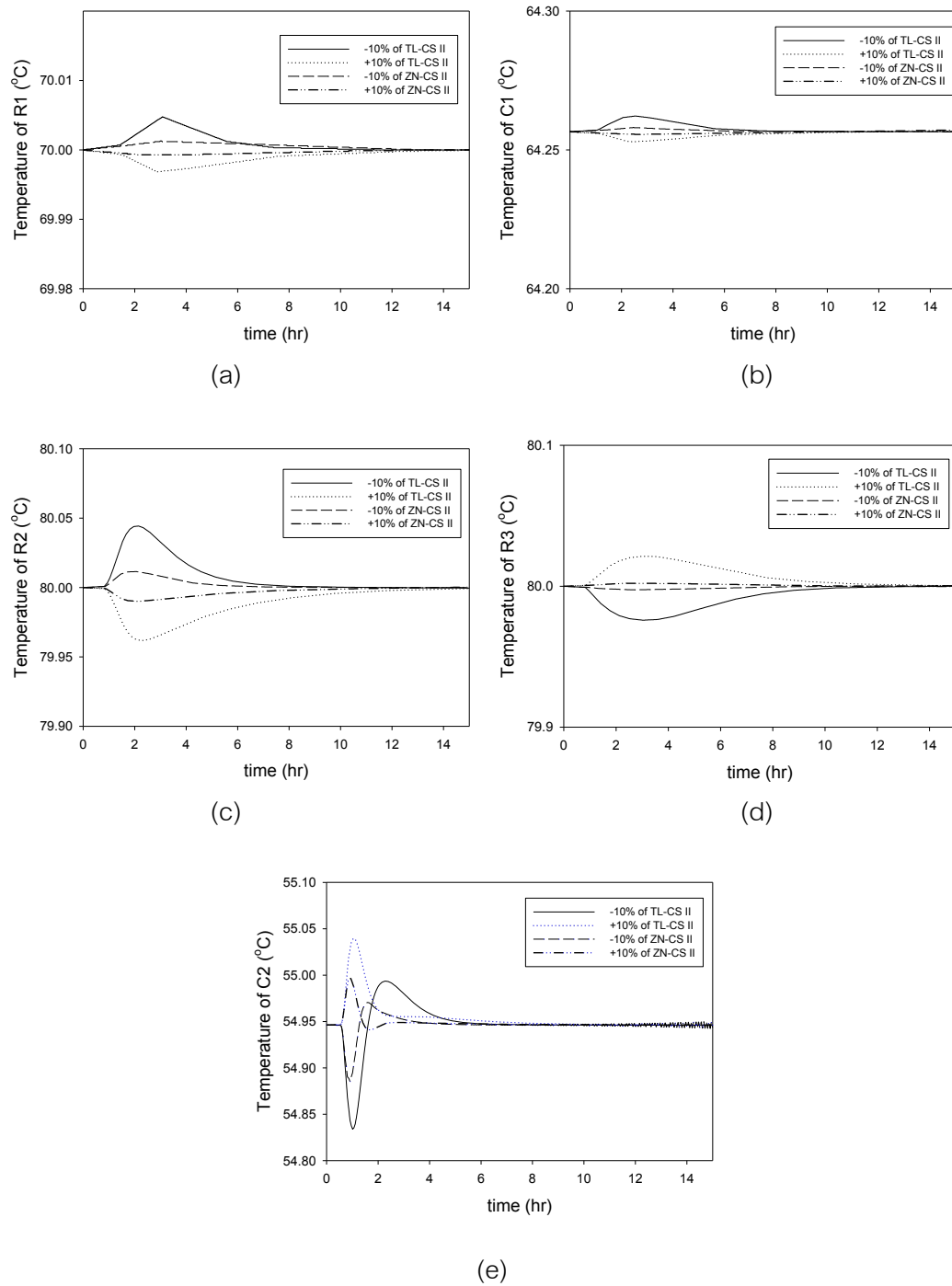


Fig. 3-29 Temperature dynamic responses of TL and ZN-tuned control structure II for production rate change.

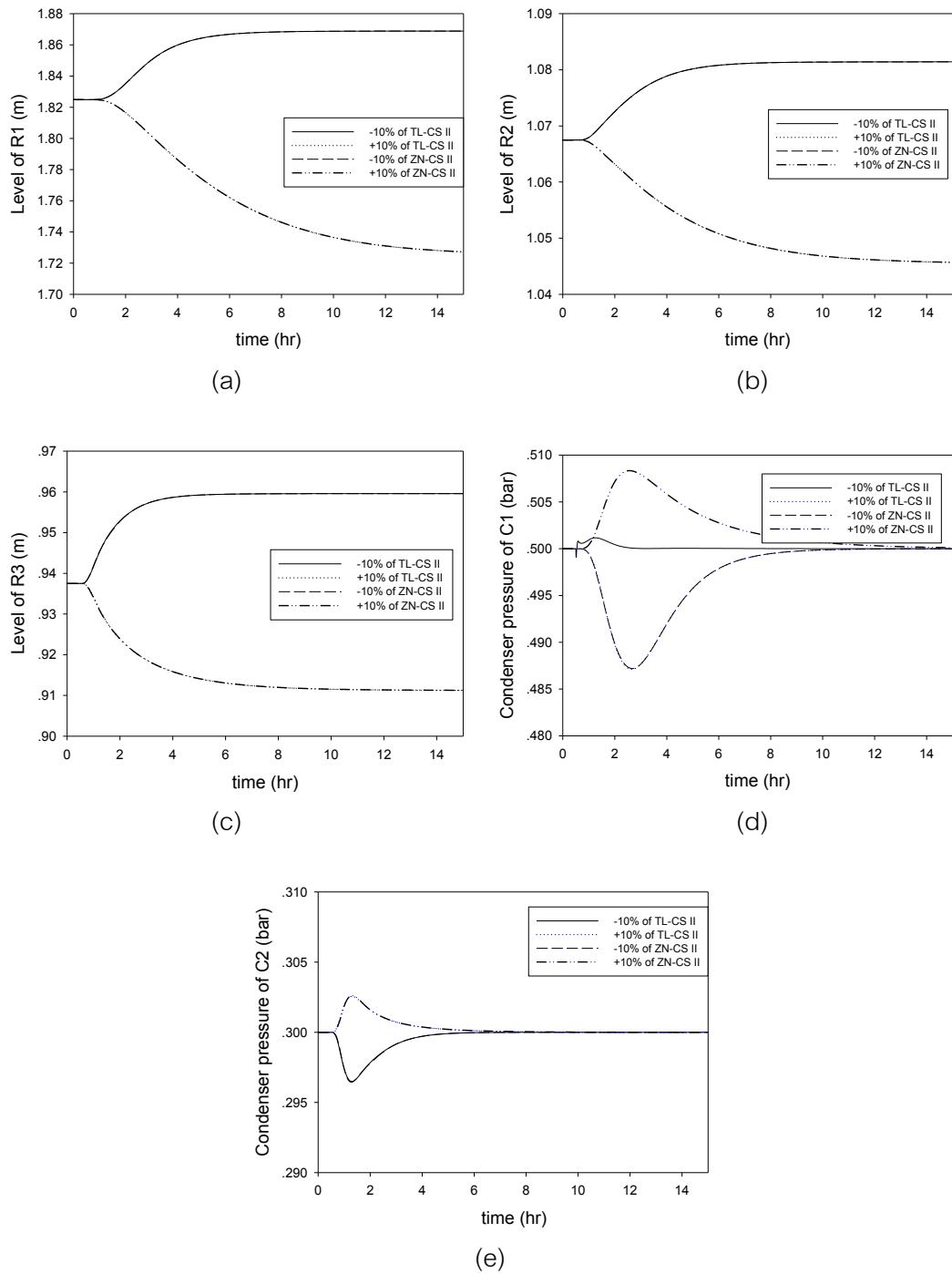


Fig. 3-30 Level and pressure dynamic responses of TL and ZN-tuned control structure II for production rate change.



The temperature controllers got tiny effect of production rate change as shown in Fig. 3-29 (a-e). For ZN tuned controllers, they gave the responses like TL tuned controllers, but ZN tuned controllers had overshoot less than TL tuned controllers such as Fig. 3-29 (e) because the TL setting made the response no oscillate, but it had a greater response time [8].

This change mainly affected to the levels of units as shown in Fig. 3-30 (a-c). The levels of units were adjusted to make the process giving the desired production rate. Because the level controls were P control, the offset of setpoint occurred. That offset could accept, and the product specification also met the standard.

Fig. 3-30 (d, e) showed pressure dynamic responses indicated that got rarely effect from this change, and they could reject the disturbance.

### 3.3.6 Dynamic performance

In this investigation, the dynamic performances of the control structures were evaluated by commonly used measure IAE. TL and ZN tuning methods were compared the performance which method gave the better dynamic performance.

PFAD feed flow rate into esterification reactor was changed; the IAE were evaluated as shown in Table 3-8. The results indicated ZN tuning method gave lower value than TL tuning method for control structure I. The biodiesel production rate of control structure II was varied, and dynamic responses were evaluated. Table 3-9 indicated that ZN tuning also gave lower value than TL tuning. For the reason, TL setting gave the greater response time than ZN setting [8]. The percentage opening of control valve was the robustness of flow that could control in the process.

For the dynamic performance of esterification reactor temperature change, ZN method performed the lower value of IAE in both control structures.

**Table 3-8** Robustness, IAE and maximum settling time of control structure I.

Testing	Robustness		IAE		Maximum settling time (hr)	
	TL	ZN	TL	ZN	TL	ZN
PFAD feed flow rate	±10%	±10%	2871.98	2718.515	4	4
Temperature of R1	±10°C	±10°C	262.462	203.447	2	2
FFA content in PFAD	92-98%	92-98%	221.173	192.540	4.5	3.5

The dynamic responses of FFA were changed in range of 92 - 98%. Both structures gave similar results, but TL tuning method performed the higher IAE values than ZN tuning method.

**Table 3-9** Robustness, IAE and maximum settling time of control structure II.

Testing	Robustness		IAE		Maximum settling time (hr)	
	TL	ZN	TL	ZN	TL	ZN
Biodiesel production rate	±10%	±10%	2817.474	2636.249	2.5	1.5
Temperature of R1	±10°C	±10°C	142.744	125.627	0.5	0.5
FFA content in PFAD	92-98%	92-98%	428.846	347.054	6.5	4.5

In addition, the controllers tuned by TL tuning rule had process settling time higher than the controllers tuned by ZN tuning method. The settling times of both tuning rules as shown in Table 3-8 and Table 3-9, respectively.

In conclusion, ZN-tuned controllers had faster response to settle steady state for any setpoint and disturbance testing. Besides, the ZN tuning method gave the less overshoot responses than TL tuning method as a result the IAE had lower value.

### 3.4 Energy management

Bottom stream of methanol recovery column II was heated to high temperature by the reboiler for removing the excess methanol. After that, it was cooled using a cooler. Hence, the removed heat was recycled to save the energy consumption. Heat exchanger was employed. The heat of the high temperature bottom stream in tubes was transferred to the water stream in shell. The heated water stream was fed into water washing column to eliminate the contaminant from biodiesel.

The heat exchanger was designed by setting outlet of hot stream to 80°C. The heat exchanger specification was shown in Table 3-10. Moreover, it had 8 m<sup>2</sup> of effective area, and countercurrent flow.

This heat exchanger was used instead of a cooler at the effluent bottom stream of column and a heater of water washing stream as shown in Fig. 3-31. It saved the heat duty for heating the water stream (25 kW) and cooler duty for cooling the bottom stream of C2 (56 kW). The heat transferred to the water stream as a result the temperature of the water stream rose to 76.5°C. It was over desire temperature 50°C, but the higher temperature water would render cleansing efficiency increase.

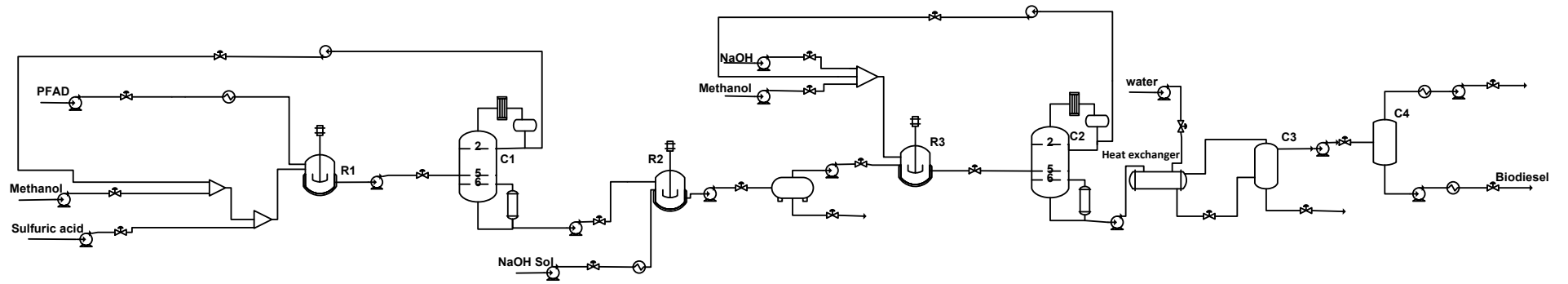


Fig. 3-31 Biodiesel production from PFAD process with heat exchanger.

**Table 3-10** Heat exchanger specification.

Specification	Tube side	Shell side
Pass	1	1
Number	51	1
Length (mm)	2700	-
Inside diameter (mm)	14.85	205

The biodiesel production process with heat exchanger was simulated in dynamic mode. The controllers were installed as previous control structures that were conventional and on demand control structures. However, controller parameters were tuned again. The ZN tuning method was employed since this method gave lower IAE value in previous work. The tuned temperature controller parameters for each control structure were shown in Table 3-11.

In control structure I, the process was tested by changing PFAD feed flow rate increased from 1000 kg/hr to 1100 kg/hr and decreased from 1000 kg/hr to 900 kg/hr at 0.5 hr as shown in Fig. 3-32 (a). Flow dynamic responses were shown in Fig. 3-32 (b-f); it showed some process variable response had the oscillation (Fig. 3-32 (d)), but the process was still stable and could adjust the process variable to settle setpoint.

Table 3-11 Controller setting by ZN tuning method for control structure I and II  
with heat exchanger.

Controlled variable	Manipulated variable	CS I		CS II	
		$K_c$	$\tau_I$ (min)	$K_c$	$\tau_I$ (min)
PFAD feed	Heat duty	50.64	6	61.74	5
R1	Reactor duty	6.14	2	3.32	5
Tray 5 <sup>th</sup> of C1	Reboiler duty	6.33	1	2.46	1
Sodium hydroxide feed to R2	Heat duty	5.77	1	12.48	2.5
R2	Reactor duty	10.81	5	24.10	3
R3	Reactor duty	103.12	5	84.8	6.5
Tray 5 <sup>th</sup> of C2	Reboiler duty	4.4	7	6.04	5
C4	Heat duty	3.66	6	3.72	6
Bottom stream of C4	Heat duty	5.52	2.5	5.27	2.5
Top stream of C4	Heat duty	2.52	1.5	1.94	1

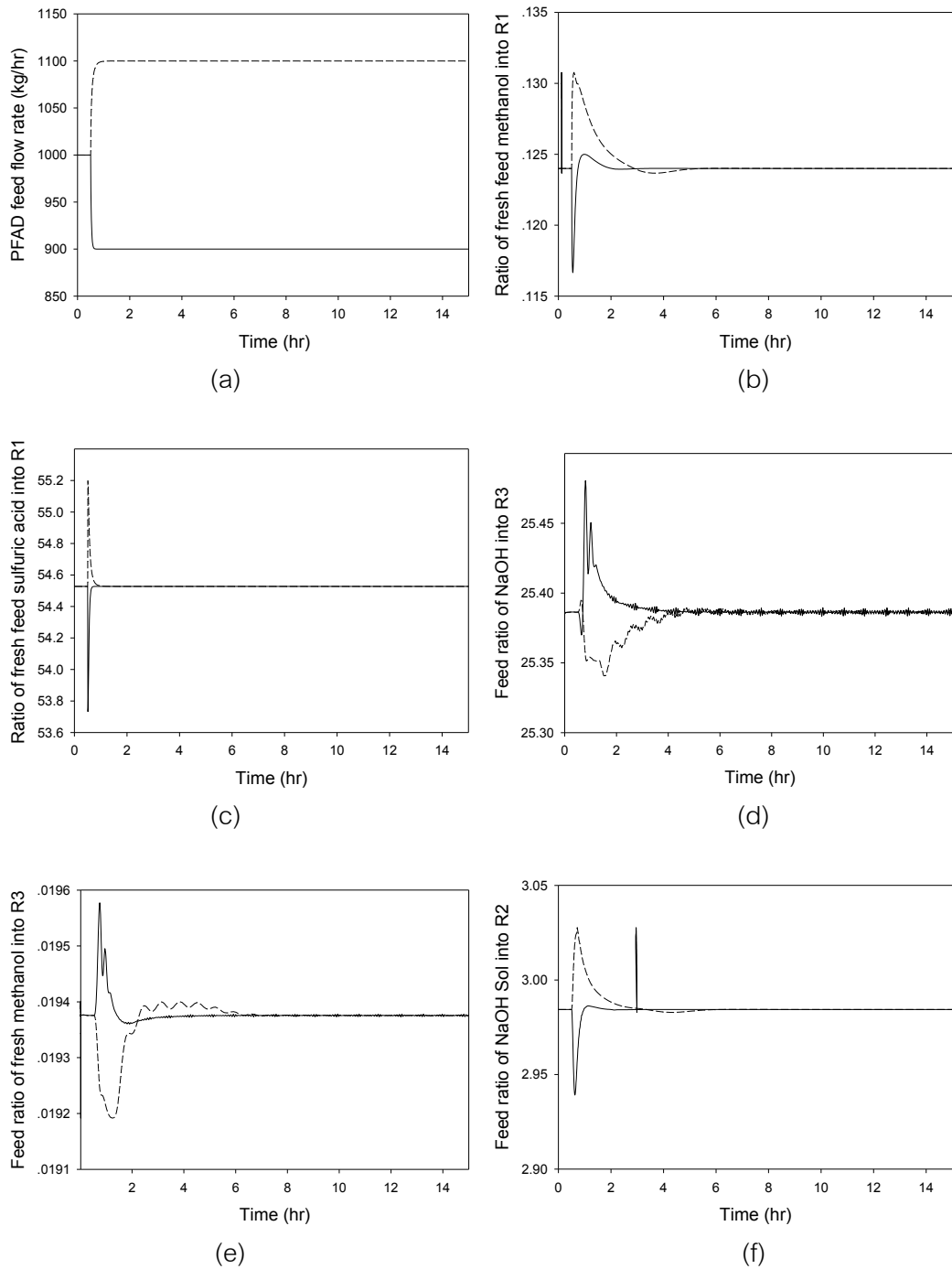


Fig. 3-32 Flow dynamic responses of ZN-tuned control structure I with heat exchanger for PFAD feed rate change. (dash line: 1100 kg/hr, solid line: 900 kg/hr)

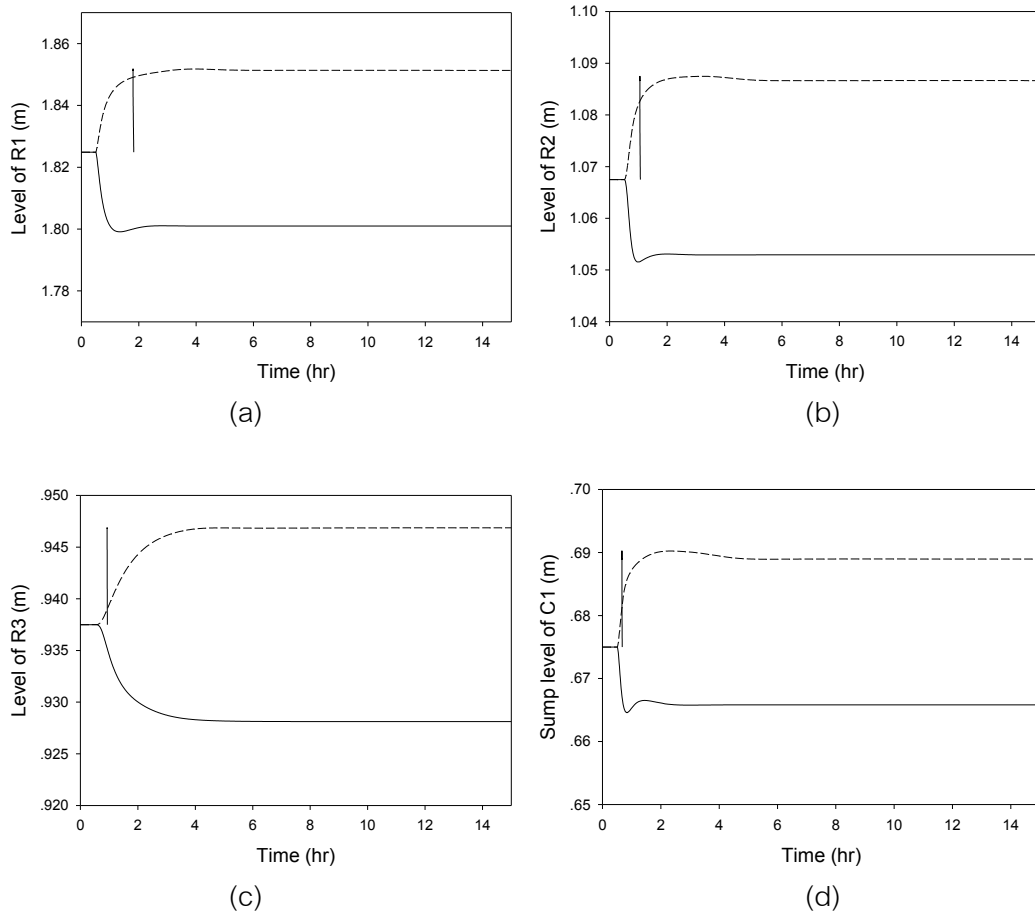


Fig. 3-33 Level dynamic responses of ZN-tuned control structure I with heat exchanger for PFAD feed rate change. (dash line: 1100 kg/hr, solid line: 900 kg/hr)

Fig. 3-33, Fig. 3-34 and Fig. 3-35 performed the dynamic responses of level, temperature, and pressure, respectively. They indicated the process could reject disturbance, PFAD feed flow rate change, and lead the process to setpoint rapidly.



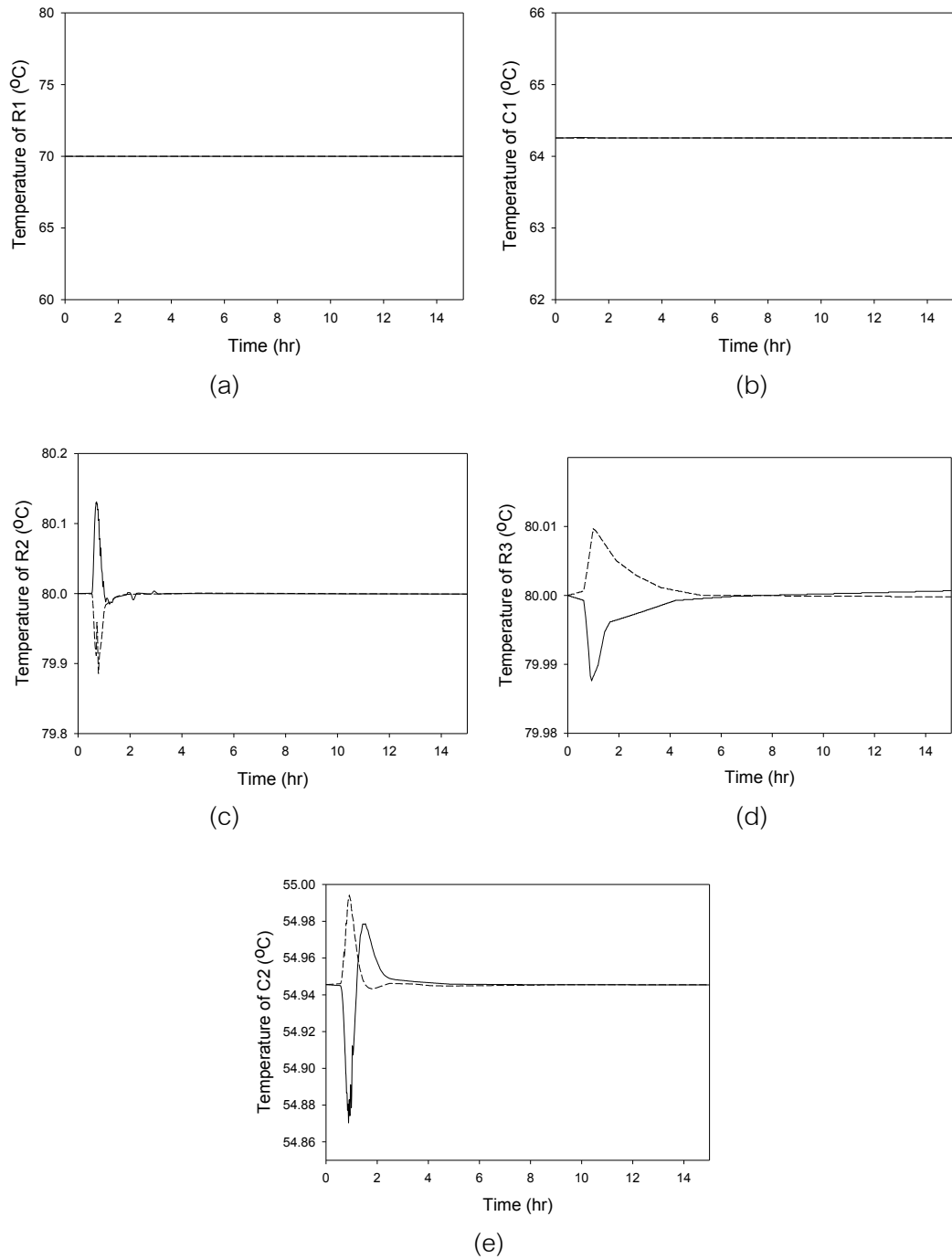
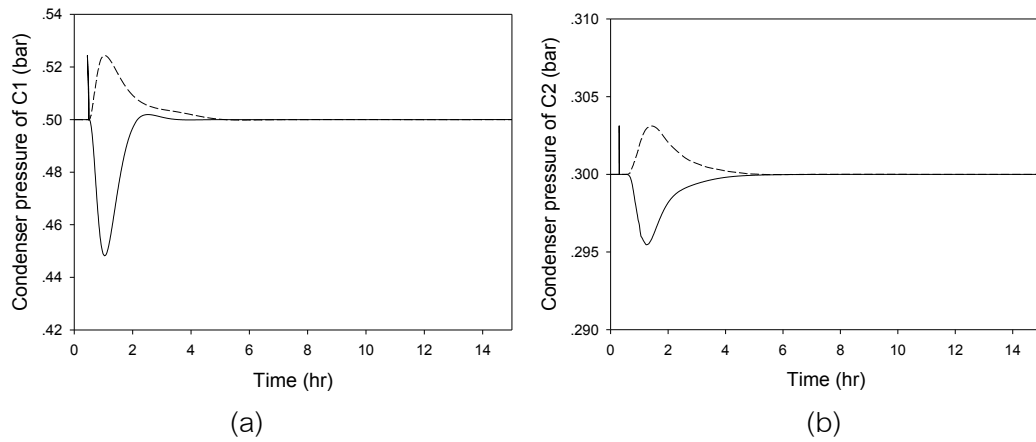


Fig. 3-34 Temperature dynamic responses of ZN-tuned control structure I with heat exchanger for PFAD feed rate change. (dash line: 1100 kg/hr, solid line: 900 kg/hr)



**Fig. 3-35** Pressure dynamic responses of ZN-tuned control structure I with heat exchanger for PFAD feed rate change. (dash line: 1100 kg/hr, solid line: 900 kg/hr)

The dynamic responses when the esterification reactor temperature was changed from  $70^{\circ}\text{C}$  to  $80^{\circ}\text{C}$  and  $70^{\circ}\text{C}$  to  $66^{\circ}\text{C}$  were shown in Fig. 3-36 (a) that had the oscillation. The temperature responses were shown in Fig. 3-36 (b-e); they oscillated in the beginning and rested to the setpoint in final.

Fig. 3-37 (a-d), Fig. 3-37 (e, f) and Fig. 3-38 (a-d) were the responses of flow, pressure, and level, respectively. They behaved like the temperature responses.

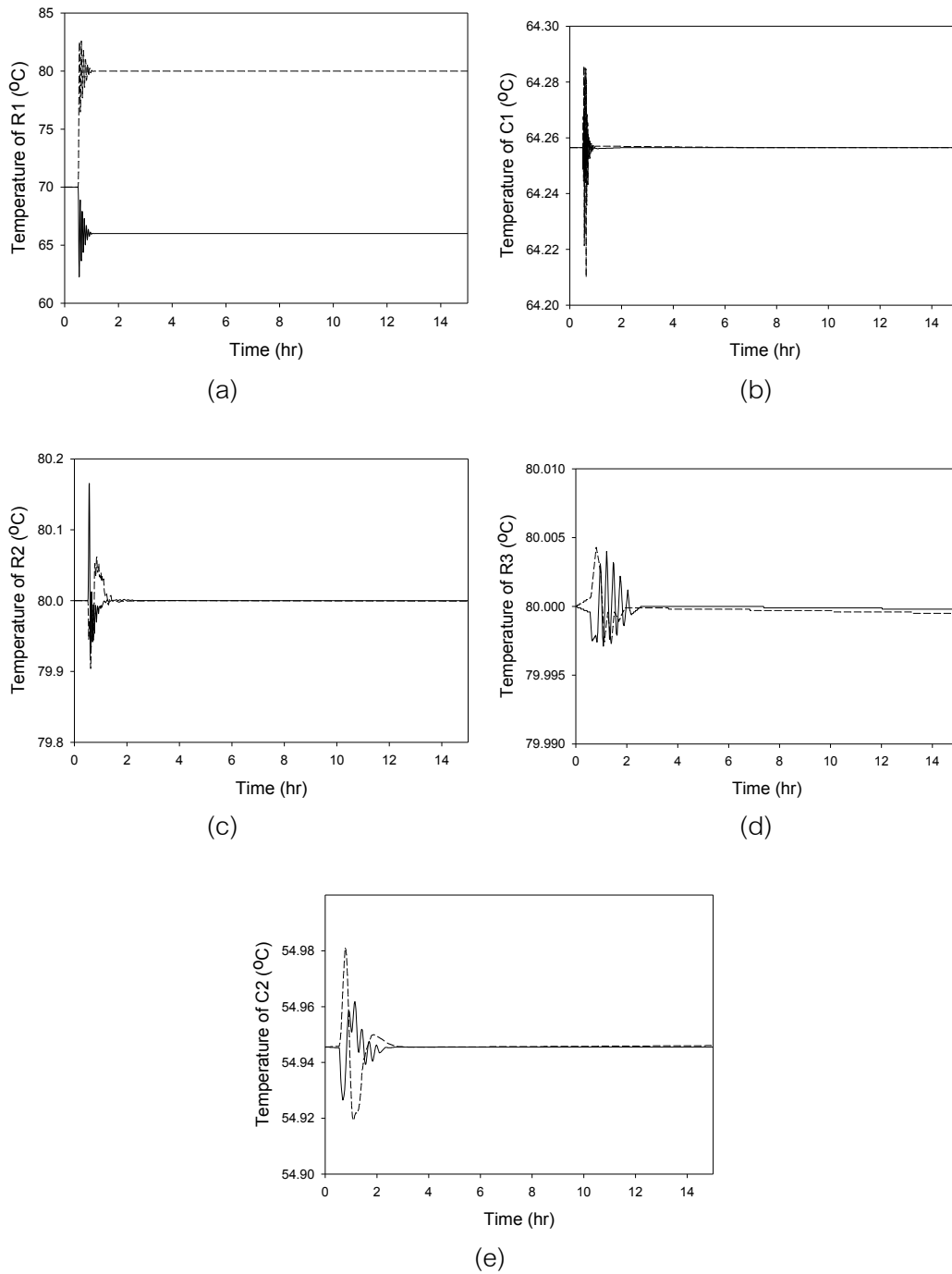


Fig. 3-36 Temperature dynamic responses of ZN-tuned control structure I with heat exchanger for R1 temperature change. (dash line: 80°C, solid line: 66°C)

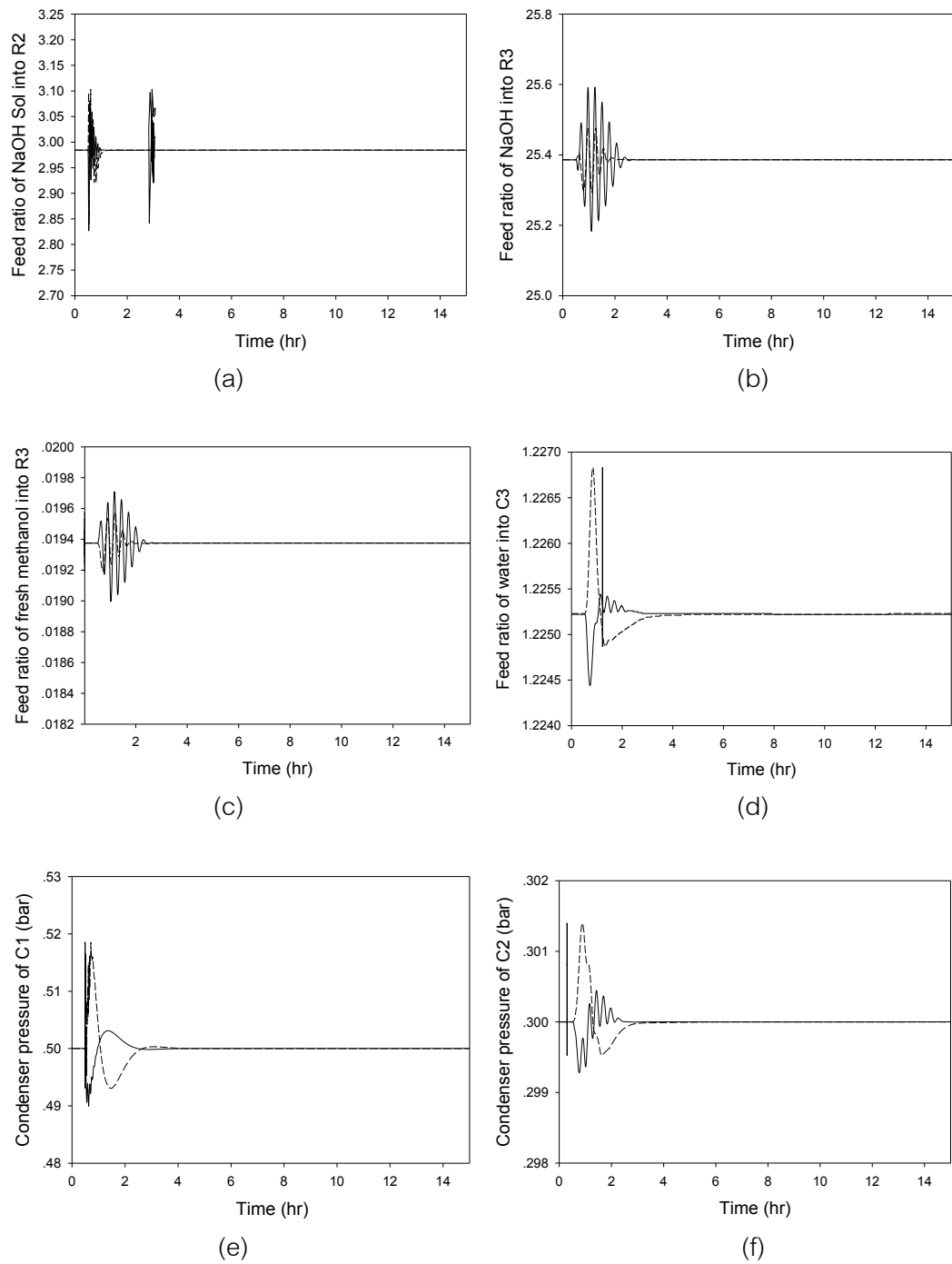


Fig. 3-37 Flow and pressure dynamic responses of ZN-tuned control structure I with heat exchanger for R1 temperature change. (dash line: 80°C, solid line: 66°C)

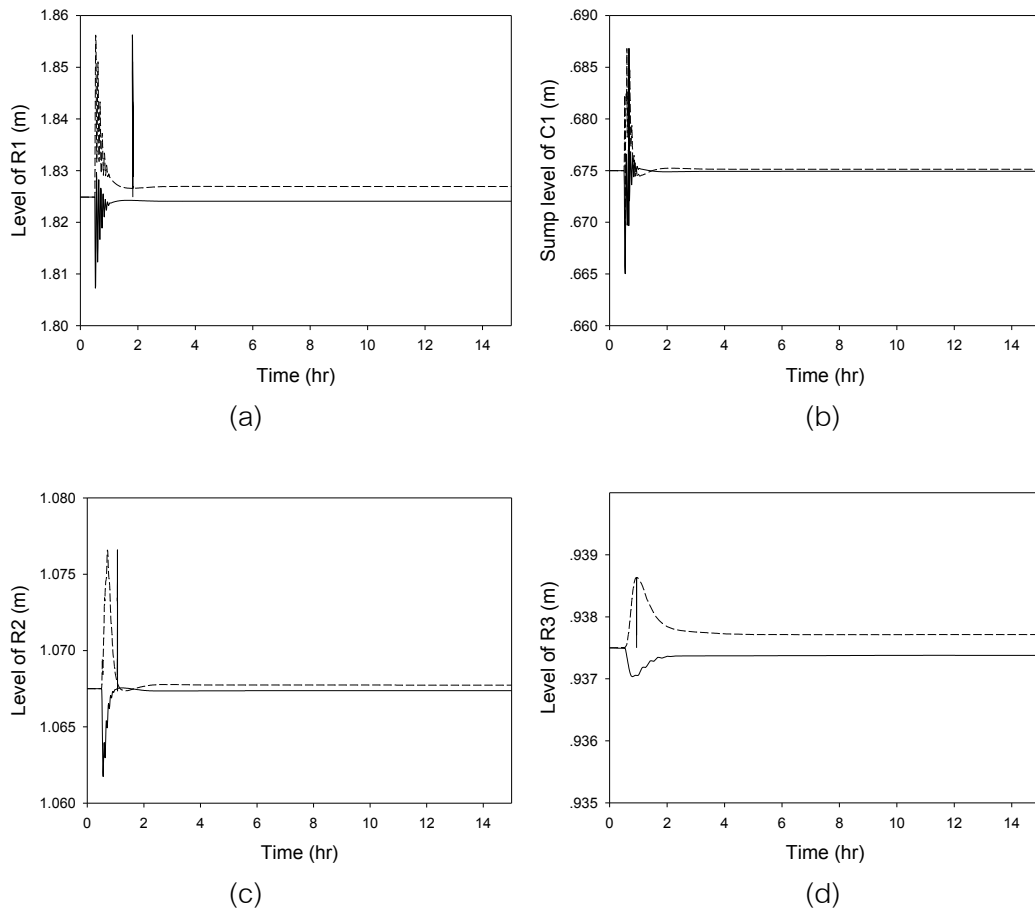


Fig. 3-38 Level dynamic responses of ZN-tuned control structure I with heat exchanger for R1 temperature change. (dash line: 80°C, solid line: 66°C)

For the FFA content changing from 92% - 98% of control structure I, it did not affect on temperature of unit operations in the process as shown in Fig. 3-39 (a-e).

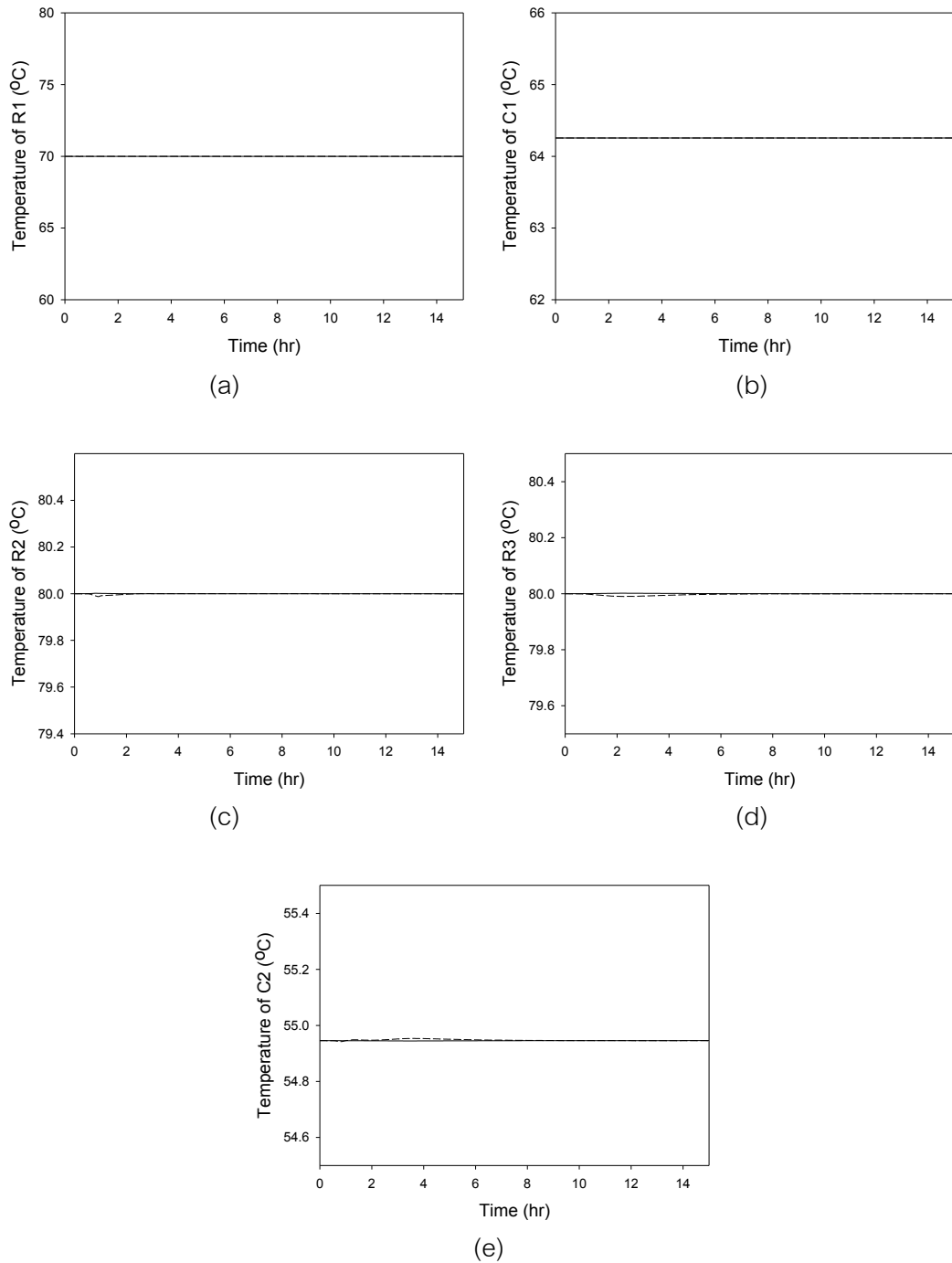


Fig. 3-39 Temperature dynamic responses of ZN-tuned control structure I with heat exchanger for FFA in PFAD change. (dash line: 98%, solid line: 92%)

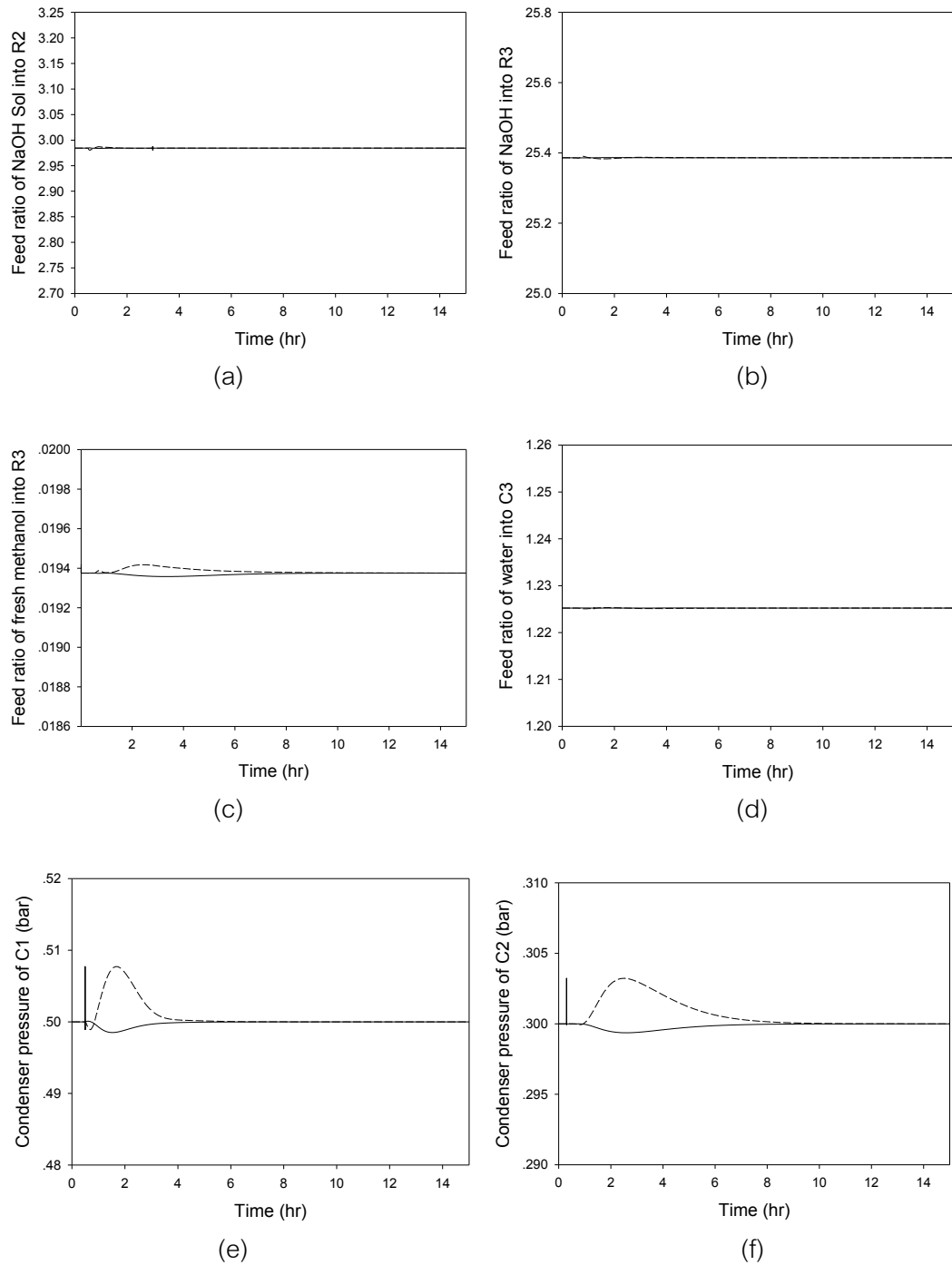


Fig. 3-40 Flow and pressure dynamic responses of ZN-tuned control structure I with heat exchanger for FFA in PFAD change. (dash line: 98%, solid line: 92%)

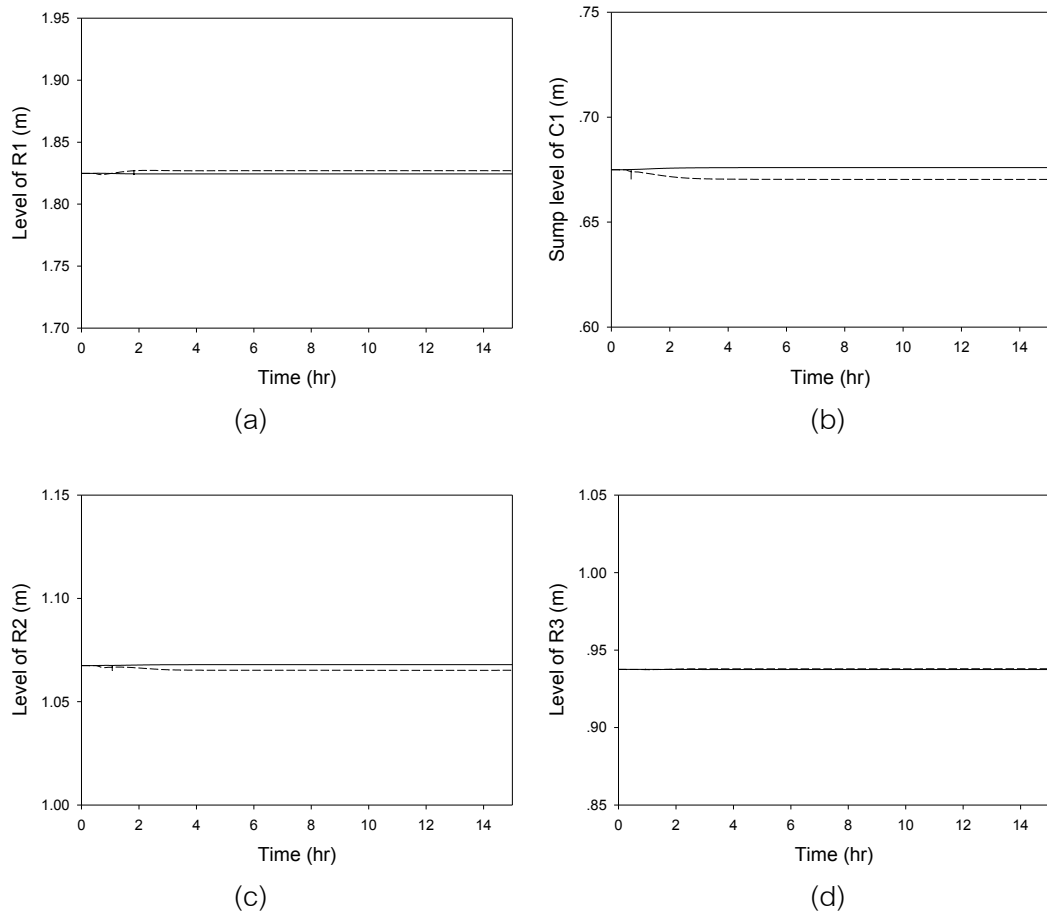


Fig. 3-41 Level dynamic responses of ZN-tuned control structure I with heat exchanger for FFA in PFAD change. (dash line: 98%, solid line: 92%)

Flow responses in Fig. 3-40 (a-d), pressure responses in Fig. 3-40 (e, f), and level responses in Fig. 3-41 (a-d) got a little effect from PFAD composition change. However, controllers could control the process reaching to steady state.

In control structure II, the biodiesel production rate was changed from 1010.7 kg/hr to 1111.8 kg/hr and 1010.7 kg/hr to 909.6 kg/hr as shown in Fig. 3-42 (a). This changing caused feed streams into R3 to vibrate as shown in Fig. 3-42 (e, f); other responses of flow were shown in Fig. 3-42 (b-d).



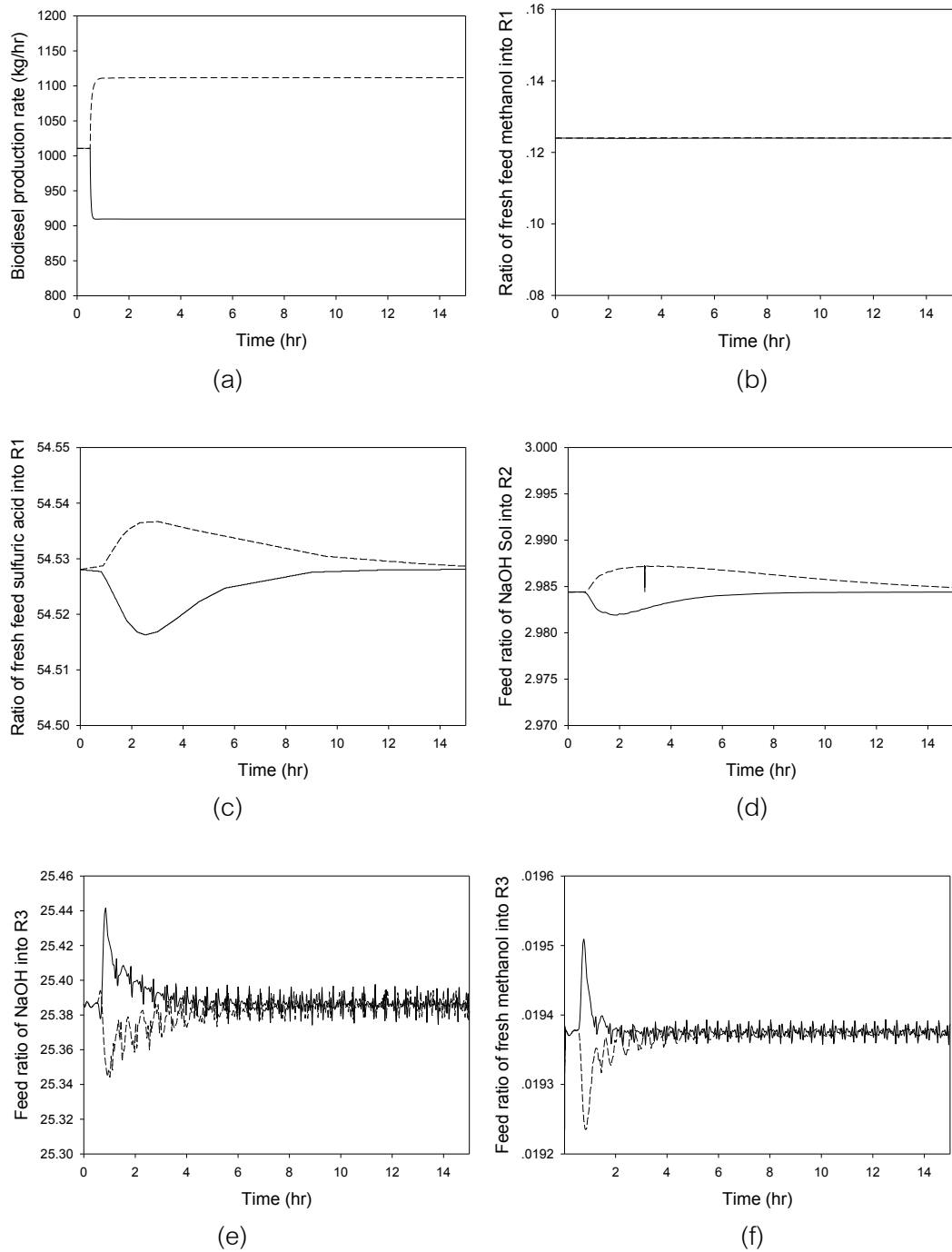


Fig. 3-42 Flow dynamic responses of ZN-tuned control structure II with heat exchanger for biodiesel production rate change. (dash line: 1111.8 kg/hr, solid line: 909.6 kg/hr)

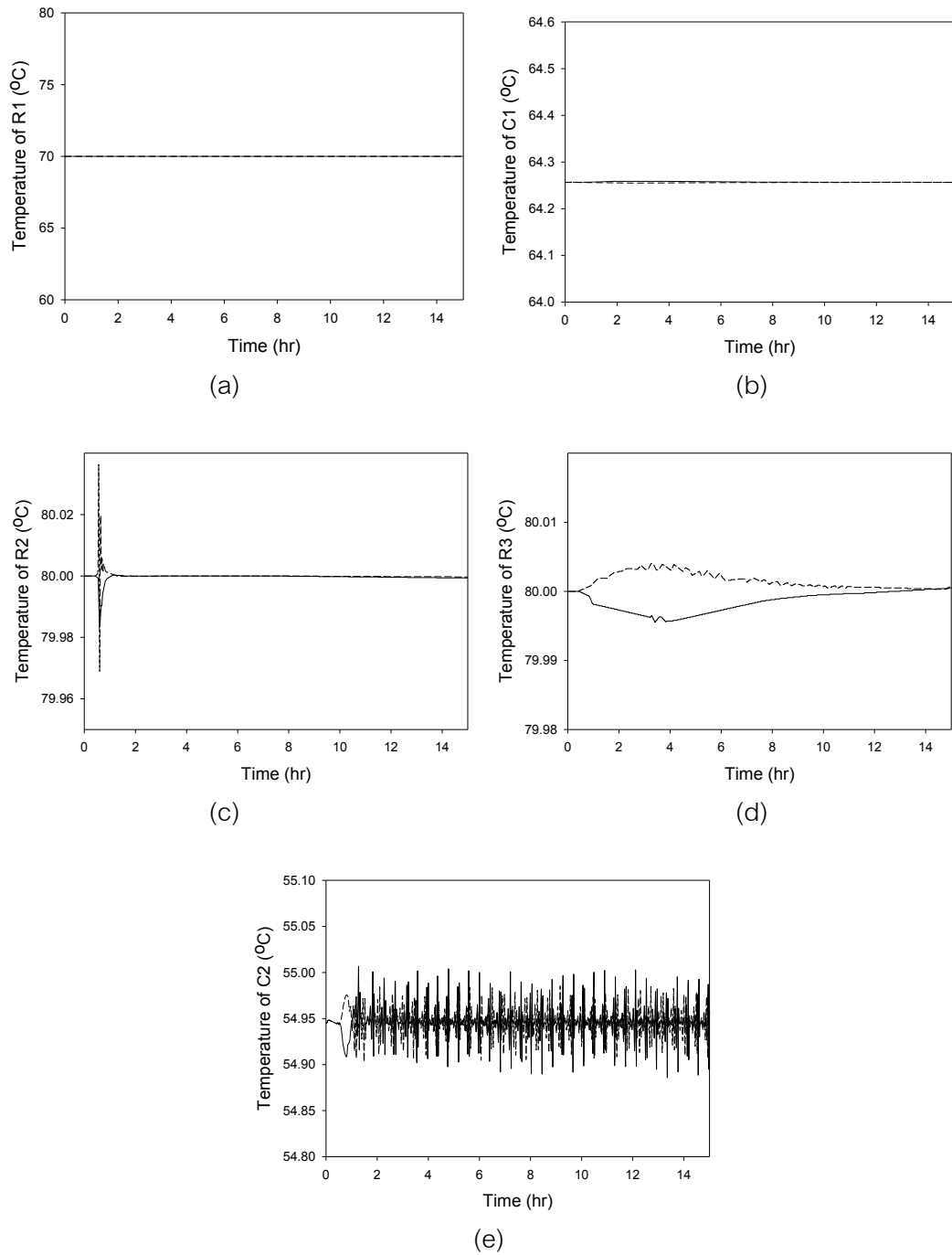


Fig. 3-43 Temperature dynamic responses of ZN-tuned control structure II with heat exchanger for biodiesel production rate change.  
(dash line: 1111.8 kg/hr, solid line: 909.6 kg/hr)

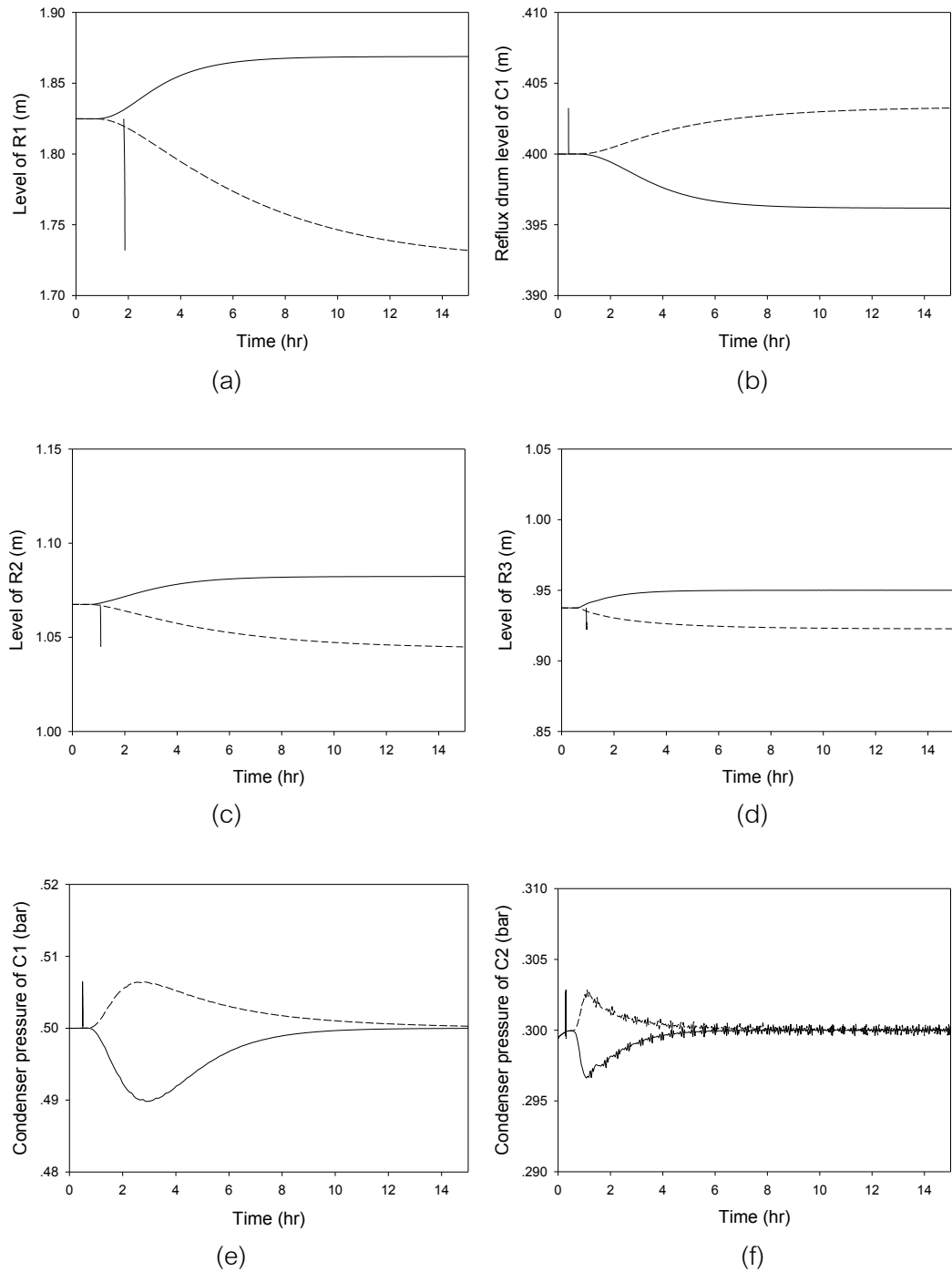


Fig. 3-44 Level and pressure dynamic responses of ZN-tuned control structure II with heat exchanger for biodiesel production rate change.

(dash line: 1111.8 kg/hr, solid line: 909.6 kg/hr)

Fig. 3-43 (a-e) show the temperature responses when the production rate was tested. Fig. 3-43 (e), the temperature of distillation column II, lightly oscillated, but it was still in a controlled temperature ( $55^{\circ}\text{C}$ ).

Fig. 3-44 (a-d) and Fig. 3-44 (e, f) show level and pressure responses, respectively. For level, they had offset because of used P controller, but the level control offset could be acceptable. For pressure, they had a little change and reached to setpoint.

After that, the temperature of R1 was changed for testing as shown in Fig. 3-45 (a). The temperature controllers could eliminate disturbance and save the stability of the process as shown in Fig. 3-45 (b-e).

Flow responses were shown in Fig. 3-46 (a-d), and pressure responses were shown in Fig. 3-46 (e, f). These controllers could control the process variables and keep the process to be stable.

Level responses were shown in Fig. 3-47 (a-d). The controllers could control the process to reach the setpoint also; they had tiny offset.

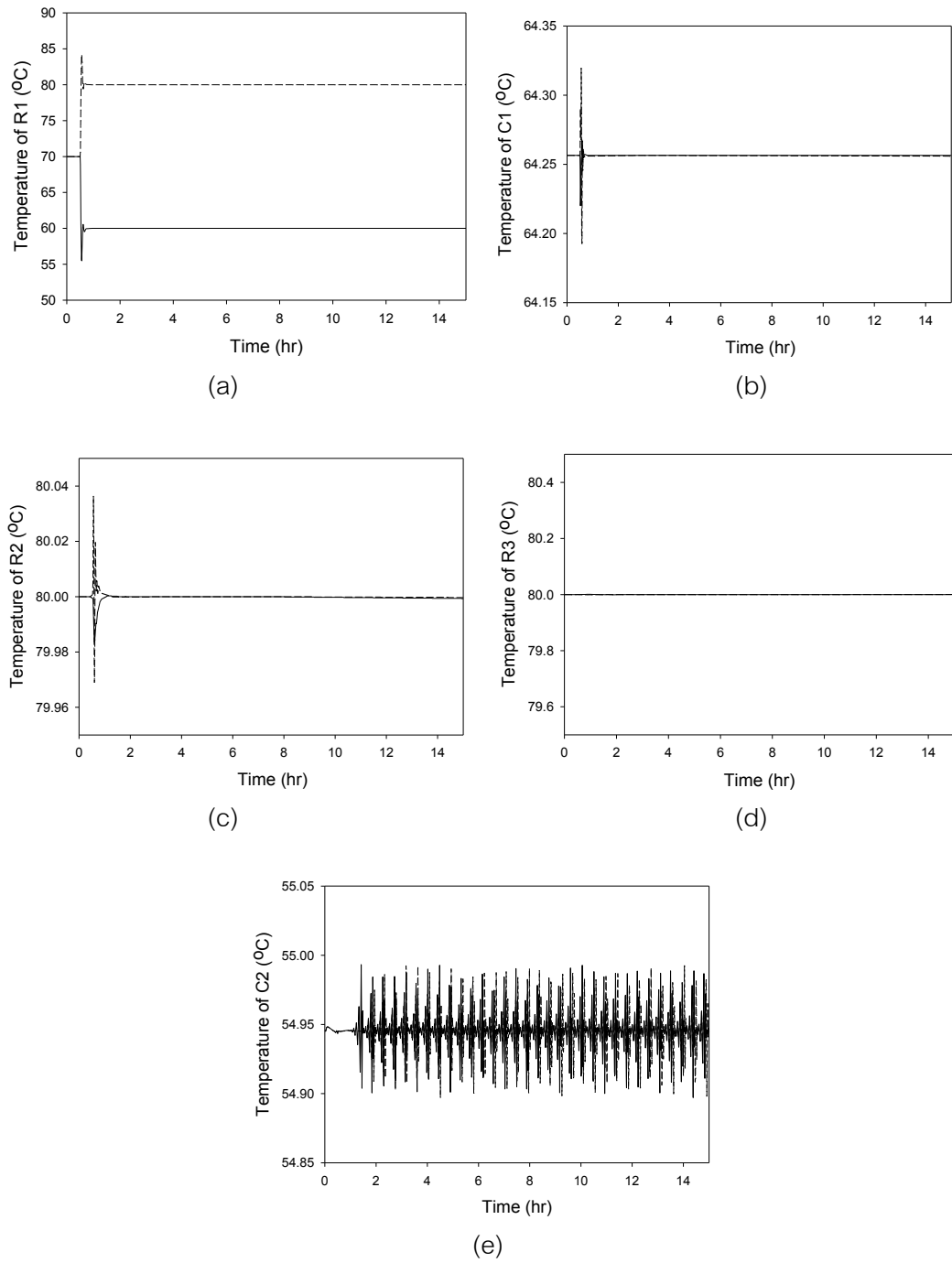


Fig. 3-45 Temperature dynamic responses of ZN-tuned control structure II with heat exchanger for R1 temperature change. (dash line: 80°C, solid line: 60°C)

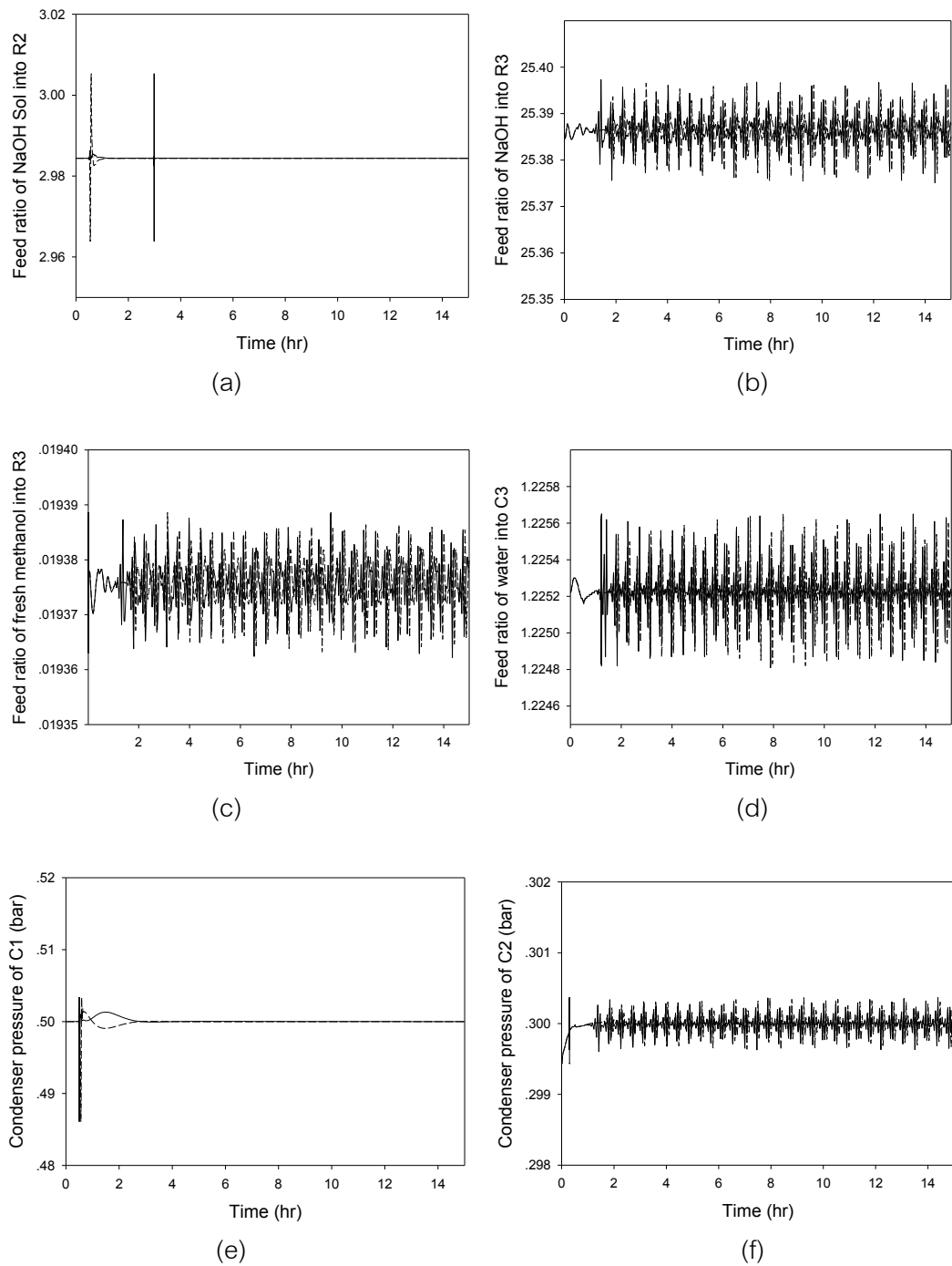


Fig. 3-46 Flow and pressure dynamic responses of ZN-tuned control structure II with heat exchanger for R1 temperature change. (dash line: 80°C, solid line: 60°C)

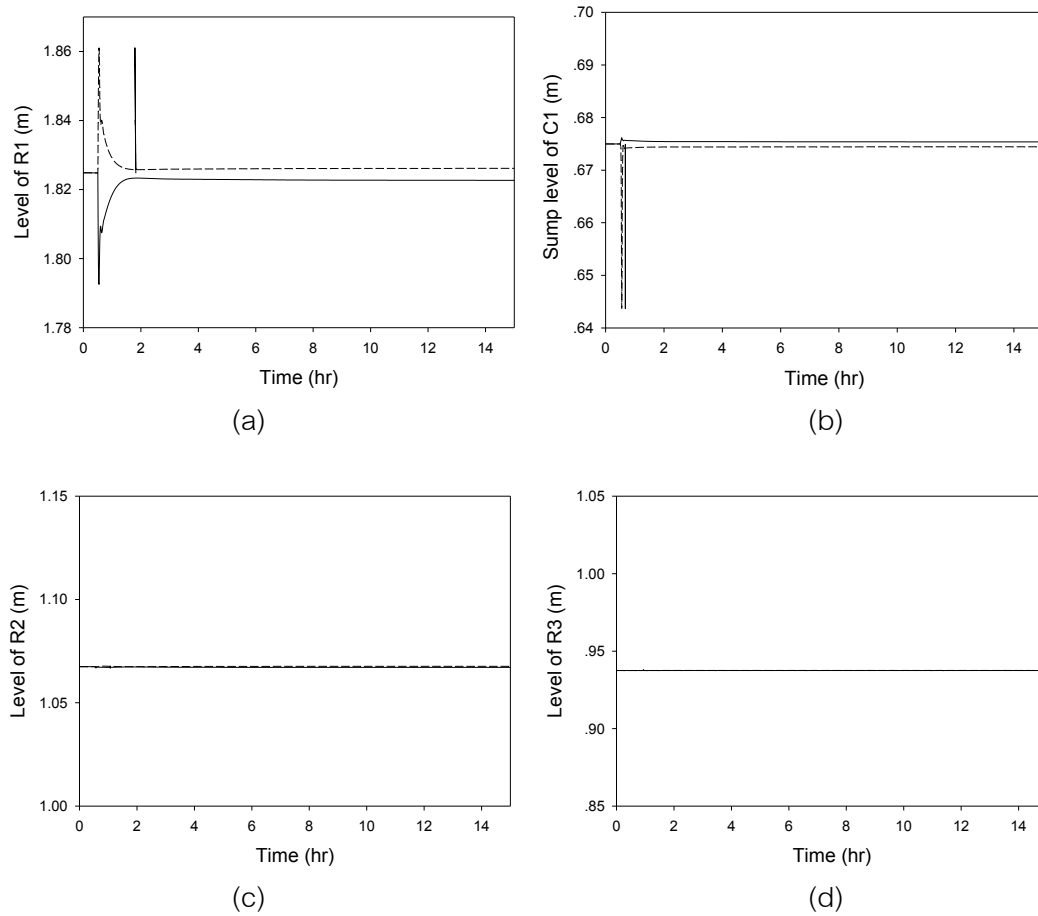


Fig. 3-47 Level dynamic responses of ZN-tuned control structure II with heat exchanger for R1 temperature change. (dash line: 80°C, solid line: 60°C)

For FFA of PFAD change (92% – 98%) in control structure II, the temperatures of the units were a little affected by variability of PFAD's composition as shown in Fig. 3-48 (a-e). Flow (Fig. 3-49 (a-d)) and pressure (Fig. 3-49 (e, f)) had the behavior like temperature also. For level as shown in Fig. 3-50 (a-d), they affected by changing PFAD composition, so the level controllers adjusted the manipulated variables for keeping the level of each unit. The steady state values of the level had offsets, while these offsets were acceptable.

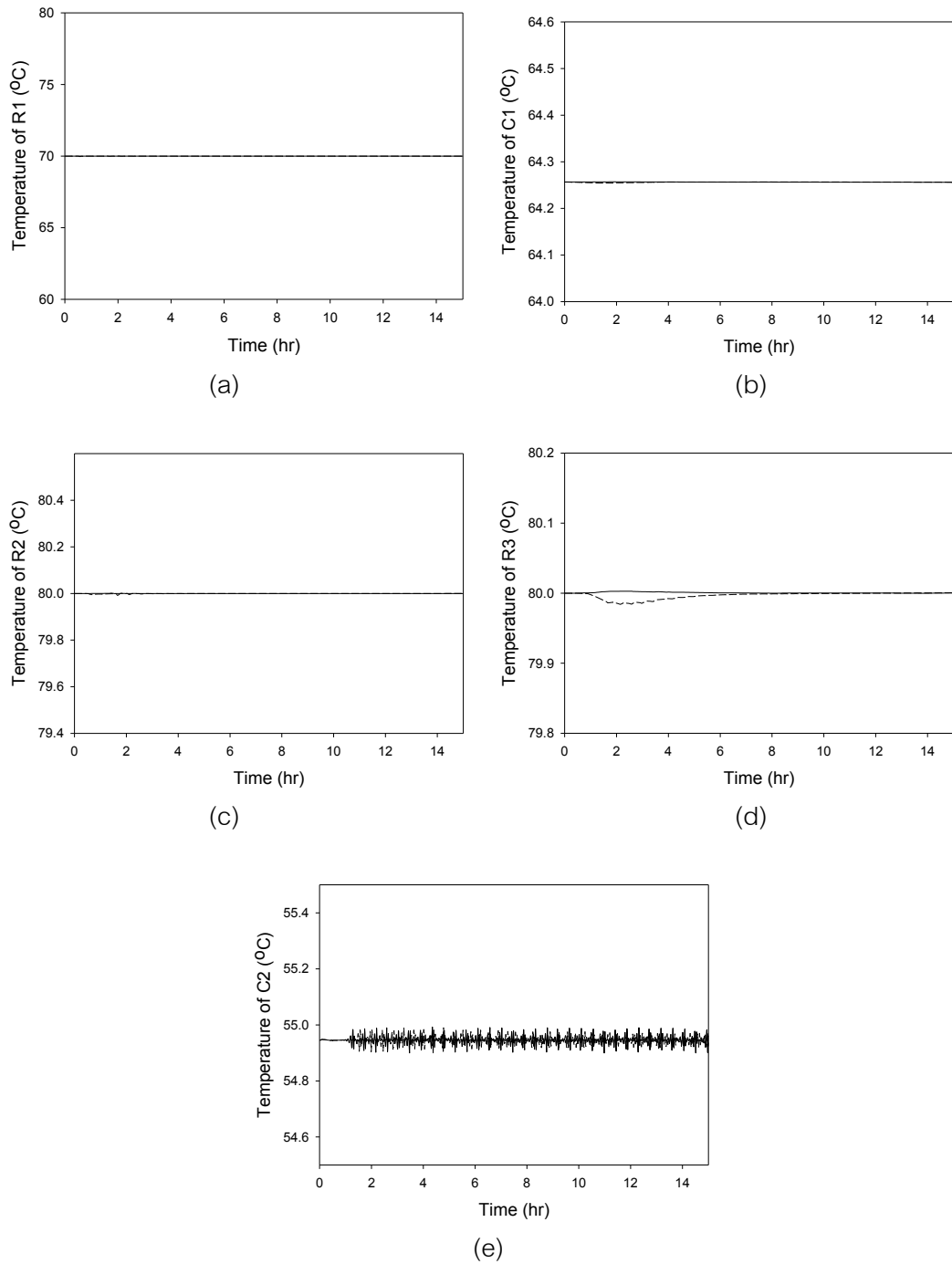


Fig. 3-48 Temperature dynamic responses of ZN-tuned control structure II with heat exchanger for FFA in PFAD change. (dash line: 98%, solid line: 92%)



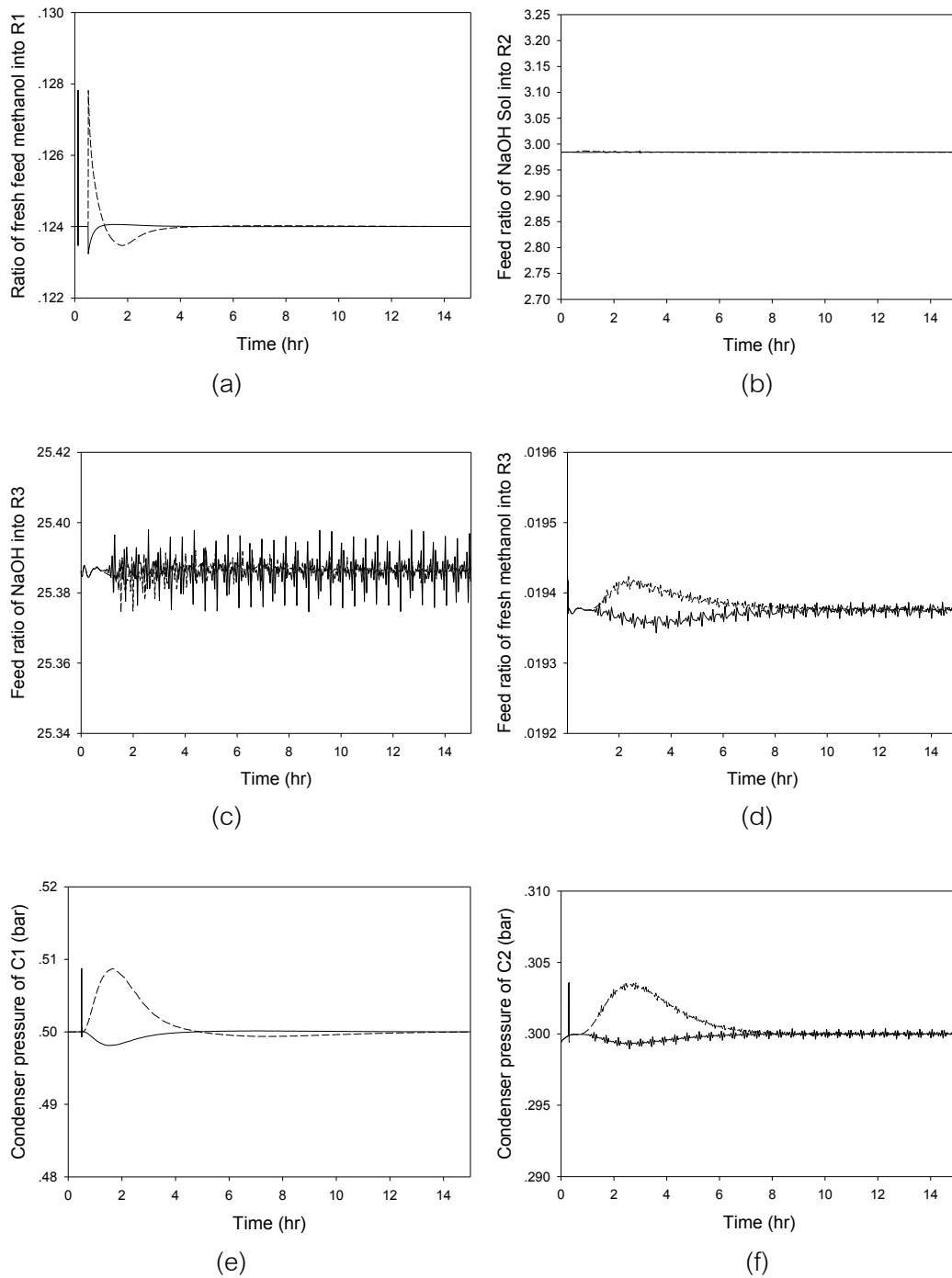


Fig. 3-49 Flow and pressure dynamic responses of ZN-tuned control structure II with heat exchanger for FFA in PFAD change. (dash line: 98%, solid line: 92%)

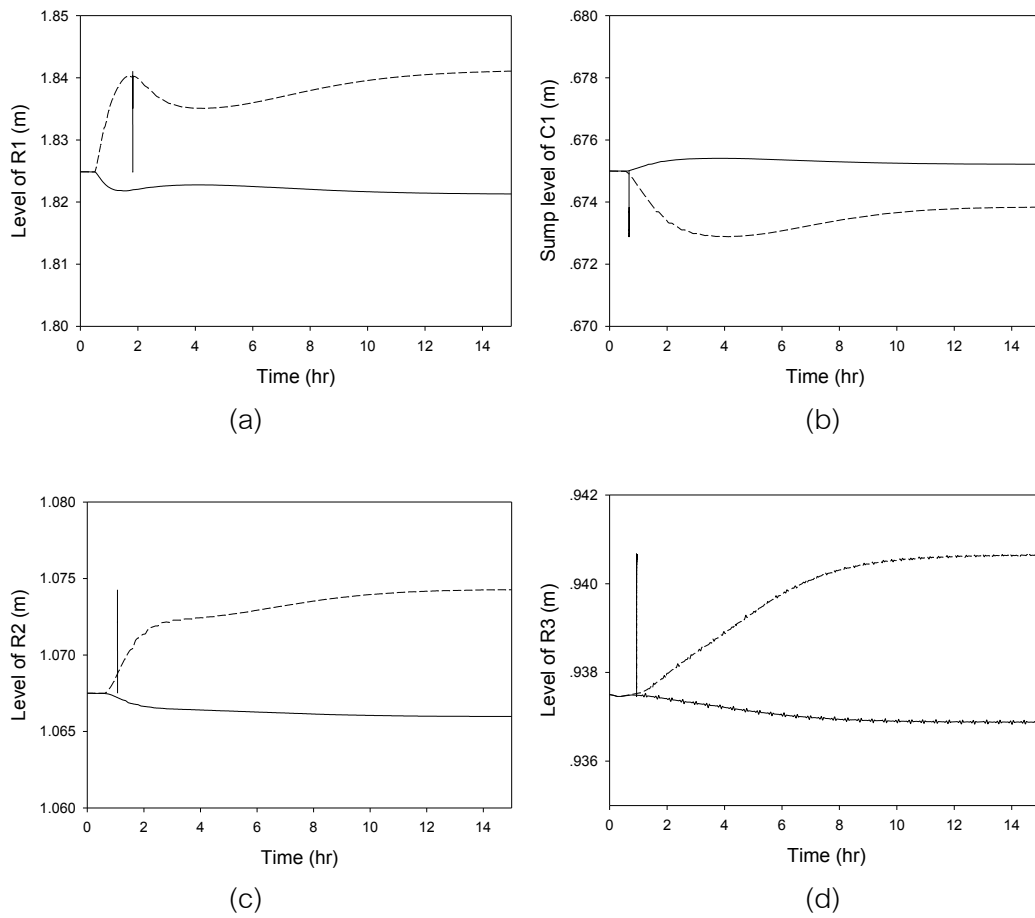


Fig. 3-50 Level dynamic responses of ZN-tuned control structure II with heat exchanger for FFA in PFAD change. (dash line: 98%, solid line: 92%)

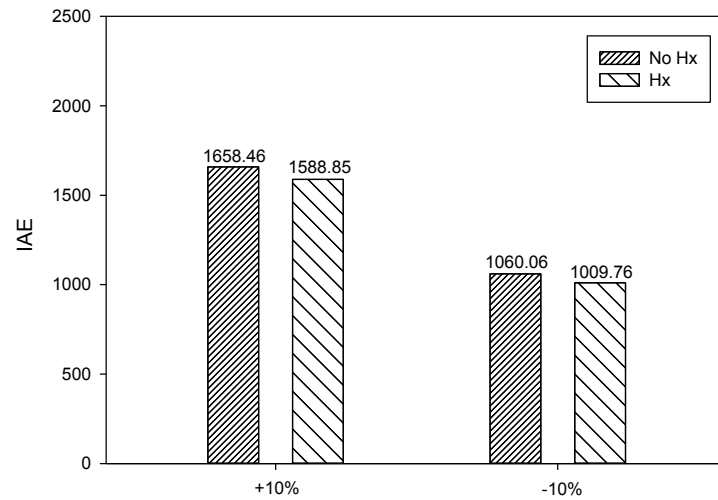


Fig. 3-51 IAE responses of  $\pm 10\%$  PFAD feed rate change of control structure I for the process with and without heat exchanger.

Fig. 3-51 shows IAE value when PFAD feed rate was changed. It indicated that the IAE of biodiesel process with heat exchanger and without heat exchanger almost the same because having heat exchanger has effect on level insignificantly which without heat exchanger process had lower value.

For the production rate change, the IAE were hardly different also as shown in Fig. 3-52.

The previous results informed that PFAD feed flow rate and production rate changes had less effect on the process variables.

Fig. 3-53 shows IAE value when esterification reactor temperature was changed. This figure indicated that IAE of the process with heat exchanger had higher values than the conventional process in both control structures because the heat exchanger made temperature responses of other units oscillate.

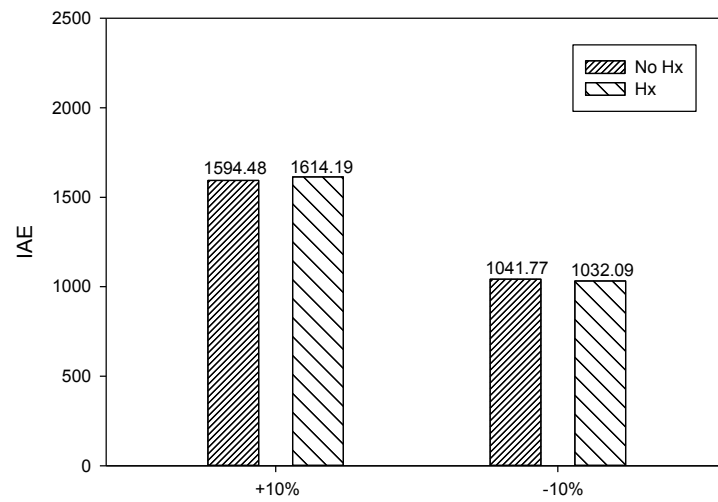


Fig. 3-52 IAE responses of  $\pm 10\%$  production rate change of control structure II for the process with and without heat exchanger.

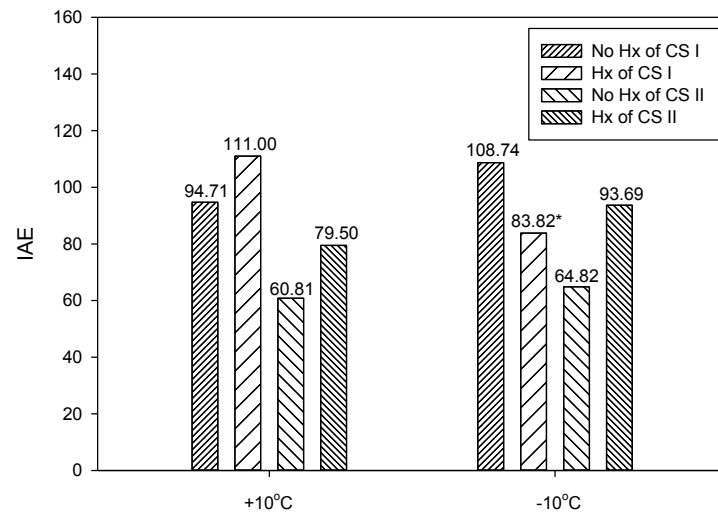


Fig. 3-53 IAE responses of  $\pm 10^{\circ}\text{C}$  of esterification reactor temperature change for the process with and without heat exchanger.

Note: \*  $-4^{\circ}\text{C}$  for control structure I with heat exchanger.

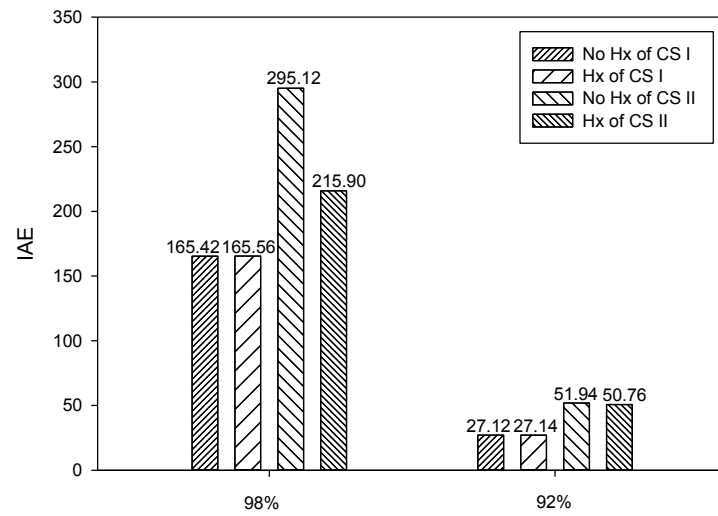


Fig. 3-54 IAE responses of FFA content in PFAD change in range of 92 - 98% for the process with and without heat exchanger.

For Fig. 3-54, the FFA in PFAD was changed in range of 92 – 98%. This result showed that IAE of 98% FFA was rarely different in control structure I. However, the IAE value of the process without a heat exchanger in control structure II when FFA was 98% had greater value than the process with heat exchanger; on the other hand, 92% FFA gave similar IAE values.

## CHAPTER 4

### CONCLUSION

#### 4.1 Conclusion

In this research, esterification reaction was found that was reversible reaction. The order of continuous esterification reaction was respect on FFA concentration in the forward reaction (first order) as well as methyl ester and water in the backward reaction (second order). The rate law is  $r = k_f [FFA] - k_b [FAME][water]$ .

From steady state operation 1000 kg/hr PFAD feed flow rate and product purity of 99.9%, the conventional and on demand plantwide control structures were proposed. These two structures had different control objectives. For the first structure, the PFAD feed flow was controlled by upstream process, so it was flow-controlled, and the setpoint of flow controller was a load disturbance to the process. For the second structure, the production rate was controlled by customer. Hence, it was flow-controlled, and the setpoint of flow controller was a load disturbance to the process. Nine steps of the plantwide process control strategy were applied to these control structures. TL and ZN tuning method were used for tuning the controllers of each structure. The ZN method gave the better result than the TL method. ZN-tuned controllers had faster response to settle steady state in both control structures, and it had less IAE value. In addition, both methods can drive the response to their setpoints in 0.5 - 6.5 hr.

In addition, the production process could save the energy by adding the heat exchanger instead of heater and cooler. A heat exchanger was installed for transferring the heat between the bottom stream of methanol recovery column II and water washing stream. It could decrease the process energy consumption with the

stable operation, but dynamic responses from these processes had oscillation more than processes without heat exchange.

#### 4.2 Recommendation

- 1) The kinetics of this process that are esterification, neutralization, and transesterification must be studied additionally. It will give accurate and real results.
- 2) This investigation is a potential feedback control study; in place of it feedforward control may give better results and improve the operations.
- 3) The different set of controlled and manipulated variables can be used if it has a different objective.

## REFERENCES

- [1] J. V. Gerpen, B. Shanks, R. Pruszko, D. Clements, and G. Knothe, "Biodiesel production technology," NREL/SR-510-362442004.
- [2] W. L. Luyben, B. D. Tyreus, and M. L. Luyben, *Plantwide Process Control*. New York: McGraw-Hill, 1999.
- [3] G. Çaylı and S. Küsefoğlu, "Increased yields in biodiesel production from used cooking oils by a two step process: Comparison with one step process by using TGA," *Fuel Processing Technology*, vol. 89, pp. 118-122, 2008.
- [4] S. Chongkhong, C. Tongurai, P. Chetpattananondh, and C. Bunyakan, "Biodiesel production by esterification of palm fatty acid distillate," *Biomass and Bioenergy*, vol. 31, pp. 563-568, 2007.
- [5] H. S. Fogler, *Elements of Chemical Reaction Engineering*, 4th ed.: Pearson Education, Inc., 2008.
- [6] S. Chongkhong, C. Tongurai, and P. Chetpattananondh, "Continuous esterification for biodiesel production from palm fatty acid distillate using economical process," *Renewable Energy*, vol. 34, pp. 1059-1063, 2009.
- [7] Thai industrial standards institute. (2005). *Specification and Quality of Fatty Acid Methyl Ester*. Available: [www.ratchakitcha.soc.go.th/DATA/PDF/2550/E/037/1.PDF](http://www.ratchakitcha.soc.go.th/DATA/PDF/2550/E/037/1.PDF)
- [8] D. E. Seborg, T. F. Edgar, and D. A. Mellichamp, *Process Dynamics and Control*, 2nd ed. Hoboken, NJ :: Wiley, 2004.
- [9] Y. Zhang, M. A. Dubé, D. D. McLean, and M. Kates, "Biodiesel production from waste cooking oil: 1. Process design and technological assessment," *Bioresource Technology*, vol. 89, pp. 1-16, 2003.
- [10] D. Aranda, R. Santos, N. Tapanes, A. Ramos, and O. Antunes, "Acid-Catalyzed Homogeneous Esterification Reaction for Biodiesel Production from Palm Fatty Acids," *Catalysis Letters*, vol. 122, pp. 20-25, 2008.
- [11] Aspen Technology, Inc. (2008), Aspen Plus Biodiesel Model.



- [12] A. H. West, D. Posarac, and N. Ellis, "Assessment of four biodiesel production processes using HYSYS.Plant," *Bioresource Technology*, vol. 99, pp. 6587-6601, 2008.
- [13] S. Glisic and D. Skala, "The problems in design and detailed analyses of energy consumption for biodiesel synthesis at supercritical conditions," *The Journal of Supercritical Fluids*, vol. 49, pp. 293-301, 2009.
- [14] R. Tesser, L. Casale, D. Verde, M. Di Serio, and E. Santacesaria, "Kinetics of free fatty acids esterification: Batch and loop reactor modeling," *Chemical Engineering Journal*, vol. 154, pp. 25-33, 2009.
- [15] P. K. S. Yadav, O. Singh, and R. P. Singh, "Palm Fatty Acid Biodiesel: Process Optimization and Study of Reaction Kinetics," *Journal of Oleo Science*, vol. 59, pp. 575-580, Nov 2010.
- [16] Y. H. Shen, J. K. Cheng, J. D. Ward, and C. C. Yu, "Design and control of biodiesel production processes with phase split and recycle in the reactor system," *Journal of the Taiwan Institute of Chemical Engineers*, vol. 42, pp. 741-750, 2011.
- [17] S. Lee, D. Posarac, and N. Ellis, "Process simulation and economic analysis of biodiesel production processes using fresh and waste vegetable oil and supercritical methanol," *Chemical Engineering Research and Design*, vol. 89, pp. 2626-2642, 2011.
- [18] A. A. Kiss and C. S. Bildea, "Design and control of an energy integrated biodiesel process," in *Computer Aided Chemical Engineering*. vol. Volume 29, M. C. G. E.N. Pistikopoulos and A. C. Kokossis, Eds., ed: Elsevier, 2011, pp. 186-190.
- [19] C. S. Bildea and A. A. Kiss, "Dynamics and control of a biodiesel process by reactive absorption," *Chemical Engineering Research and Design*, vol. 89, pp. 187-196, 2011.

- [20] H. J. Cho, J.-K. Kim, S. W. Hong, and Y.-K. Yeo, "Development of a novel process for biodiesel production from palm fatty acid distillate (PFAD)," *Fuel Processing Technology*, vol. 104, pp. 271-280, 2012.
- [21] J.-K. Cheng, C.-C. Chao, J. D. Ward, and I. L. Chien, "Design and control of a biodiesel production process using sugar catalyst for oil feedstock with different free fatty acid concentrations," *Journal of the Taiwan Institute of Chemical Engineers*, vol. 45, pp. 76-84, 2014.
- [22] D. S. Patle, Z. Ahmad, and G. P. Rangaiah, "Plantwide Control of Biodiesel Production from Waste Cooking Oil Using Integrated Framework of Simulation and Heuristics," *Industrial & Engineering Chemistry Research*, vol. 53, pp. 14408-14418, Sep 2014.
- [23] The American Oil Chemists' Society, "Official Methods and Recommended Practices of the AOCS Ca 5a-40," 5 ed. Champaign, 1997.
- [24] W. L. Luyben, *Plantwide Dynamic Simulators in Chemical Processing and Control*: Marcel Dekker, 2002.
- [25] R. Lin, Y. Zhu, and L. L. Tavlarides, "Mechanism and kinetics of thermal decomposition of biodiesel fuel," *Fuel*, vol. 106, pp. 593-604, 2013.

APPENDIX

## APPENDIX A

Calibration curve of the pump

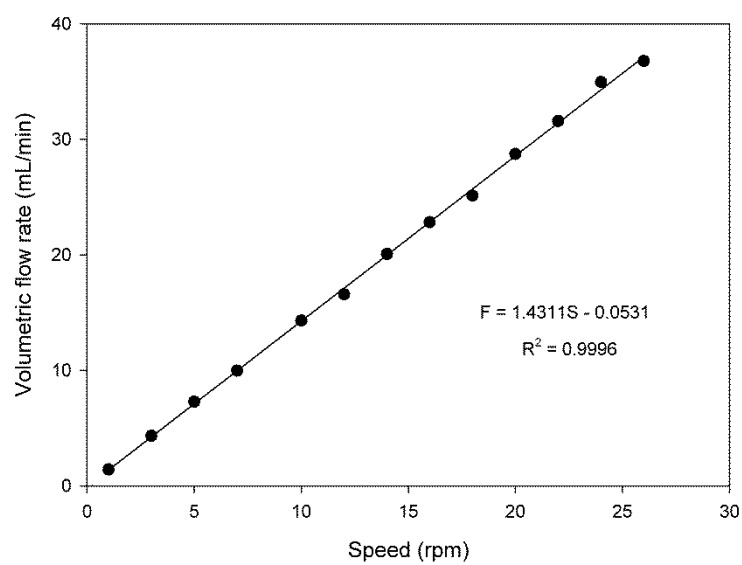


Fig. A-1 Calibration curve of methanol-sulfuric acid solution pump.

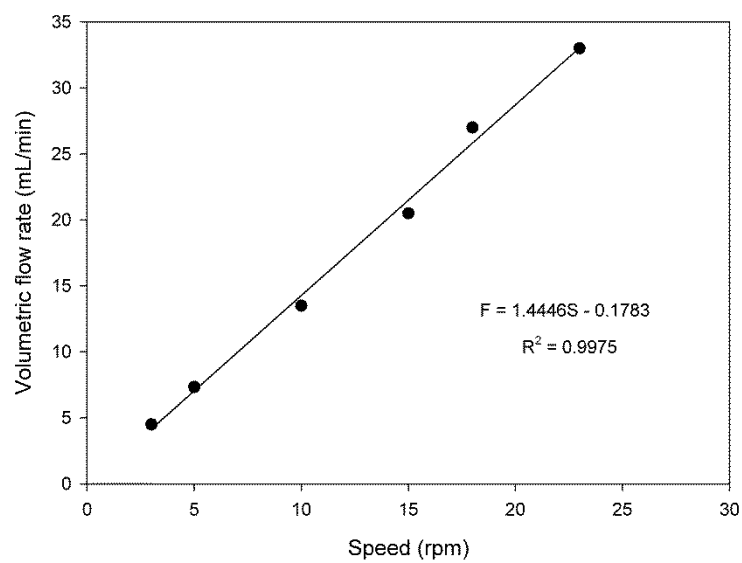


Fig. A-2 Calibration curve of heated PFAD pump.

## APPENDIX B

## Ultimate gain and Ultimate period of the process

Table B-1 Ultimate gain and Ultimate period of process in control structure I.

Controlled variable	Manipulated variable	$K_U$	$P_U$ (min)
PFAD feed	Heat duty	137.16	6
R1	Reactor duty	7.32	6
Tray 5 <sup>th</sup> of C1	Reboiler duty	5.03	1.2
Sodium hydroxide feed to R2	Heat duty	10.61	6
R2	Reactor duty	24.23	6
R3	Reactor duty	290.58	6
Tray 5 <sup>th</sup> of C2	Reboiler duty	10.35	8.4
Bottom stream of C2	Heat duty	24.23	1.2
Water feed to C3	Heat duty	27.71	3.6
C4	Heat duty	9.13	7.2
Bottom stream of C4	Heat duty	11.52	3
Top stream of C4	Heat duty	3.42	1.2

**Table B-2** Ultimate gain and Ultimate period of process in control structure II.

Controlled variable	Manipulated variable	$K_U$	$P_U$ (min)
PFAD feed	Heat duty	137.16	6
R1	Reactor duty	7.87	5.4
Tray 5 <sup>th</sup> of C1	Reboiler duty	12.55	1.2
Sodium hydroxide feed to R2	Heat duty	13.16	1.8
R2	Reactor duty	21.71	6
R3	Reactor duty	110.16	6
Tray 5 <sup>th</sup> of C2	Reboiler duty	35.42	12
Bottom stream of C2	Heat duty	16.74	3.6
Water feed to C3	Heat duty	30.23	4.2
C4	Heat duty	8.65	7.2
Bottom stream of C4	Heat duty	11.39	3
Top stream of C4	Heat duty	2.26	1.8

## APPENDIX C

## Conference proceeding

A. Saejio and K. Prasertsit, "Design and control of biodiesel production in esterification section," in *19th Regional Symposium on Chemical Engineering*, Bali, Indonesia, 2012, pp. B-22-1.

## VITAE

Name Mr. Apichat Saejio

Student ID 5310130034

### Educational Attainment

Degree	Name of Institution	Year of Graduation
Bachelor of Engineering (Chemical Engineering)	Prince of Songkla University	2010

### Scholarship Awards during Enrollment

Prince of Songkla scholarship

Graduate School Research Support Funding for Thesis

### List of Publication and Proceeding

A. Saejio and K. Prasertsit, "Design and control of biodiesel production in esterification section," in *19th Regional Symposium on Chemical Engineering*, Bali, Indonesia, 2012, pp. B-22-1.